# MODELLING DOPAMINE AND GLUTAMATE SIGNAL INTEGRATION INFLUENCE ON NEUROADAPTATION

Lu Li
St John's College



A Dissertation submitted to the University of Cambridge for
the degree of Doctor of Philosophy

European Molecular Biology Laboratory
European Bioinformatics Institute
Wellcome Trust Genome Campus
Hinxton, Cambridge, CB10 1SD
United Kingdom

luli@ebi.ac.uk

9th August 2010

Lu Li: *Modelling Dopamine and Glutamate Signal Integration Influence on Neuroadaptation,* A Dissertation submitted to the University of Cambridge for the degree of Doctor of Philosophy, © 9th August 2010

Supervisor:
Nicolas Le Novère

Thesis Advisory Committee:
Stephen Eglen, Cambridge University
Wolfgang Huber, EMBL Heidelberg
Liliana Minichiello, EMBL Monterotondo

Cambridge, 9th August 2010

To my parents

## DECLARATION

This dissertation is my own work and includes nothing which is the outcome of work done in collaboration except as specified in the text. It is not substantially the same as any I have submitted for a degree, diploma or other qualification at any other university; and no part has already been, or is currently being submitted for any degree, diploma or other qualification.

This dissertation does not exceed the specified length limit of 300 single-sided pages of double-spaced text as defined by The Biology Degree Committee.

*Cambridge, 9th August 2010*

Lu Li

# MODELLING DOPAMINE AND GLUTAMATE SIGNAL INTEGRATION INFLUENCE ON NEUROADAPTATION

<div style="text-align: right;">Lu Li</div>

Mechanisms underlying reward processes and drug addiction include the neuroadaptation of striatal cells. Integration of cortico-striatal glutamate input and mesencephalic dopamine signalling has been shown to be important. In this thesis, I investigate this transmission cross-talk by studying quantitative models of key molecular processes involved in short-term synaptic plasticity and long-term cellular remodelling.

Using a detailed quantitative computational model of calmodulin function, I investigate the effect of calcium signals by varying spike frequency, spike amplitude, and signal duration. I show that the effective activation of calmodulin depends on calcium spike frequencies rather than the total amount of calcium ions. Furthermore, high frequencies of calcium inputs shift the balance of relative activation from calcineurin to calcium/calmodulin-dependent protein kinase II (CaMKII), inducing long-term potentiation. Dopamine-mediated inhibition of protein phosphatase 1 (PP1) extends the activation of CaMKII by high calcium spiking frequencies, therefore modulating short-term synaptic plasticity.

I also investigate how dopamine and glutamate signals converge on the activity of extracellular signal regulated kinase (ERK), a crucial protein regulating structural changes such as dendritic remodelling and density of synaptic connections. Comparison of alternative models, where either calcineurin or PP1 directly stimulates striatal-enriched tyrosine phosphatase (STEP), with existing experimental data, provides evidence for a direct stimulation of STEP by PP1. However, my experiments conducted on primary striatal neuron cultures after one week or two weeks show a switch of glutamate influence on ERK activity, from activation to inhibition. Detailed computational models provide a tentative explanation why dopamine regulated PP1 activ-

ity displays opposite effects on ERK activity according to different neuronal differentiation and, in particular, the type of *N*-methyl-ᴅ-aspartate (NMDA) receptors expressed.

This thesis sheds light on some biochemical cascades involved in striatal neuroadaptation, and provides accurate models that can be reused and extended to study other aspects of this neuroadaptation.

*I hear and I forget.*
*I see and I remember.*
*I do and I understand..*

— *Confucius*

## ACKNOWLEDGEMENTS

First of all, I would like to thank my supervisor Nicolas Le Novère for his support and supervision. I am very grateful for having worked in the exciting field of computational modelling, as well as being involved in wet lab experiments.

I would like to express my gratitude to the members of my thesis advisory committee: Stephen Eglen, Wolfgang Huber and Liliana Minichiello, for providing invaluable comments and suggestions.

Many thanks to Denis Hervé and Jean-Antoine Girault for their patience and encouragement while I was in the lab in Paris. I would also like to give special thanks to Miriam Sanchez Matamales and Emmanuelle Jordi, who spared their precious time to teach me how to successfully perform some crucial experiments and made my stay in Paris so enjoyable.

I have a special thought for everyone in the Compneur group: thank you for making me feel involved in a big family.

I want to say Xie Xie to my parents, Camille Laibe, Chen Li, and Penny Coggill for love and understanding.

Finally, I want to thank my supervisor again, without him, it would have been impossible to finish this thesis on time.

# CONTENTS

## LIST OF FIGURES

# LIST OF TABLES

# INTRODUCTION

## 1.1 SYNAPTIC BASIS OF NEUROADAPTATION

### 1.1.1 *Reward and neuroadaptation*

Reward-driven learning is essential for obtaining the resources necessary for survival behaviours such as feeding and reproduction (Hyman *et al.*, 2006). Drugs of abuse are perceived as a kind of reward, and induce persistent compulsive drug intake. Research indicates that neuronal systems can adapt to repeated long-term drug intake, and store drug-associated cues as memory (Berke and Hyman, 2000; Robbins and Everitt, 2002; Everitt and Robbins, 2005; Hyman, 2005). Thus, drug addiction results from the distorted reward-related learning, and from neuroadaptation.

A common feature of reward is the increased dopamine input generated from the ventral tegmental area (VTA) of the midbrain to the nucleus accumbens (NAc) of the ventral striatum (Fig. 1) (Wise, 1998; Chiara, 1998). The NAc, in particular its shell region, is an important target of drugs of abuse (Pontieri *et al.*, 1995; Ito *et al.*, 2004). The NAc also receives glutamatergic afferents from the cerebral cortex, and projects to the pallidum, as part of the cortico-striato-thalamic loop (Parent and Hazrati, 1995). Precise information about specific experiences, cues and actions can be encoded by the induction of bidirectional alterations of synaptic strength, a process termed 'synaptic plasticity'. In this case, cortico-striatal glutamate inputs and mesencephalic dopamine signals are integrated in the NAc, converting drug associated information and response into long-term memory, via alteration in synaptic plasticity and physical remodelling of the synaptic connections (Berke and Hyman, 2000; Hyman and Malenka, 2001).
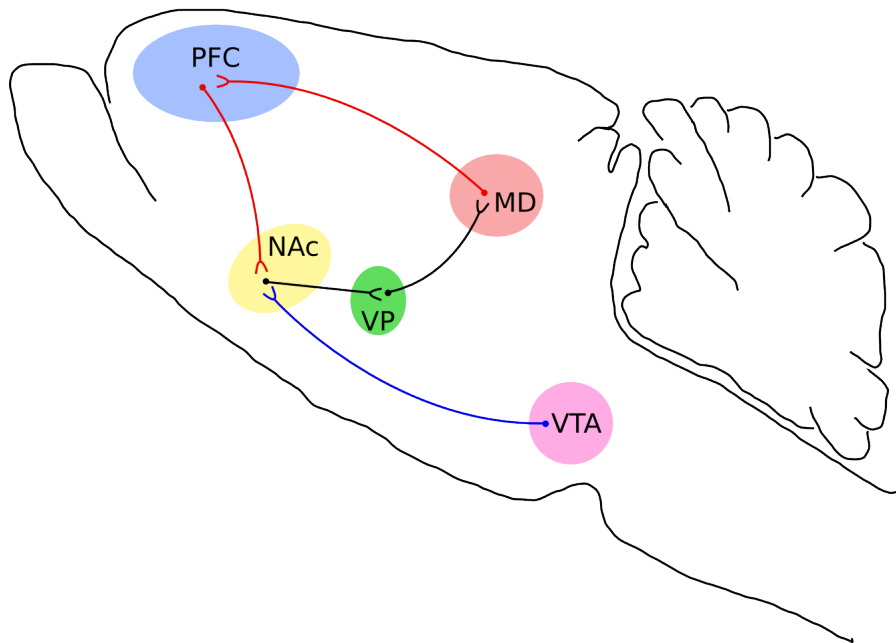
Figure 1: **Dopamine-glutamate interactions in the NAc and the cortico-striato-thalamic loop.** This figure illustrates how the glutamate afferent (red line) from the prefrontal cortex (PFC) and dopamine projection (blue line) from ventral tegmental area (VTA) interact at spines in the NAc. The output neurons of NAc, the medium-sized spiny neurons (MSNs), project $\gamma$-aminobutyric acid (GABA) (black line) to the ventral analog of the globus pallidus, known as the ventral pallidum (VP). GABAergic VP neurons project to mediodorsal thalamic nucleus (MD), which in turn projects glutamate to PFC.

1.1.2  *Synaptic plasticity*

Neuronal circuits are largely composed of dendrites, axons, and the synapses that connect them, with neuronal information transferred through these connections. A chemical synapse transforms an electrical signal into a chemical one, and consists of a presynaptic active zone, a synaptic cleft and a protein dense region of the spine head called the postsynaptic density (PSD) (Harris *et al.*, 1992). PSD determines the strength of the response to an incoming signal. Bidirectional alterations of this strength are called synaptic plasticity, a process at the origin of learning and memory (Malenka, 2003; Lynch, 2004).

*Short term synaptic plasticity*

NMDA receptor-dependent long-term potentiation (LTP) and long-term depression (LTD) are two of the most extensively studied prototypic forms of synaptic plasticity. At resting membrane potential, the NMDA receptor is blocked by magnesium. When presynaptic glutamate release coincides with postsynaptic membrane depolarization, the NMDA receptor becomes activatable due to magnesium removal. Glutamate may cause the NMDA receptor to open, and permit calcium ions to flow through the receptor pore (Bliss and Collingridge, 1993; Magee and Johnston, 1997; Markram *et al.*, 1997). The influx of calcium induces the activation of calmodulin, which in turn stimulates the CaMKII (Lisman *et al.*, 2002). The activated CaMKII phosphorylates the GluR1 subunit of the $\alpha$-amino-3-hydroxy-5-methyl-4-isoxazolepropionic acid (AMPA) receptor (Lee *et al.*, 2000, 2003a), mediating the delivery of AMPA receptors to the postsynaptic membrane (Hayashi *et al.*, 2000; Malinow and Malenka, 2002; Bredt and Nicoll, 2003). This strengthens the pre- and postsynaptic connections, inducing NMDA receptor-dependent LTP (Fig. 2).

Paradoxically, the NMDA receptor-dependent elevation of calcium level is also necessary for the induction of LTD that is characterised by weakened pre- and postsynaptic connections (Mulkey and Malenka, 1992; Kandler *et al.*, 1998). Calcium influx through the NMDA receptor results in the activation of calcineurin and the subsequent activation of PP1, leading to the reduced CaMKII activity and eventually to the rapid reduction in the expression of AMPA receptors in

the postsynaptic membrane (Fig. 2) (Mulkey *et al.*, 1994; Groth *et al.*, 2003).
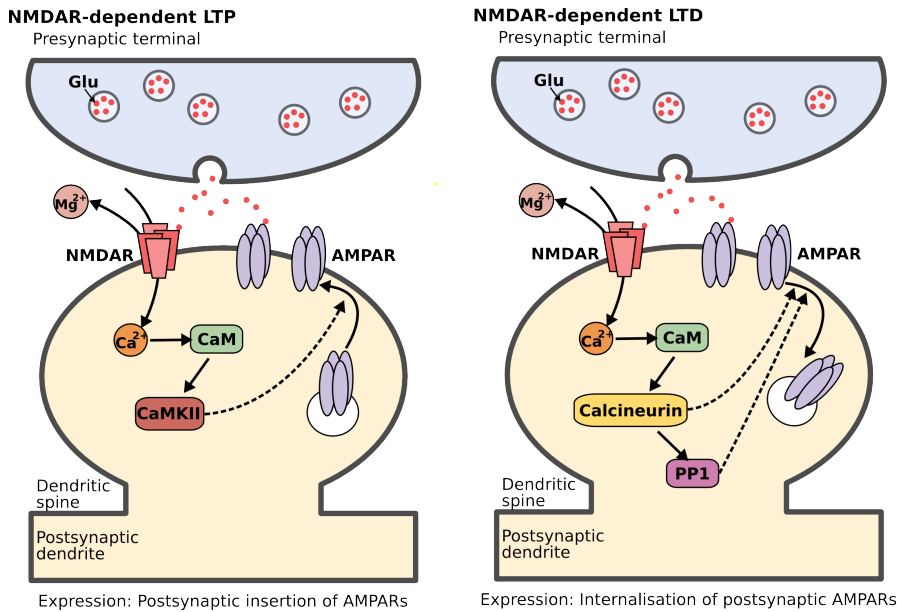


Figure 2: **NMDA receptor-dependent LTP and LTD**. This figure shows a simplified view of NMDA receptor-dependent short-term synaptic plasticity. *Left*: NMDA receptor-dependent long-term potentiation (LTP). The calcium/calmodulin-dependent protein kinase II (CaMKII)-mediated AMPA receptor insertion into postsynaptic membrane is a major mechanism underlying the initiation of LTP. *Right*: NMDA receptor-dependent long-term depression (LTD). Calcineurin- and protein phosphatase 1 (PP1)-mediated internalisation of postsynaptic AMPA receptor is a primary mechanism of this process.

Therefore, calcium is responsible for triggering both NMDA receptor-dependent LTP and LTD. Surprisingly, however, little is known about the quantitative properties of the postsynaptic calcium signals that can distinguish the activation of these two opposing events.

*Structural plasticity*

Recording memories of neuronal activity is initiated by alterations in glutamate-dependent synaptic transmission. Changes are thereafter stabilised by structural modifications in synaptic connections on dendritic spines. These structural changes, whether dependent on protein synthesis or not, encode persistent long-term memory,

and are referred to as 'structural plasticity' (Lamprecht and LeDoux, 2004).

The morphology of spine, the protrusion on dendrites, consists of an expanded head and a neck that connects to the dendritic shaft (Nimchinsky *et al.*, 2002). The excitatory synapse contains the PSD that is developed to efficiently respond to synaptic transmission. Therefore, the shape and number of spines control the characteristics of neurotransmission, and the spines themselves are dynamically regulated by synaptic activity.

Much evidence indicates that induction of synaptic plasticity leads to changes in spine shape (Nikonenko *et al.*, 2002; Yuste and Bonhoeffer, 2001; Fifková and Anderson, 1981), and density (Engert and Bonhoeffer, 1999; Toni *et al.*, 1999; Fiala *et al.*, 2002; Harris *et al.*, 2003). Modifications in spine morphology and number, induced by learning procedures, have also been demonstrated (Leuner *et al.*, 2003; Geinisman *et al.*, 2001; Kleim *et al.*, 2002; Knafo *et al.*, 2001). Spine morphological changes can be observed in as little as two minutes poststimulation and can last up to months.

The onset of structural change is too rapid to be regulated via nuclear events such as gene expression modifications, or even by direct dendritic protein synthesis. Conversely, it has been shown that more persistent changes require regulation at the level of gene expression and protein translation (Kandel, 2001). Thus, dendritic structural plasticity includes at least two parallel and correlated processes. One process controls the rapid remodelling of cytoskeletal and adhesion proteins (Matus, 2000; Maletic-Savatic *et al.*, 1999), thereby stabilising synaptic connections and consolidating the early phase of synaptic plasticity into late phase. The second process induces the regulation of gene expression and protein synthesis over longer periods of time, consolidating synaptic connections, thus entering the late phase of synaptic plasticity (Fig. 3 and Fig. 4).

The underlying structure of the spine is built upon cytoskeletal filaments composed of actin (Harris and Kater, 1994). Individual actin filaments are transient structures, and filament polymerisations contribute both to the shape of a spine, and to new spine formation (Fischer *et al.*, 1998; Dunaevsky *et al.*, 1999). Indeed, the activation of NMDA receptor, which leads to postsynaptic calcium elevation, has

been shown to induce actin polymerisation (Fukazawa *et al.*, 2003) and to alter spine morphology (Fig. 3) (Maletic-Savatic *et al.*, 1999).

Cytoskeletal rearrangement requires stabilisation, a process that involves the AMPA receptors. These receptors have been demonstrated to maintain spine morphology by sequestering protrusive actin from the surface of the spine head into the core of a spine (Fig. 3) (Fischer *et al.*, 2000). The basal activities of AMPA receptors, induced by spontaneous glutamate release, are able to maintain spine shape in mature synapses (McKinney *et al.*, 1999). Furthermore, the morphological changes of spine, triggered by synaptic activity, can be enhanced by insertion of AMPA receptors into postsynaptic membrane, which maintains LTP (Lamprecht and LeDoux, 2004) and retains memory (Schafe *et al.*, 2001; Lee *et al.*, 2003a; Esteban *et al.*, 2003).

In fact, these morphological changes are correlated with short-term synaptic plasticity. Activation of NMDA receptors induces the activation of CaMKII and the initiation of actin dynamics. Actin-based alterations in spine shape, or the formation of new spines, strengthens synaptic connections. In the meantime, CaMKII facilitates the insertion of AMPA receptors which, in turn, stabilise the actin based structural plasticity. However, similar to the induction of LTD, NMDA receptor-dependent calcium influx can also disrupt the stability of synaptic structure by the activation of calcineurin (Halpain *et al.*, 1998).

The fast rearrangement of the cytoskeleton in spines provides a transition between initial expression of synaptic plasticity and more persistent structural remodelling of dendritic spines via regulation of gene expression and protein synthesis. Protein synthesis can happen locally in dendrite regions proximal to stimulated synapses (Steward and Schuman, 2001; Martin *et al.*, 2000). The synapse-associated polyribosome complexes (SPRCs) are localised precisely at the base of the spine (Steward and Levy, 1982). The mRNA for the CaMKII $\alpha$ subunit is associated with SPRCs, and mRNA levels increase during synaptic activity (Scheetz *et al.*, 2000; Bagni *et al.*, 2000). Many mRNAs encoding different dendritic proteins are locally transcribed in a cell type-dependent manner (Steward and Schuman, 2001). A key advantage of local protein synthesis is that it allows transcription-dependent changes to rapidly occur, which in turn can initiate quickly the late phase of synaptic plasticity.
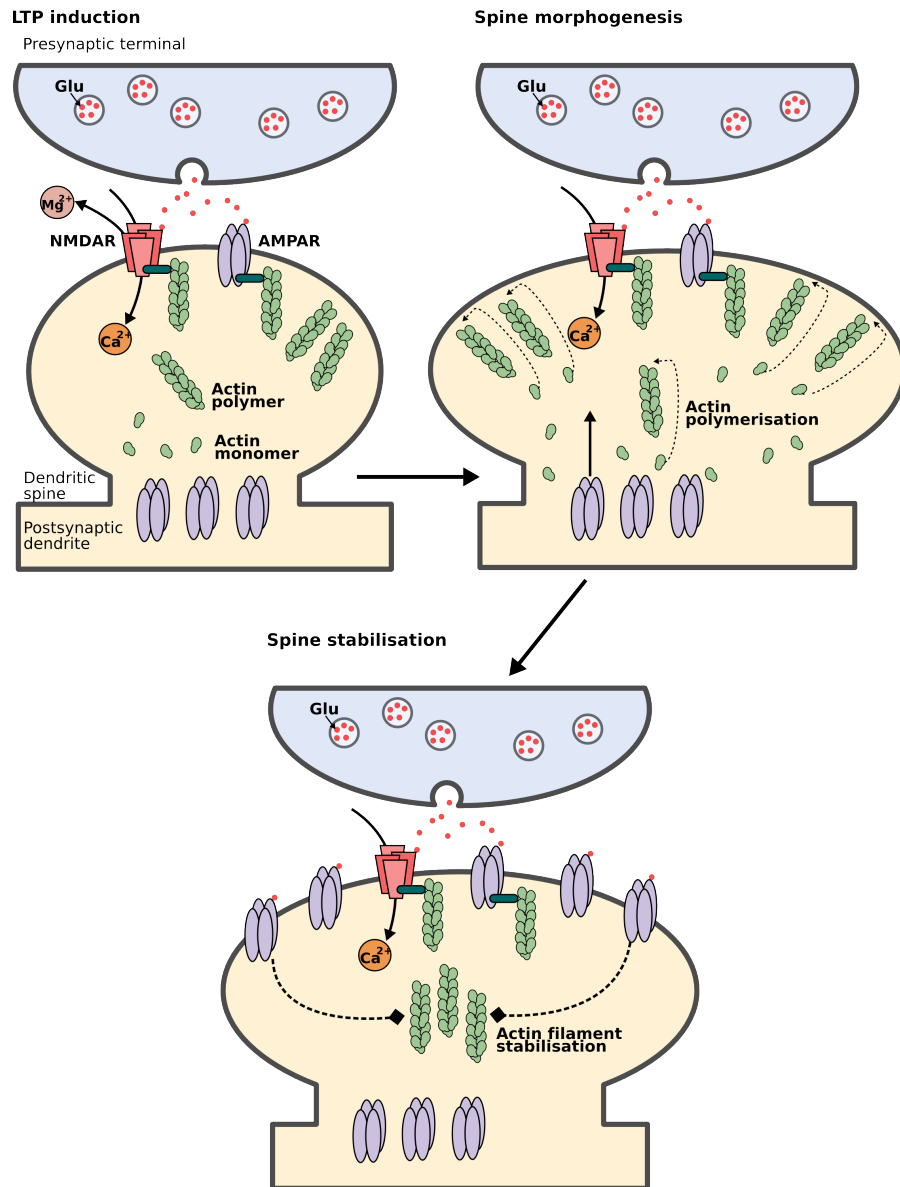
Figure 3: **Actin-based spine morphology changes and stabilisation**. Synaptic activity induces glutamate release, which activates NMDA receptor, resulting in increased postsynaptic calcium level (*top left*). Rapid actin polymerisation leads to the changes in spine shape (*top right*). The increase of AMPA receptors in the postsynaptic membrane enhances glutamate transmission and stabilises actin filaments (*bottom*).

Sustained structural changes of dendritic spines also require controls at the level of gene expression (Fig. 4). One of the most extensively studied transcription factors, cyclic AMP-response-element-binding protein (CREB), plays a crucial role in establishing and maintaining long-term memory (Kandel, 2001). CREB-mediated gene expression has also been shown to be involved in the long-term effects of drugs of abuse (Blendy and Maldonado, 1998; Carlezon *et al.*, 2005). The targets of CREB include genes encoding brain-derived neurotrophic factor (BDNF), which can lead to structural changes in synapses (Tao *et al.*, 1998; Poo, 2001). Synaptic activity induced phosphorylation and activation of CREB is mediated by calcium-dependent activation of the mitogen-activated protein (MAP) kinase pathway (Wu *et al.*, 2001a; Dolmetsch *et al.*, 2001). However, calcium elevation induced by neuronal activity can also trigger CREB dephosphorylation, through the activation of calcineurin and the subsequent activation of PP1. This NMDA receptor-induced negative regulation of CREB may be affected by the compositional changes of NMDA receptors, and the changes of the associated signalling complexes (Sala *et al.*, 2000; Hardingham *et al.*, 2002).

Long-term exposure to drugs of abuse also leads to large-scale dendritic structural changes, for example, resulting in altered dendritic branching (Robinson and Kolb, 2004). Unlike that of spines, the dendritic cytoplasm is dominated by microtubules (MTs) (Matus, 2000). MTs are in a dynamic state, being constantly polymerised and depolymerised in stable dendrites (Georges *et al.*, 2008). Dendritic branching is initiated by the depolymerisation of MTs and the subsequent MT invasion into filopodia (Georges *et al.*, 2008) that may be newly formed during the induction state of LTP. Many intracellular proteins play roles in regulating dendritic morphology, regulating neurite outgrowth, branching, and stabilisation (reviewed in Arimura and Kaibuchi (2007); Barnes *et al.* (2008); Barnes and Polleux (2009)).

In summary, structural plasticity due to cytoskeleton rearrangement is rapidly initiated during synaptic activity, followed by a parallel protein synthesis-dependent structural plasticity. This allows both the rapid changes in neurotransmission and the formation of persistent long-term memory.
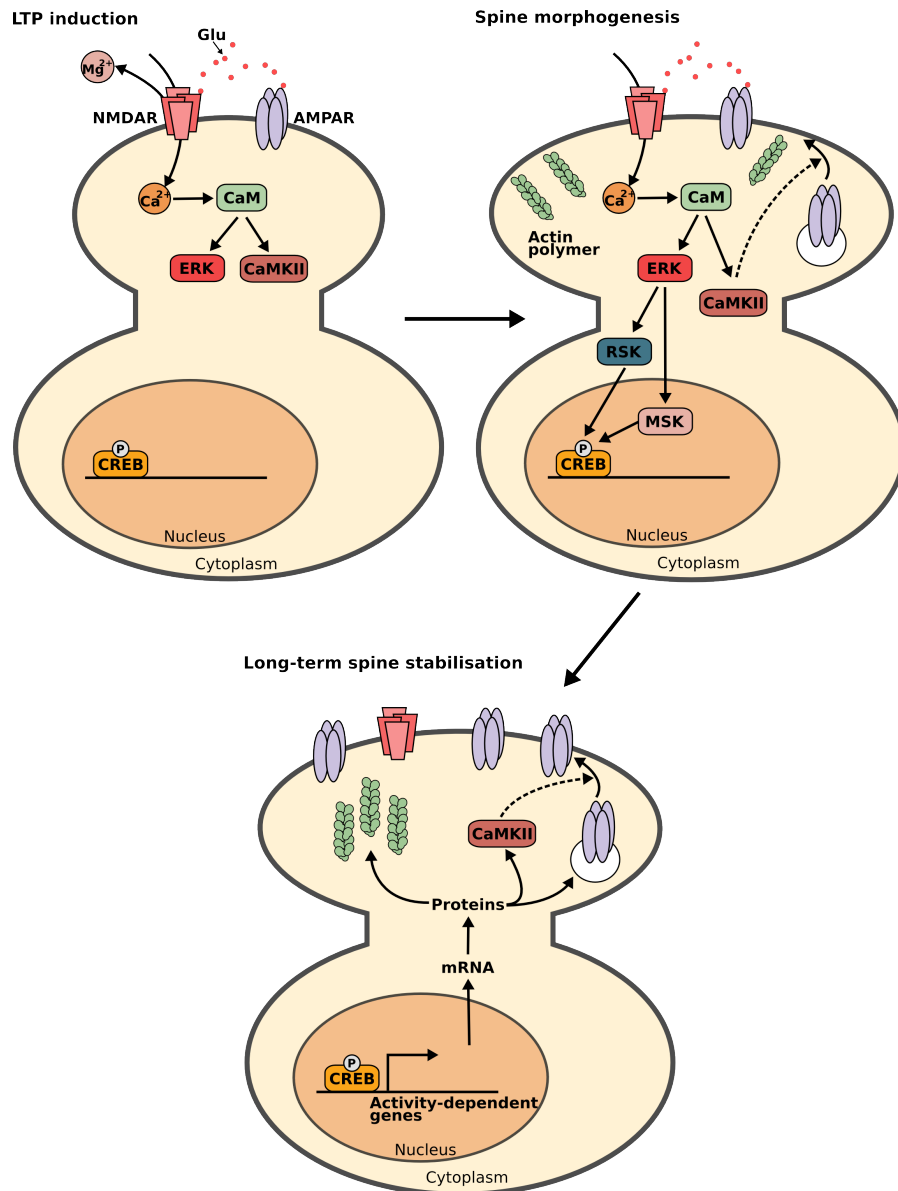
Figure 4: **The involvement of gene expression and protein synthesis in spine morphogenesis.** Synaptic activity-dependent glutamate release leads to activations of NMDA receptors and second messenger pathways. These result in increased activities of extracellular signal regulated kinases (ERK) and calcium/calmodulin-dependent protein kinase II (CaMKII) (*top left*). The fast spine morphogenesis is companioned with the altered nuclear gene expression, mediated by the action of ribosomal protein S6 kinases (RSKs), mitogen- and stress-activated kinases (MSKs), and their substrate cyclic AMP-response-element-binding protein (CREB) (*top right*). The newly synthesised proteins, for example, AMPA receptors, CaMKII, and actin, promote structural changes of the synapses (*bottom*).

### 1.1.3    *Signalling pathways responding to dopamine inputs*

Dopamine was first shown to be a neurotransmitter in the late 1950s by Carlsson (1959). Since then, dopamine has been found to control many aspects of brain function, including voluntary motor activity, motivation, positive reinforcement and reward-related learning. Because of its importance in those functions, modification of dopamine transmission is also involved in many pathologies such as Parkinson's disease, schizophrenia, and drug addiction. The dopaminergic neurons involved in reward related learning are located in the midbrain, within the ventral tegmental area and the substantia nigra compacta. They project primarily to the striatum, prefrontal cortex, amygdala, and hippocampus. Dopamine receptors belong to the superfamily of G-protein coupled receptors (GPCRs) and consist of five distinct receptor sub-types in mammals, regrouped in two subfamilies, D1R-like (D1R, D5R) and D2R-like (D2R, D3R, and D4R) (Missale *et al.*, 1998). Dopamine innervation from the midbrain to the striatum exerts its effect mainly through dopamine D1 and D2 receptor subtypes (Berthet and Bezard, 2009). GABAergic medium-sized spiny neuron (MSN), the predominant cell type of the striatum, can be classified into two neuronal populations depending on their projections. MSNs directly projecting to the internal globus pallidus and substantia nigra pars reticulata, and having a stimulatory effect on the cortico-striato-thalamic loop, express mainly dopamine D1 receptors; whereas MSNs projecting to the same nuclei via relays in the external globus pallidus and the subthalamic nucleus, and having an inhibitory effect on the cortico-striato-thalamic loop, express preferentially dopamine D2 receptors (Alexander and Crutcher, 1990). Recent research reveals that different drugs of abuse may exert their long-term effect through different populations of striatal output neurons. For instance, in mouse, acute cocaine injection increases extracellular signal regulated kinases-1/2 (ERK1/2) activity in dopamine D1R-expressing striatonigral neurons (Bertran-Gonzalez *et al.*, 2008).

Dopamine is not an excitatory or inhibitory neurotransmitter, but a neuromodulator. Dopamine exerts effects via adjusting the responses of intracellular signalling pathways to other neurotransmitters, such as glutamate. Because of its positive effect on adenylyl cyclase (AC),

via a olfactory isoform of GTP-binding protein $\alpha$ subunit ($G\alpha_{olf}$) in the striatum (Corvol *et al.*, 2001), a major effect of dopamine D1 receptor is to stimulate cyclic adenosine monophosphate (cAMP) production, thus increasing the activation of cyclic AMP-dependent protein kinase (PKA). PKA can directly phosphorylate and activate AMPA receptors to control corticostriatal neurotransmission (Esteban *et al.*, 2003). Dopamine can also act on regulatory proteins that are crucial for the convergence of dopamine- and glutamate-activated signalling cascades, one of which is dopamine- and cAMP-regulated phosphoprotein of 32 kDa (DARPP-32) (Walaas *et al.*, 1983; Greengard, 2001a).

DARPP-32 is highly expressed in MSN (Ouimet *et al.*, 1984, 1998). It is a potent PP1 inhibitor once phosphorylated at Thr34 by PKA (Hemmings *et al.*, 1984a). DARPP-32 interacts with PP1 via two binding domains, both of which contribute to inhibition (Hemmings *et al.*, 1990; Desdouits *et al.*, 1995a; Kwon *et al.*, 1997; Huang *et al.*, 1999). DARPP-32 and inhibitor I (I1) share similar characteristics and, in particular, both inhibit PP1. However, DARPP-32 possesses three other phosphorylation sites, Thr75 by cyclin-dependent protein kinase 5 (CDK5), Ser102 by casein kinase 2 (CK2), and Ser137 by casein kinase 1 (CK1), which make it a signalling hub for kinases and phosphatases. Phosphorylation on Thr75 converts DARPP-32 into an inhibitor of PKA (Bibb *et al.*, 1999). Ser102 phosphorylated DARPP-32 is able to be phosphorylated by PKA more efficiently on Thr34 *in vitro* (Girault *et al.*, 1989). Furthermore, phosphorylation on Ser137 decreases the rate of Thr34 dephosphorylation by calcineurin (Hemmings *et al.*, 1990; Desdouits *et al.*, 1995b). In short, CK1 and CK2 increase the phosphorylation state of Thr34, thus enhancing D1 dopaminergic signalling and the inhibition of PP1, whereas CDK5 mediates inhibitory effects on dopamine-stimulated signalling pathways. The dephosphorylation of Thr34 is mediated by calcineurin (King *et al.*, 1984) that is activated by calcium and calmodulin (Groth *et al.*, 2003). However, there is evidence indicating that protein phosphatase 2A (PP2A) may also dephosphorylate Thr34, albeit with relatively low efficiency, despite its preferential activity on Thr75 (Nishi *et al.*, 1999). Phospho-Ser137 can be dephosphorylated by protein phosphatase 2C (PP2C) (Desdouits *et al.*, 1998) and Ser102 by PP2A *in vitro* (Girault *et al.*, 1989). Thus, glutamate-induced activation of calcineurin impairs the

effect of dopamine signalling by releasing DARPP-32 inhibition of PP1. PP2C may produce a synergistic effect with calcineurin by increasing its phosphatase efficiency. The dephosphorylation of Thr34 and Ser102 by PP2A negatively impacts D1 dopaminergic signalling; on the other hand, PP2A effects on Thr75 can enhance dopamine inhibitory effect on PP1 through releasing phospho-Thr75 inhibition on PKA (Fig. 5).
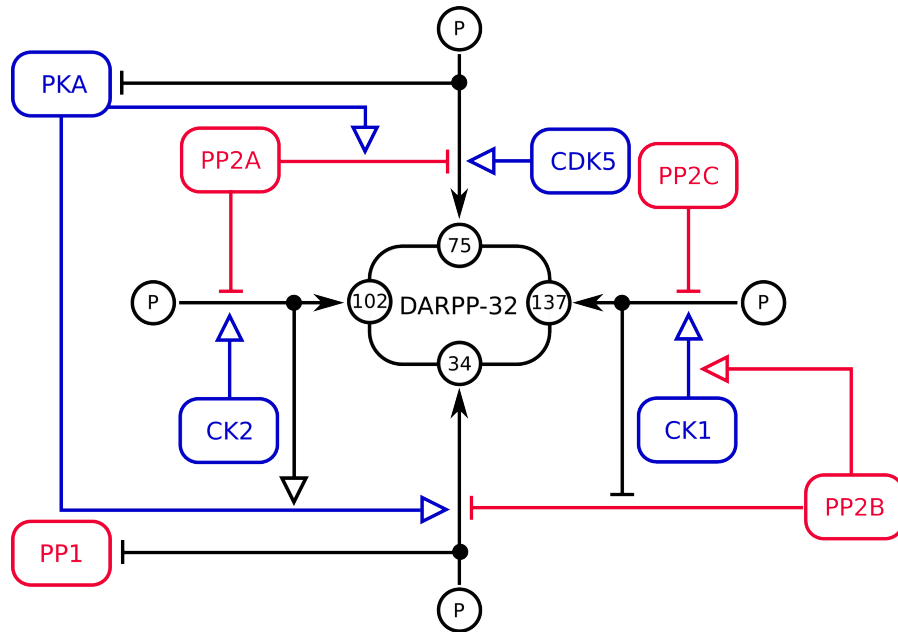


Figure 5: **Regulation of DARPP-32 phosphorylation.** This figure illustrates the regulation of the four phosphorylation sites of dopamine- and cAMP-regulated phosphoprotein of 32 kDa (DARPP-32) and its inhibitory role on cyclic AMP-dependent protein kinase (PKA) and protein phosphatase 1 (PP1), modified, with permission, from Le Novère *et al.* (2008). Phosphatases and kinases are represented in red and blue respectively. The graphical conventions are those of the Entity Relationship language of Systems Biology Graphical Notation (SBGN) (Le Novère *et al.*, 2009). Rectangular box with rounded corners: entity, circle on entity: state, circle not on entity: state value, harpoon arrow: assignment, black dot: outcome, empty arrow head: stimulation, bar arrow head: inhibition.

An additional layer of complexity comes from the intricacy of the regulation of these kinases and phosphatases. The cAMP-regulated PKA phosphorylates and increases the phosphatase activity of PP2A. PP2A dephosphorylates DARPP-32 on Thr75 and thereby forming a positive feedback loop on dopamine signal efficiency (Nishi *et al.*,

2000; Ahn *et al.*, 2007a). However, PKA can also activate cyclic nucle-otide phosphodiesterase (PDE), which in turn catalyses the degrada-tion of cAMP, reducing the duration of dopamine signal transmission. Glutamate induced calcium elevation not only activates calcineurin but also PP2A, enhancing dopamine signal efficiency via dephos-phorylation of Thr75 (Nishi *et al.*, 2002; Ahn *et al.*, 2007b). Further-more, DARPP-32 can translocate to the nucleus upon dephosphoryla-tion at Ser102 by PKA-dependent activation of PP2A. Thus, drugs of abuse cannot only induce DARPP-32 phosphorylation on Thr34 but also cause rapid nuclear accumulation, resulting in PP1 inhibi-tion in the nucleus. PP1 has very broad range of substrates, including promoting the histone H3 phosphorylation, thus controlling nuclear function and long-term drug effect (Stipanovich *et al.*, 2008).

Therefore, DARPP-32 cannot be simply considered as a switch that either inhibits PP1 or PKA, corresponding to dopamine or glutamate transmission. More precisely, DARPP-32 acts as an integrator, combin-ing the activities of enzymes regulated by dopamine and/or glutam-ate into graded inhibition of PP1 and PKA, in a temporal and spatial manner (Le Novère *et al.*, 2008). DARPP-32 plays a very important role in dopamine induced phosphorylation of NMDA and AMPA re-ceptors, and the induction of LTP and LTD in striatal neurons (Yan *et al.*, 1999; Fienberg *et al.*, 1998; Snyder *et al.*, 1998; Flores-Hernández *et al.*, 2002; Calabresi *et al.*, 2000). Besides, DARPP-32 modulates do-pamine D1 receptor-induced gene transcription (Svenningsson *et al.*, 2000), which is important for initiating drug-induced long-term ad-aptive morphological changes. All in all, dopamine, via DARPP-32, regulates the potency of PKA and PP1 to control the plasticity of corticostriatal connections and long-term neuroadaptation of basal ganglia.

## 1.2 Modelling signalling pathways in neurons

Neurons can process and store information through the activation of biochemical signalling networks. Neurotransmitters released in syn-apses can activate membrane receptors, where these activations result in increased or decreased second messenger levels, which themselves can affect many signalling pathways. These pathways are densely

connected, and several characteristics enable the postsynaptic compartments to act as complex signal processors.

First of all, neuronal signalling is based on precise timing. The activation of NMDA receptor requires the binding of glutamate to coincide with postsynaptic membrane depolarization, which then allows calcium influx, triggering specific neuronal responses (Bliss and Collingridge, 1993; Magee and Johnston, 1997; Markram *et al.*, 1997). In reward-related learning, the reward signal-inducing dopamine release must pair with the sensory-motor input-triggering glutamate release, so that dopamine modulates glutamate signalling pathways and increases the expression of molecules involved in learning (Centonze *et al.*, 2001; Wickens *et al.*, 2003).

Secondly, neuronal biochemical networks are able to distinguish signals with temporal patterns (Bhalla, 2003). For instance, central to this thesis are the different frequencies of calcium spikes triggering distinct responses, including calcineurin and CaMKII, that results in the induction of LTD or LTP.

Thirdly, signalling proteins, especially the ones located in the vicinity of the postsynaptic membrane, are assembled and organised in a way that allows the initiation of selective modulations of synaptic activity (Kennedy, 2000). One example is the NMDA receptor signalling complex. The cytoplasmic tail of the NR2 subunit of NMDA receptor serves as a scaffold protein, associating many crucial kinases and phosphatases, including CaMKII and synaptic Ras GTPase activating protein (SynGAP). These will be explored in more detail later in this thesis.

Last, but not least, the characteristic activities of neuronal signalling networks span multiple timescales. Fast synaptic transmission occurs in less than 1 millisecond, whereas slow transmission takes place over periods of hundreds of milliseconds to minutes (Greengard, 2001b). Glutamate-induced MAP kinase activation can last for hours, whereas changes in neuronal morphology may require days.

These properties are difficult to control and manipulate during *in vivo* experiments. Therefore we need to build quantitative computational models in order to interpret the results from molecular experiments, to predict the consequences of our various hypotheses, and

finally to map and gain a system-level understanding of the different relevant pathways.

Several mathematical approaches are available for representing and analysing neuronal biochemical signalling, which can be classified into three major categories (reviewed by Eungdamrong and Iyengar (2004) and Tölle and Le Novère (2006)): deterministic simulations of continuous variables, population based stochastic simulations and particle based stochastic approach.

### 1.2.1  *Deterministic simulations of continuous variables*

Simulations of deterministic systems do not involve any stochastic considerations. Therefore, the changes in concentrations of components over time are predictable if the initial conditions and boundaries are specified.

*Continuous models based on homogeneous systems*

Most deterministic simulations assume that chemical reactions happen in well-stirred compartments, and models are therefore built on continuous ordinary differential equation (ODE) systems. Typical examples are kinetic models based on Mass Action kinetics (Guldberg and Waage, 1864), which relate the velocity of an elementary reaction to the product of the concentrations of its reactants, to the powers of their respective stoichiometries. The speed at which a component changes depends on the rates of reactions at which this component is consumed or produced.

This kind of modelling is computationally efficient, and many ODE solvers have been implemented. If each chemical species in the model is present in a large quantity, these homogeneous and continuous ODE systems can provide a good approximation of the behaviour of a large network (for example, see Bhalla and Iyengar (1999)). Since these models can be efficiently simulated, they are amenable to large-scale parameter scanning for initial concentrations and kinetic constants, therefore providing useful insights on parameter constraints for the behaviours of the relevant signalling pathways (see for example Fernandez *et al.*, 2006)).

*Deterministic models based on heterogeneous systems*

Space homogeneity is not always the reality. For example, neuronal activity is often regulated by localised constructs, as demonstrated by the signalling complexes within the PSD. Often, a more realistic approach is to consider multiple compartments in order to emulate concentration gradients, different cellular organelles, and scaffolds-based signalling complexes. In these instances, the diffusion of molecules between the different compartments can be modelled as transport reactions. Within each compartment, molecules may be considered as being distributed homogeneously, thus compartmentalised interactions can still be modelled by continuous ODE systems (for example, see Naoki *et al.* (2005)). However, when a chemical component appears in different compartments, each compartment needs to be treated as an independent pool, thus increasing the complexity of the model. Furthermore, the rates of diffusion between compartments are usually only roughly estimated.

Another realistic approach is to use reaction-diffusion equations based on partial differential equations (PDE). In this modelling approach, the concentration change of a component depends not only on the net rate of consuming and producing reactions, but also on its diffusion in space. Therefore, the concentration changes depend on multiple independent variables, including time and the location of the molecule in the concentration gradients. To numerically solve reaction-diffusion equations requires not only the initial conditions, but also the concentrations at the boundaries of the specified compartments (Fall *et al.*, 2002) (for examples, see Fink *et al.* (2000), Haugh (2002), and Shvartsman *et al.* (2002)). The drawbacks of this modelling approach are increased complexity and computing time. Moreover, the values for diffusion constants *in vivo* are generally unavailable.

### 1.2.2   *Population-based stochastic simulations*

Biochemical components participate in reactions as integer numbers, which define the discrete nature of a biological system. Many biochemical activities do not follow predicted trajectories when the initial conditions are specified. This is due to the noise and randomness

in neuronal signalling, both of which are unavoidable because of reactions occurring in space-restricted environments, and because of the small numbers of each species involved. In this case, the changes in concentration of components over time cannot be precisely predicted, and continuous deterministic approaches may lead to inaccurate results. Probabilistic descriptions of chemical reactions are therefore preferred.

A family of widely used algorithms for simulating stochastic biochemical models was proposed by Gillespie (1976, 1977), based on the kinetic Monte Carlo Method (Bortz *et al.*, 1975). In Gillespie-type methods, reactions occur with certain probabilities defined by their kinetic rates and the number of molecules present. Random numbers are used to decide the delay before the next step, and which reactions will occur (for examples, see Bhalla (2004a) and Bhalla (2004b)). Stochastic simulation approaches can also be incorporated within a spatially heterogeneous reaction-diffusion model (Lee *et al.*, 2003b).

In many circumstances, however, reactions with small numbers of reactants coexist with reactions involving great numbers of signalling molecules. An ideal approach, in terms of speed and accuracy, would be to use a hybrid system incorporating both stochastic and deterministic simulation methods, as demonstrated in Tian *et al.* (2007).

### 1.2.3  *Particle-based stochastic approach*

All simulation approaches described above treat reacting components as population pools. One problem arising from this implementation is the potential combinatorial explosion resulting from multi-state molecules (reviewed by Tölle and Le Novère (2006)). An attractive alternative is to use particle-based stochastic approaches, in which each individual molecule is treated as an object. This allows understanding of the contribution of each individual particle within the whole system. Another advantage of a particle-based approach is that positional information, orientation, and geometry for each molecule can be monitored, which has significant effects in the study of spatially heterogeneous system. However, this also means that additional parameters need to be obtained or estimated (for example, see Franks *et al.* (2002) and Franks *et al.* (2003)).

# SHORT-TERM SYNAPTIC PLASTICITY

## 2.1 INTRODUCTION

NMDA receptor-dependent LTP and LTD are two forms of activity-dependent synaptic plasticity, a process at the origin of learning and memory (Malenka, 2003; Lynch, 2004). It has been shown that a high-frequency of synaptic stimulation leads to LTP (Bliss and Collingridge, 1993), while a low-frequency stimulation results in LTD (Dudek and Bear, 1992). In both cases, stimulation triggers postsynaptic membrane depolarization, which leads to the activation of synaptic NMDA receptors, and the subsequent elevation of intracellular calcium concentration. Calcium, via calmodulin, activates the CaMKII, inducing LTP (McGlade-McCulloh *et al.*, 1993; Lledo *et al.*, 1995), or calcineurin, triggering LTD (Mulkey *et al.*, 1994).

It has been proposed that substantial increases in postsynaptic calcium concentration selectively activate CaMKII, while moderate rises activate calcineurin (PP2B) (Artola and Singer, 1993; Lisman, 1989). However, several observations suggest this hypothesis is inadequate. First of all, intracellular calcium level increases in the form of spikes rather than by gradually reaching a steady level. This is due to the large number of calcium-binding proteins, which acts as the calcium buffer, and to calcium efflux mechanisms, which lower calcium concentration back to a basal level within a few hundred milliseconds (Sabatini *et al.*, 2002). This fast calcium transient suggests that the increase in calcium level depends not only on the amplitude of each input, but also on the frequency and duration of these inputs. Second, a brief sub-molar increase of calcium has been found to trigger LTP and LTD with similar probabilities (Neveu and Zucker, 1996). Third, the different temporal patterns of postsynaptic calcium elevation have been shown to selectively induce LTP or LTD (Yang *et al.*, 1999). Taken together, these findings suggest that the temporal patterns of calcium increase, rather than its amplitude, are the key signal carrying sig-

nificant biological information. The question remains, however, as to how signalling pathways are able to decipher the temporally-encoded calcium signals through key signalling molecules such as calmodulin, or CaMKII.

Calmodulin, an important calcium-dependent regulatory protein, possesses four EF-hand calcium-binding domains (Babu *et al.*, 1988), and can exist in two distinct conformations: the inactive T state (Kuboniwa *et al.*, 1995) and the active R state (Babu *et al.*, 1985). Calcium cooperatively binds to calmodulin (Crouch and Klee, 1980). The binding of four calcium ions is not necessary for calmodulin function, since unsaturated calmodulin can also activate its targets (Shifman *et al.*, 2006). Stefan *et al.* (2008) proposed an allosteric model for calmodulin activation, illustrating how the binding of calcium ions progressively stabilises the high-affinity R state. Furthermore, in this model, calmodulin can differentially activate calcineurin and CaMKII according to static calcium concentration values. This raises the question of whether this allosteric device is also able to decode patterns of calcium spikes.

CaMKII is a crucial mediator for NMDA receptor-dependent synaptic plasticity (Lisman *et al.*, 2002; Malenka and Nicoll, 1999). CaMKII holoenzyme is a dodecamer structure composed of two rings of hexamers (Rosenberg *et al.*, 2005; Kolodziej *et al.*, 2000). Binding of calmodulin activates the CaMKII monomer (Hanley *et al.*, 1988), and initiates its autophosphorylation on threonine 286 (Thr286). This autophosphorylation requires the catalytic ability from an active neighbour subunit within the hexameric ring (Hanson *et al.*, 1994; Mukherji and Soderling, 1994). Phosphorylated CaMKII remains in a constant active state, independent of calmodulin activity (Payne *et al.*, 1988; Hanson *et al.*, 1994). This autophosphorylation also increases the apparent affinity of calmodulin binding to CaMKII (Meyer *et al.*, 1992). CaMKII autophosphorylation has been shown to be a decoder of calcium spike frequency *in vitro* (De Koninck and Schulman, 1998). Many questions, however, remain open. How does CaMKII respond to calcium inputs in the presence of phosphatases? What is the relative activity of CaMKII and calcineurin regulated during high-frequency calcium oscillations?

Calcineurin exerts its effect on synaptic plasticity in MSN by dephosphorylating DARPP-32 on Thr34 (Hemmings *et al.*, 1984a), relieving inhibition on PP1, thereby dephosphorylating CaMKII on Thr286 (Strack *et al.*, 1997a). The fact that PP1 inhibition blocks the induction of LTD demonstrates the important modulatory roles played by inhibitors of PP1 (Kirkwood and Bear, 1994; Mulkey *et al.*, 1993, 1994). Drugs of abuse cause extracellular dopamine increase, which enhances DARPP-32 phosphorylation on Thr34, and PP1 inhibition. Then, how drugs of abuse affect CaMKII activity?

To answer these questions, detailed quantitative computational models are required, since for example, biochemical experiments are often constrained by the limitations of available chelators able to produce different patterns of calcium spikes (Yang *et al.*, 1999). A few models have already investigated the effect of calcium on postsynaptic plasticity. For instance, based on a spatial model, Franks *et al.* (2001) showed that calmodulin activation depends on the frequencies of calcium spikes, and this response to frequency can be modulated by the availability of calmodulin and calcium binding proteins. Bhalla (2002) demonstrated that signalling pathways can discriminate between eight complex calcium input patterns, and raise distinct activities of kinases and phosphatases. D'Alcantara *et al.* (2003) provided insight into how a calcium increase of high amplitude and short duration could induce AMPA receptor activation; while a low amplitude, long duration signal triggers AMPA receptor inactivation. Naoki *et al.* (2005) studied how different spike frequencies and shapes of calcium can influence calmodulin activation in the area near calcium channels, especially when calmodulin is exchangeable to other local regions within the dendritic spine. Urakubo *et al.* (2008) set up an allosteric model of NMDA receptor and showed that presynaptic glutamate release followed by postsynaptic membrane depolarization induces activation of NMDA receptors and large postsynaptic calcium spikes, resulting in LTP. Pepke *et al.* (2010) revealed that calmodulin with fewer than four bound calcium ions and its sensitivity to calcium spike frequency contribute primarily to CaMKII activation. However, none of these models accurately modelled calmodulin activation in the first place, nor considered CaMKII autophosphorylation in the context of a hexamer. Besides, the correlation between the frequency

of calcium inputs and the total amount of calcium ions has never been systematically studied before.

In the present study, I used an existing model of calmodulin developed by Stefan *et al.* (2008) based on the allosteric framework. The model accurately reproduces the activation of calmodulin by calcium as observed experimentally. I expanded this model to include CaMKII autophosphorylation, using a rate based on the probability of having an active neighbour subunit, at each simulation step. Reactions describing the dephosphorylation of CaMKII by PP1, the inhibition of PP1 by DARPP-32, and the dephosphorylation of DARPP-32 by calcineurin were included in addition (as shown in Fig. 6). A detailed calcium buffering system was embedded, with each calcium spike accurately modelled and in accord with published experimental data (Sabatini *et al.*, 2002). The effects of a wide range of calcium frequencies, amplitudes, and durations were studied. The activation of calcineurin and CaMKII were compared, based on the amplitudes and durations of their activation.

In the following sections, I show that the activation of calmodulin depends on the frequency of calcium inputs. With a total amount of calcium ions kept constant, high frequency pulses stimulate calmodulin more efficiently. Calcium inputs activate both calcineurin and CaMKII at all frequencies, but increased frequencies shift the balance of relative activation from calcineurin to CaMKII. Independent of the input amplitude and duration, the total amount of calcium ions injected adjusts the sensitivity of the system towards calcium-input frequencies. At a given frequency, the quantity of CaMKII activated is proportional to the total amount of calcium. Thus, a small amount of calcium input at high frequency can induce the same activation of CaMKII as observed for larger amounts, at lower frequencies. Finally, the extent of activation of CaMKII at high calcium signal frequency is further controlled by other factors, including by the availability of calmodulin, and the potency of phosphatase inhibitors.
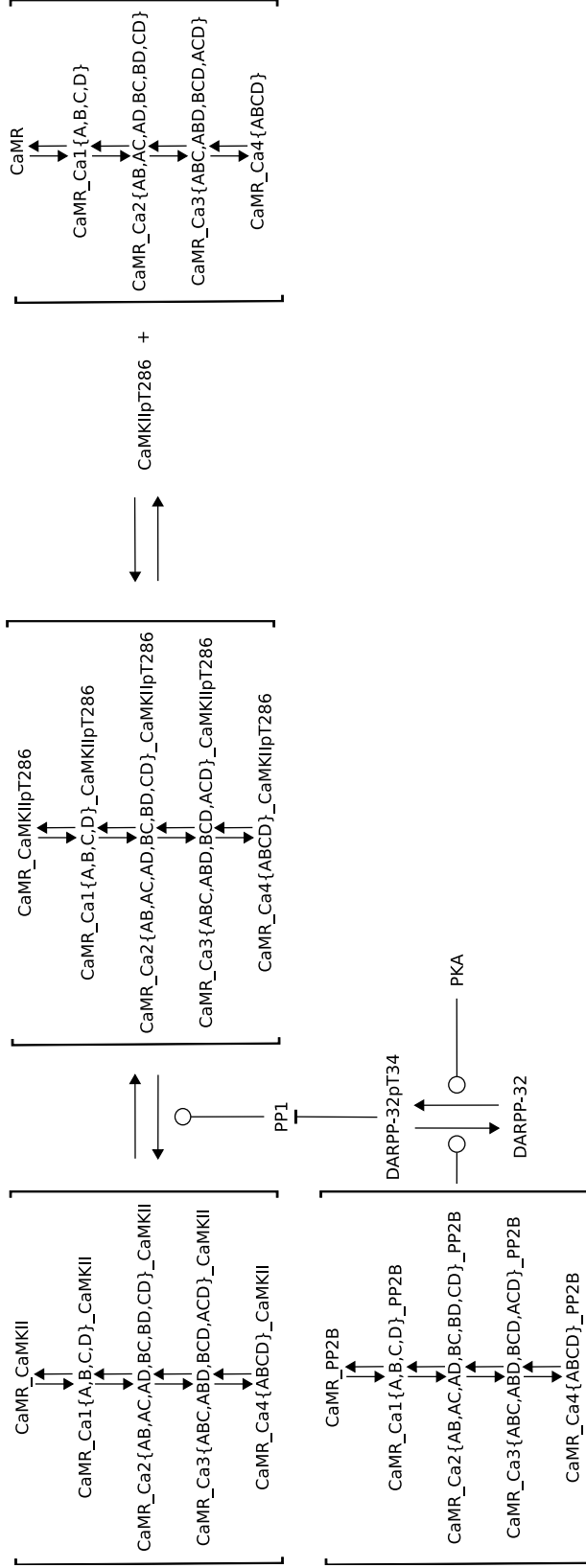
Figure 6: **Reaction diagram of calmodulin regulated pathways.** Graphical representation of the model implemented in this study. Part of this model is based on a published allosteric model of calmodulin function (Stefan *et al.*, 2008). Only the extension is displayed here. Filled arrow: yield, bar arrow: inhibition, circle: catalyse, CaMR: calmodulin in active state, PP2B: calcineurin. CaMKII: calcium/calmodulin-dependent protein kinase II. PP1: protein phosphatase 1. PKA: cyclic AMP-dependent protein kinase. DARPP-32: dopamine- and cAMP-regulated phosphoprotein of 32 kDa.

## 2.2 Modelling methods

### 2.2.1 *Modelling and simulation software*

Models were based on the description of biochemical processes using continuous variables, that were simulated with a deterministic method. Modelling and simulation were performed using the E-cell system, version 3 (Takahashi *et al.*, 2004). E-Cell system is a module based, object-oriented simulation environment suitable for modelling, simulating and analysing of large-scale cell biological models. E-Cell defines the simulation model as a set of objects connected to each other. A biochemical reaction can be built by connecting variable, process, and stepper objects, where a variable represents a molecular species (an entity pool), a process represents the kinetic law that results in changes in the values of several variables, and a stepper attaches a specific simulation algorithm to a set of processes. E-cell supports various stepper functions, and can incorporate different algorithms and time scales into one model via its unique discrete integration meta-algorithm.

A generic ODEStepper, based on the combined Radau 5 and Dormand-Prince 5(4)7M (Dormand and Prince, 1980) algorithms, was used for the elementary reactions. E-Cell switches between these two algorithms depending on the stiffness of the system of equations at a given time point. Simulations were performed on the computing cluster of the European Bioinformatics Institute, which is composed of Intel-based nodes under GNU/Linux. The simulations were launched concurrently with the calcium firing at one frequency running on an individual core.

### 2.2.2 *Reaction and parameters*

My models presented in this thesis were based on a single homogeneous compartment, with a volume of $10^{-15}$ L representing the spine (Nimchinsky *et al.*, 2002). Reactions were modelled with Mass Action Law (MAL) processes. Each enzymatic reaction was represented by each of the three elementary steps for binding (1), dissociation (2), and catalysis (3). Michaelis-Menten kinetics were not used for

enzymatic reactions, since it assumes substrate concentration greatly exceeds the enzyme concentration. Based on this assumption, an enzyme may be characterised as an independent catalyst, and the concentration of an enzyme-substrate complex may always be assumed to be constant (quasi-steady state approximation) (Briggs and Haldane, 1925). However, when the system contains similarly distributed enzymes and substrates, the differences between the macro-level (*e.g.* Michaelis-Menten kinetics) and the micro-level descriptions (*e.g.* reaction rate for elementary steps) should not be neglected (Kholodenko and Westerhoff, 1995). Thus, the elemental step description is always a more precise way to gain an accurate and quantitative understanding of enzyme kinetics.

$$E + S \xrightarrow{k_{on}} ES \qquad (1)$$
$$ES \xrightarrow{k_{off}} E + S \qquad (2)$$
$$ES \xrightarrow{k_{cat}} E + P \qquad (3)$$
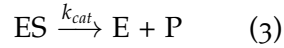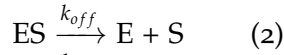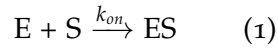
The association ($k_{on}$), dissociation ($k_{off}$), and catalytic ($k_{cat}$) constants were mainly obtained from published kinetic constants, retrieved from the Database Of Quantitative Cellular Signalling (`http://doqcs.ncbs.res.in/`), or estimated.

### 2.2.3 *Pathway activation*

$Ca^{2+}$ inputs were implemented using Python scripts, consisting of repeated increases of the calcium influx constant of a zero-order reaction in the model. The duration for each increase was 8 milliseconds. Throughout most of the study, the number of calcium ions inserted in the system at each input was 43200 molecules (that is the product of influx rate multiplied by duration). To study the effect of input size, the number of calcium ions for each input was increased, by increasing the influx rate. The delay before the next calcium increase varied according to the frequency. However, when the input frequency was too high to have the time interval between two spikes longer than 8 milliseconds, the influx constant and opening duration would be recalculated in order to keep the number of calcium ions in each input constant. For instance, a 50 Hz signal was composed of a train of calcium inputs, each of which lasted 8 milliseconds, and a 12 milliseconds interval between each pair of inputs. However, at 200 Hz, the

delay between each opening was 5 milliseconds. Since this was below the 8 milliseconds threshold, the system considered the opening was 5 milliseconds, and calculated the new influx constant based on this new opening time.

## 2.3 Postsynaptic calcium affects the ratio of calcineurin and CaMKII activation

### 2.3.1 *Model structure*

The activation of calmodulin by calcium was modelled as described previously (Stefan *et al.*, 2008). In the following sections, I first introduce this existing calmodulin model. The extention of this model is explained afterwards.

*Allosteric model of calmodulin by Stefan et al.*

This model describes two states of calmodulin, the active (R) and the inactive (T) state. In either state, calmodulin can bind up to four calcium ions, with calcium affinity being higher for R state than for T state. Each calcium-binding site is considered unique and modelled explicitly, with its own specific dissociation constant. Calmodulin, regardless of the number of calcium ions bound, can undergo transitions between R and T states. The binding of calcium progressively lowers more the free energy of the R state than that of T state. As a consequence, calcium ions cooperatively bind to calmodulin, facilitating the transition from T to R state. Once calmodulin is in the R conformation, it can bind to target proteins, calcineurin and CaMKII in the model, and can activate them (Fig. 7).

The allosteric isomerisation constant L ($L = [T_0]/[R_0]$) and the ratio of R and T affinity for each site ($c_i = K_i^R/K_i^T$) are estimated by assuming all four $c_i$ values are identical and all four binding sites are equivalent. Then, the experimental data of calcium-binding in the presence and absence of an allosteric activator for mutant and wild-type forms of calmodulin (Peersen *et al.*, 1997), is fitted in the equation describing the fractional occupation correspondingly (Rubin and Changeux, 1966) to obtain L and c values. Then the microscopic dissociation constants for R state ($K_i^R$) are estimated by fitting experimen-

tal data of calmodulin binding to calcium under different experimental conditions (Bayley *et al.*, 1996; Shifman *et al.*, 2006; Peersen *et al.*, 1997), into a generalised equation for fraction occupation of calmodulin with non-equivalent calcium-binding sites (Monod *et al.*, 1965).
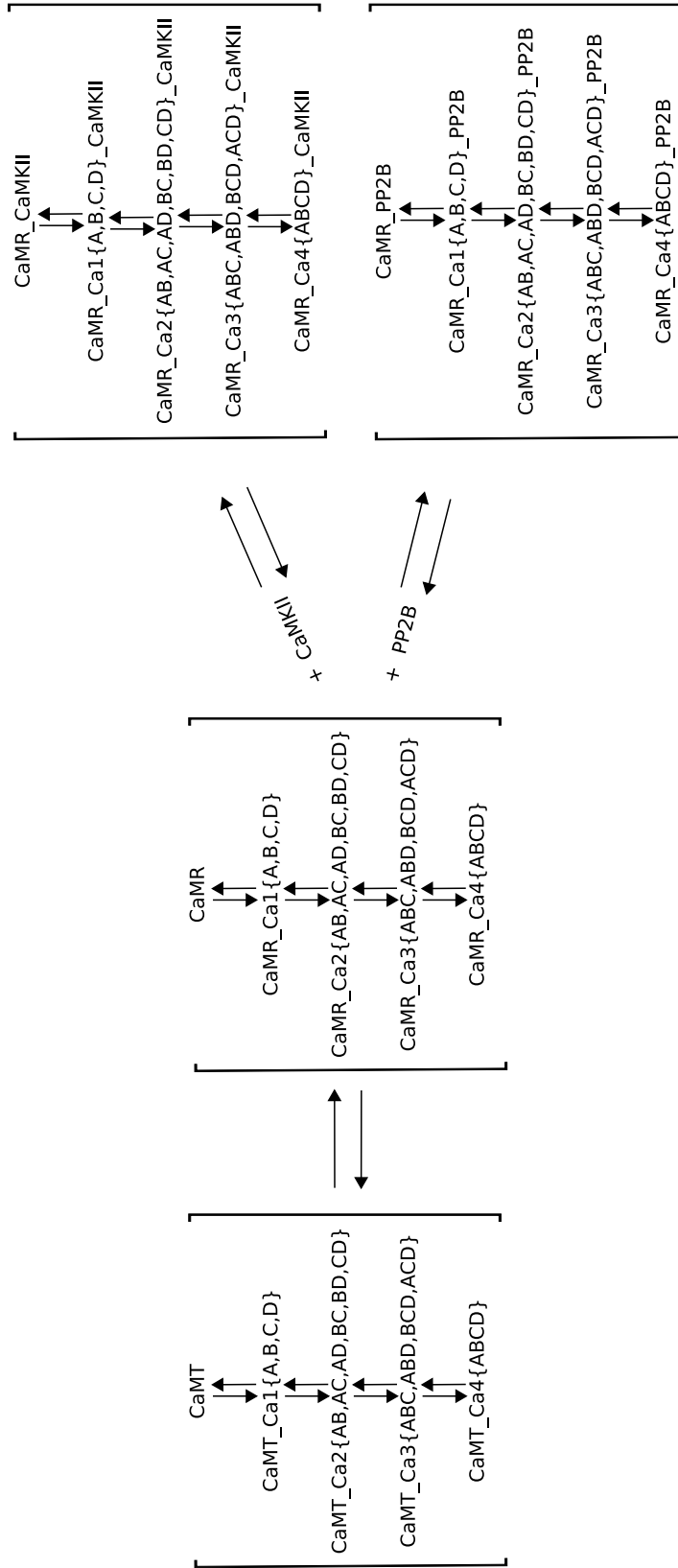
Figure 7: **Allosteric model of calmodulin by Stefan *et al.*.** Graphical representation of the published allosteric model of calmodulin (Stefan *et al.*, 2008). The four binding sites of calmodulin are designated as A,B,C, and D. Filled arrow: yield, CaMT: calmodulin in inactive state, CaMR: calmodulin in active state, PP2B: calcineurin. CaMKII: calcium/calmodulin-dependent protein kinase II

*Extention of the model of calmodulin*

The model described above was extended by including a detailed description of the processes controlling CaMKII autophosphorylation. Only monomers of CaMKII were considered and the autophosphorylation was modelled in a first order reaction upon calmodulin binding. In order to accurately model the autophosphorylation on Thr286 within the context of the hexamer and take into account the fact that this is a trans-phosphorylation between adjacent subunits (Hanson *et al.*, 1994), I computed a correction of the rate based on the probability that monomers have active neighbours. I proceeded in two steps. On the one hand, for each number of active monomers per hexamer, I computed the probability for a given subunit of having an active neighbour. On the other hand, I set up a random simulator to calculate the distributions of active CaMKII subunits within hexamers as a function of the total amount of active subunits (`http://www.ebi.ac.uk/~luli/thesis/calcium/`). For a given quantity of active CaMKII monomers, I randomly picked the location of active monomers within the hexamers, and recorded the number of hexamers containing a specific number of active subunits. After 1000 repeats of this random simulation, the average fraction of each number of active monomers per hexamer was multiplied by its corresponding probability of having an active neighbour computed in the first step. The sum of these six numbers was then used as a coefficient to adjust the autophosphorylation rate. The whole procedure was repeated for every 1% increase of active monomers. Finally, these 100 generated values were fitted by a polynomial function of degree 5. This polynomial function was embedded in the model for E-Cell, dynamically changing the autophosphorylation rate (the detailed procedure for this calculation is illustrated in Fig. 8, the fitted polynomial function is plotted in Fig. 9). Once CaMKII was phosphorylated, its affinity for calmodulin increased in the model, according to Meyer *et al.* (1992).
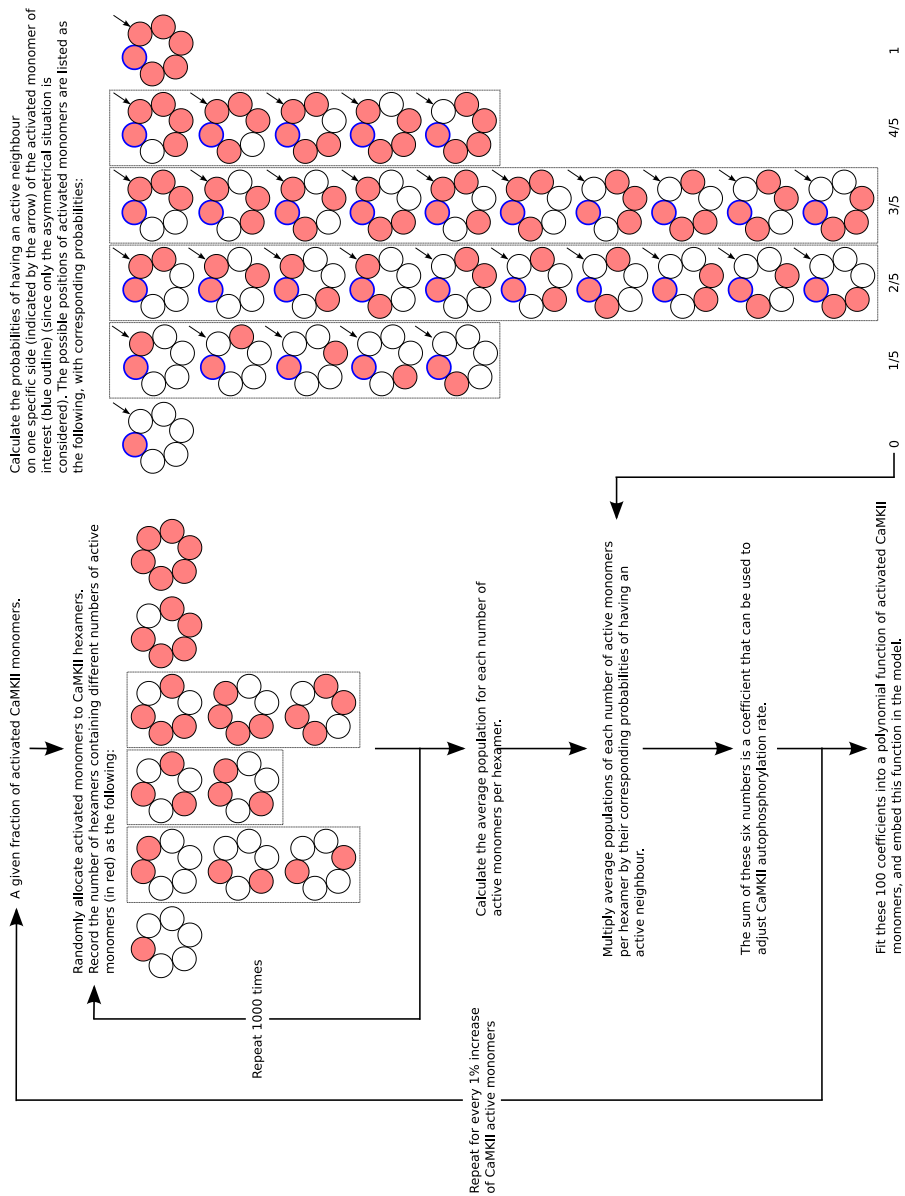
Figure 8: **Calculation the rate of CaMKII autophosphorylation** . This figure shows the procedure for calculating the correction of the autophosphorylation rate as a function of active CaMKII monomers.
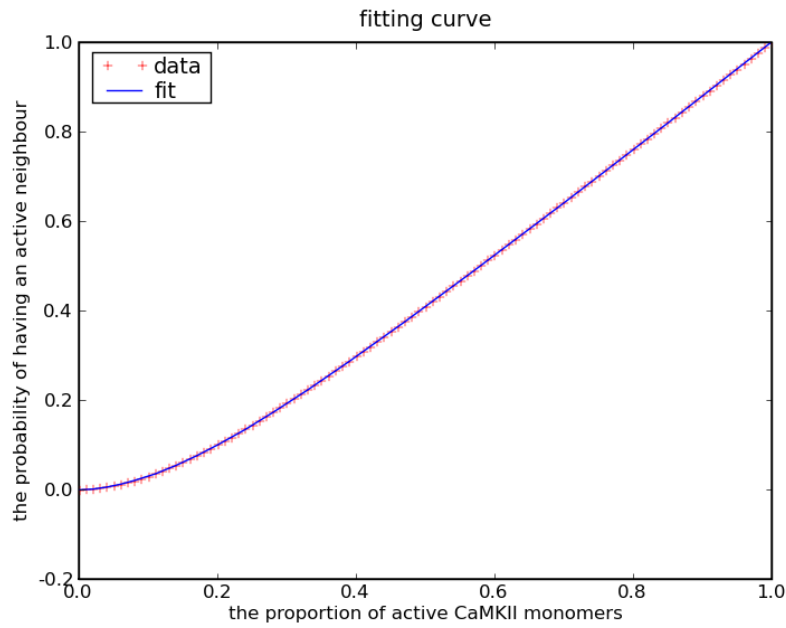
Figure 9: **The fitted polynomial function for the rate of CaMKII autophosphorylation**. The polynomial function was fitted by 100 corrections of the rate of CaMKII autophosphorylation. The 100 corrections were calculated in terms of the distribution of activated CaMKII monomer and the probability of having an active neighbour.

The catalytic subunit of calcineurin (calcineurin A or CNA) is activated upon association with $Ca^{2+}$/calmodulin (Klee *et al.*, 1998). Calcineurin has a relatively higher affinity for calmodulin binding than other calmodulin-binding proteins (Quintana *et al.*, 2005; Perrino *et al.*, 2002) and, in particular, CaMKII, which facilitates its sensitive response to calcium-mediated synaptic stimulation (Groth *et al.*, 2003). Activated calcineurin dephosphorylates DARPP-32 on Thr34 (Hemmings *et al.*, 1984a).

PP1 is a major eukaryotic protein serine/threonine phosphatase that regulates diverse cellular processes, including the dephosphorylation of CaMKII and the induction of LTD (Mulkey *et al.*, 1994). The catalytic subunit of PP1 is inhibited by DARPP-32 upon its phosphorylation on Thr34 by PKA (Hemmings *et al.*, 1984a; Svenningsson *et al.*, 2004). In this model, approximately 40% of DARPP-32 was activated by the basal level of PKA. The phosphorylated DARPP-32, in turn, inhibited almost 90% of the total PP1. The inhibition was

modelled following a competitive inhibition mechanism. Only phosphorylation on Thr34 of DARPP-32 was considered in this model.

The calcium efflux was modelled assuming a single clearance process, using Michaelis-Menten kinetics. The calcium influx was modelled through a zero-order reaction with a fixed rate. The vast number of calcium buffer proteins, with different dissociation constants were adopted in order to provide an efficient calcium reservoir (Naoki *et al.*, 2005).

All the quantitative parameters used in this model are listed in Table 1, and abbreviations are explained in Table 2. This model and the Python script used for simulation in E-Cell are available online (`http://www.ebi.ac.uk/~luli/thesis/calcium/`).

Table 1: List of parameters used for simulation of the short-term synaptic plasticity model.

| Parameter | Value | Reference |
|---|---|---|
| *Ca*$^{2+}$ binding calmodulin (CaM): | | |
| $k_{on}$ | $10^6\,M^{-1}s^{-1}$ | (Stefan *et al.*, 2008)*,[1] |
| $k_{off_A}^R$ | $8.32\,s^{-1}$ | (Stefan *et al.*, 2008)*,[1] |
| $k_{off_B}^R$ | $1.66 \times 10^{-2}\,s^{-1}$ | (Stefan *et al.*, 2008)*,[1] |
| $k_{off_C}^R$ | $17.4\,s^{-1}$ | (Stefan *et al.*, 2008)*,[1] |
| $k_{off_D}^R$ | $1.45 \times 10^{-2}\,s^{-1}$ | (Stefan *et al.*, 2008)*,[1] |
| $k_{off_A}^T$ | $2.10 \times 10^3\,s^{-1}$ | (Stefan *et al.*, 2008)*,[1] |
| $k_{off_B}^T$ | $4.19\,s^{-1}$ | (Stefan *et al.*, 2008)*,[1] |
| $k_{off_C}^T$ | $4.39 \times 10^3\,s^{-1}$ | (Stefan *et al.*, 2008)*,[1] |
| $k_{off_D}^T$ | $3.66\,s^{-1}$ | (Stefan *et al.*, 2008)*,[1] |
| $k_{RT}^{CaM}$ | $1 \times 10^6\,s^{-1}$ | (Stefan *et al.*, 2008)*,[1] |
| $k_{TR}^{CaM}$ | $48.38\,s^{-1}$ | (Stefan *et al.*, 2008)*,[1] |
| $k_{RT}^{CaMCa}$ | $6.2829 \times 10^4\,s^{-1}$ | (Stefan *et al.*, 2008)*,[1] |
| $k_{TR}^{CaMCa}$ | $768.81\,s^{-1}$ | (Stefan *et al.*, 2008)*,[1] |
| $k_{RT}^{CaM2Ca}$ | $3.96 \times 10^3\,s^{-1}$ | (Stefan *et al.*, 2008)*,[1] |
| $k_{TR}^{CaM2Ca}$ | $1.2217 \times 10^4\,s^{-1}$ | (Stefan *et al.*, 2008)*,[1] |
| $k_{RT}^{CaM3Ca}$ | $249.2\,s^{-1}$ | (Stefan *et al.*, 2008)*,[1] |

Table 1: continued

| | | |
|---|---|---|
| $k_{TR}^{CaM3Ca}$ | $1.94144 \times 10^5\,s^{-1}$ | (Stefan *et al.*, 2008)*,[1] |
| $k_{RT}^{CaM4Ca}$ | $15.6816\,s^{-1}$ | (Stefan *et al.*, 2008)*,[1] |
| $k_{TR}^{CaM4Ca}$ | $3.085144 \times 10^6\,s^{-1}$ | (Stefan *et al.*, 2008)*,[1] |

$Ca^{2+}$ binding calcium buffer protein (CBP):

| | | |
|---|---|---|
| $k_{on_{CBP_{fast}}}$ | $10^9\,M^{-1}s^{-1}$ | (Markram *et al.*, 1998)*,[2] |
| $k_{off_{CBP_{fast}}}$ | $10^3\,s^{-1}$ | (Markram *et al.*, 1998)*,[2] |
| $k_{on_{CBP_{medium}}}$ | $10^8\,M^{-1}s^{-1}$ | (Markram *et al.*, 1998)*,[2] |
| $k_{off_{CBP_{medium}}}$ | $10^2\,s^{-1}$ | (Markram *et al.*, 1998)*,[2] |
| $k_{on_{CBP_{slow}}}$ | $10^7\,M^{-1}s^{-1}$ | (Markram *et al.*, 1998)*,[2] |
| $k_{off_{CBP_{slow}}}$ | $10\,s^{-1}$ | (Markram *et al.*, 1998)*,[2] |
| $k_{on_{CBP_{vslow}}}$ | $10^6\,M^{-1}s^{-1}$ | (Markram *et al.*, 1998)*,[2] |
| $k_{off_{CBP_{vslow}}}$ | $1\,s^{-1}$ | (Markram *et al.*, 1998)*,[2] |

$Ca^{2+}$ pump:

| | | |
|---|---|---|
| $v_{max}$ | $4 \times 10^{-3}\,Ms^{-1}$ | (cf. Markram *et al.*, 1998)*,[3] |
| $K_m$ | $1 \times 10^{-6}\,M$ | (Markram *et al.*, 1998)* |

$Ca^{2+}$ leak:

| | | |
|---|---|---|
| $k$ | $4 \times 10^{-5}\,Ms^{-1}$ | (cf. Markram *et al.*, 1998)*,[3] |

$CaM^R$ binding substrates:

| | | |
|---|---|---|
| $k_{on_{CaMKII}}$ | $3.2 \times 10^6\,M^{-1}s^{-1}$ | (Tzortzopoulos and Török, 2004)[4] |
| $k_{off_{CaMKII}}$ | $0.343\,s^{-1}$ | (Tzortzopoulos and Török, 2004)[4] |
| $k_{on_{CaMKIIp}}$ | $3.2 \times 10^6\,M^{-1}s^{-1}$ | (Tzortzopoulos and Török, 2004)[4] |
| $k_{off_{CaMKIIp}}$ | $0.001\,s^{-1}$ | (Meyer *et al.*, 1992)[5] |
| $k_{on_{PP2B}}$ | $4.6 \times 10^7\,M^{-1}s^{-1}$ | (Quintana *et al.*, 2005)[6] |
| $k_{off_{PP2B}}$ | $0.4\,s^{-1}$ | (Perrino *et al.*, 2002)[7] |

*CaMKII* autophosphorylation on *Thr*286:

Table 1: continued

| | | |
|---|---|---|
| $k_{Thr286p}$ | $6.3\,s^{-1}$ | (Lučić *et al.*, 2008)[8].This parameter is further refined during simulation run. |

*PKA* phosphorylates DARPP-32 on *Thr*34:

| | | |
|---|---|---|
| $k_{on_{D\_PKA}}$ | $5.6 \times 10^6\,M^{-1}s^{-1}$ | (Hemmings *et al.*, 1984b)[9] |
| $k_{off_{D\_PKA}}$ | $10.8\,s^{-1}$ | (Hemmings *et al.*, 1984b)[9] |
| $k_{cat_{D\_PKA}}$ | $2.7\,s^{-1}$ | (Hemmings *et al.*, 1984b)[9] |

Calcineurin (*PP2B*) dephosphorylates DARPP-32 on *Thr*34:

| | | |
|---|---|---|
| $k_{on_{Dp\_PP2B}}$ | $4.1 \times 10^6\,M^{-1}s^{-1}$ | (King *et al.*, 1984)[10] |
| $k_{off_{Dp\_PP2B}}$ | $6.4\,s^{-1}$ | (King *et al.*, 1984)[10] |
| $k_{cat_{Dp\_PP2B}}$ | $0.2\,s^{-1}$ | (King *et al.*, 1984)[10] |

DARPP-32$_{Thr34p}$ binding *PP1*:

| | | |
|---|---|---|
| $k_{on_{Dp\_PP1}}$ | $4.0 \times 10^6\,M^{-1}s^{-1}$ | (Desdouits *et al.*, 1995a)[11] |
| $k_{off_{Dp\_PP1}}$ | $0.4\,s^{-1}$ | (Desdouits *et al.*, 1995a)[11] |

*PP*1 dephosphorylates *CaMKII*:

| | | |
|---|---|---|
| $k_{on_{CaMKIIp\_PP1}}$ | $3.0 \times 10^6\,M^{-1}s^{-1}$ | this study*,[12] |
| $k_{off_{CaMKIIp\_PP1}}$ | $0.5\,s^{-1}$ | this study*,[12] |
| $k_{cat_{CaMIIp\_PP1}}$ | $2.0\,s^{-1}$ | (Zhabotinsky, 2000)* |

Concentrations:

| | | |
|---|---|---|
| $[CaM^T]_0$ | $3 \times 10^{-5}\,M$ | (Kakiuchi *et al.*, 1982)[13] |
| $[Ca^{2+}]_{basal}$ | $1 \times 10^{-8}\,M$ | (Allbritton *et al.*, 1992)[14] |
| $[PP2B]$ | $1.6 \times 10^{-6}\,M$ | (cf. Goto *et al.*, 1986)[15] |
| $[CaMKII]$ | $7 \times 10^{-5}\,M$ | (cf. Petersen *et al.*, 2003)[16] |
| $[DARPP-32]$ | $3 \times 10^{-6}\,M$ | (estimated from Halpain *et al.*, 1990)[17] |
| $[PKA]$ | $1.2 \times 10^{-8}\,M$ | (estimated from Bacskai *et al.*, 1993)[18] |
| $[PP1]$ | $2 \times 10^{-6}\,M$ | (cf. Ingebritsen *et al.*, 1983)[19] |
| $[CBP_{fast}]$ | $8 \times 10^{-5}\,M$ | (Naoki *et al.*, 2005)* |
| $[CBP_{medium}]$ | $8 \times 10^{-5}\,M$ | (Naoki *et al.*, 2005)* |

Table 1: continued

| | | |
|---|---|---|
| $[CBP_{slow}]$ | $2 \times 10^{-5}\,M$ | (Naoki *et al.*, 2005)* |
| $[CBP_{vslow}]$ | $2 \times 10^{-5}\,M$ | (Naoki *et al.*, 2005)* |
| Compartment: | | |
| spine volume | $10^{-15}\,l$ | (Nimchinsky *et al.*, 2002)[20] |

Table 1: List of parameters used for simulation of the short-term synaptic plasticity model. Asterisk indicates that this reference refers to a computational model. [1]: Stefan *et al.* (2008) did parameter searching according to experimental data from Bayley *et al.* (1996); Peersen *et al.* (1997); Shifman *et al.* (2006) (details see section 2.3.1). [2]: Markram *et al.* (1998) estimated these parameters according to Falke *et al.* (1994). [3]: Parameters were estimated according to Markram *et al.* (1998), and adjusted to maintain the resting calcium level at 10 nM. [4,5,6,7,8,9,10,11]: Parameters were obtained from *in vitro* experiments. [12]: The affinity between CaMKII and PP1 was estimated to be identical as that between DARPP-32 and PP1. [13]: Measurement was obtained from cerebral cortex tissue extract from rat. [14]: Data obtained from cytosolic extract from Xenopus laevis oocytes. [15]: Measurement was obtained from dorsal striatum tissue extract from rat. [16]: Measurement was obtained from immunogold labelling on isolated PSD extract from rats forbrain. [17]: Measurement was obtained from immunoblotting of striatal slices of rats. [18]: The concentration of catalytic subunit of PKA was estimated according to basal cAMP concentration in sensory neurons of marine snail *Aplysia*, measured by Bacskai *et al.* (1993). [19]: Experimental measurement was obtained from rabbit brain extract. [20]: Measurement was obtained from apical spine of CA1 pyramidal neuron.

Table 2: List of abbreviations used in the short-term synaptic plasticity model.

| Abbreviations | Definition/Reference |
|---|---|
| CaM | calmodulin |
| | UniProt:P62158 |
| PP2B | calcineurin/protein phosphatase 2B |
| | GO:0005955 |
| CaMKII | calcium/calmodulin-dependent protein kinase II |
| | GO:0005954 |
| DARPP-32 | dopamine- and cAMP-regulated phosphoprotein of 32 kDa |

|      | Table 2: continued |
|------|--------------------|
|      | UniProt:Q9UD71     |
| PKA  | cyclic AMP-dependent protein kinase |
|      | GO:0005952         |
| PP1  | protein phosphatase 1 |
|      | GO:0000164         |
| CBP  | calcium binding protein |

Table 2: List of abbreviations used in the short-term synaptic plasticity model.

### 2.3.2 *Calcium spikes and simulation design*

Calcium signals in the spine are crucial for synaptic plasticity. Their transient changes are shaped by many factors including the calcium sources, calcium extrusion mechanisms, and the distribution of calcium buffer proteins. In this study, I focused on the calcium spikes induced by synaptic stimulation. Using the model described in the methods section, I showed that a single calcium input of 43200 molecules induced free intracellular calcium transient to reach the peak level, 1 micromolar (corresponding to 602 molecules), within 10 milliseconds, and decayed to basal level within 220 milliseconds (Fig. 10), which is in agreement with the amplitude and time course of NMDA receptor mediated calcium transient in an individual spine in partial depolarised conditions (Sabatini *et al.*, 2002). This single input was repeated to induce a train of calcium spikes, with varied intervals, to form signals with different frequencies.

First, I modulated the calcium signal purely on frequency, by applying the same number of inputs, with the same input size. This generated a prolonged low-frequency stimulation, while a higher-frequency stimulus was relatively short-lived. In total, 34 different frequencies of calcium inputs, ranging from 0.1 Hz to 200 Hz, were studied in these simulations. For each frequency, 100 calcium inputs were applied after the system reached steady state (800 seconds after initiation, labelled as 0 second in the following figures). Therefore,
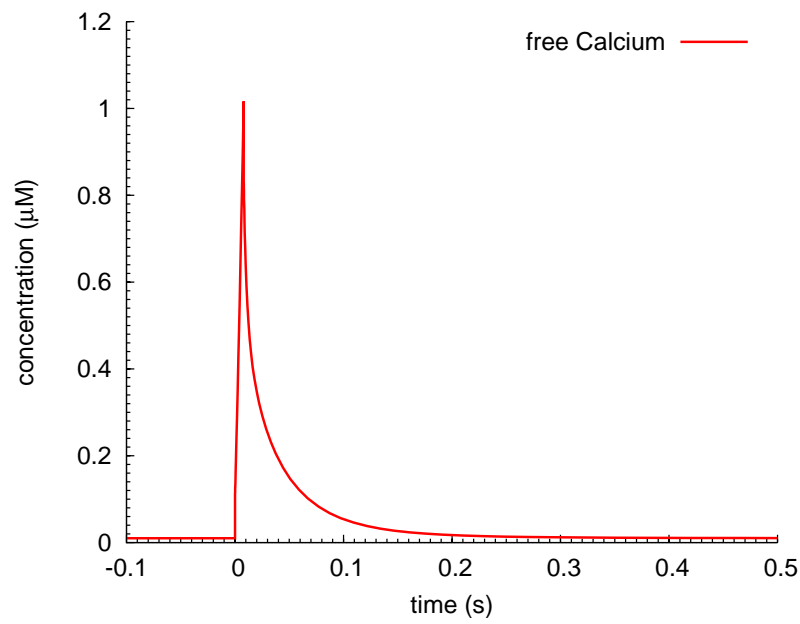
Figure 10: **Intracellular free calcium concentration increase induced by a single calcium input**. Increase of postsynaptic free calcium concentration triggered by a single calcium input. With a single input (43200 molecules), intracellular free calcium reaches maximal level, 1 micromolar (corresponding to 602 molecules), within 10 milliseconds, and decays back to basal level within 200 milliseconds.

while the simulations used different frequencies, equivalent amounts of calcium ions were used.

A train of inputs at 1 Hz did not change the peak level of intracellular free calcium (Fig. 11), when compared with a single input (Fig. 10). In contrast, a succession of inputs at 10 Hz and 25 Hz gradually raised not only the peak free intracellular calcium level but also the basal value (Fig. 11).
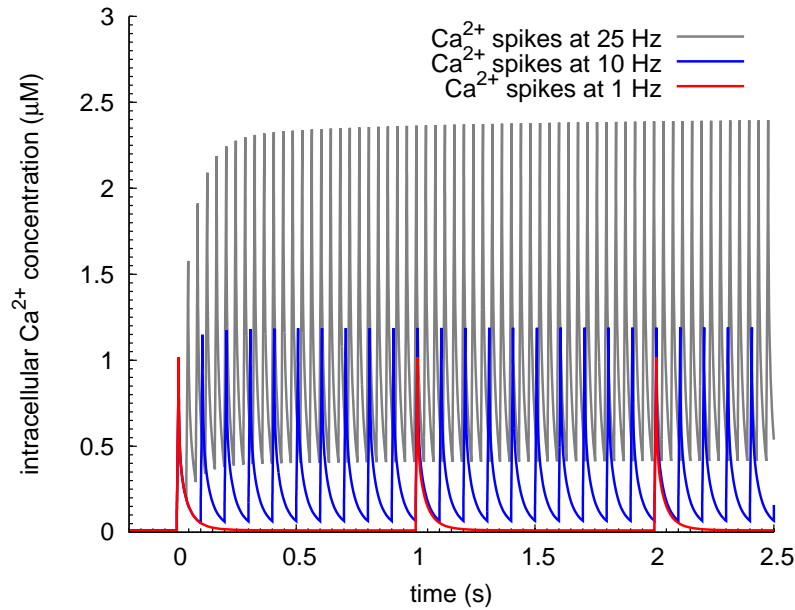


Figure 11: **Intracellular free calcium concentration increase induced by a train of calcium inputs**. Increase of postsynaptic free calcium concentration triggered by a train of inputs at 1 Hz (red line), 10 Hz (blue line), and 25 Hz (grey line). As the frequency of calcium inputs increases, the free calcium concentration rises both in its basal level and its maximal value.

Finally, the total number of calcium ions entering the spine was alternated in two ways. Firstly, the number of inputs was varied from 1 to 180, while the input size remained the same. Secondly, the input size was changed while the spike number was kept identical.

### 2.3.3 *Parameter definition: the activated area*

The activation of calcineurin and CaMKII by calmodulin displays distinct temporal characteristics. I integrated the concentration over time

of activated calcineurin and CaMKII, and calculated the area above the basal level of activity. This is defined as the 'activated area' (Fig. 12). This area represents both the duration and the amplitude of a stimulated enzyme and, since the catalytic activity is a constant, this effectively reflects the amount of substrate which will be affected (Le Novère *et al.*, 2008). The ratio between the activated area of calcineurin and that of CaMKII was computed as a parameter to judge the preferential activation on calcineurin and CaMKII, after calcium stimulation at that specific frequency.
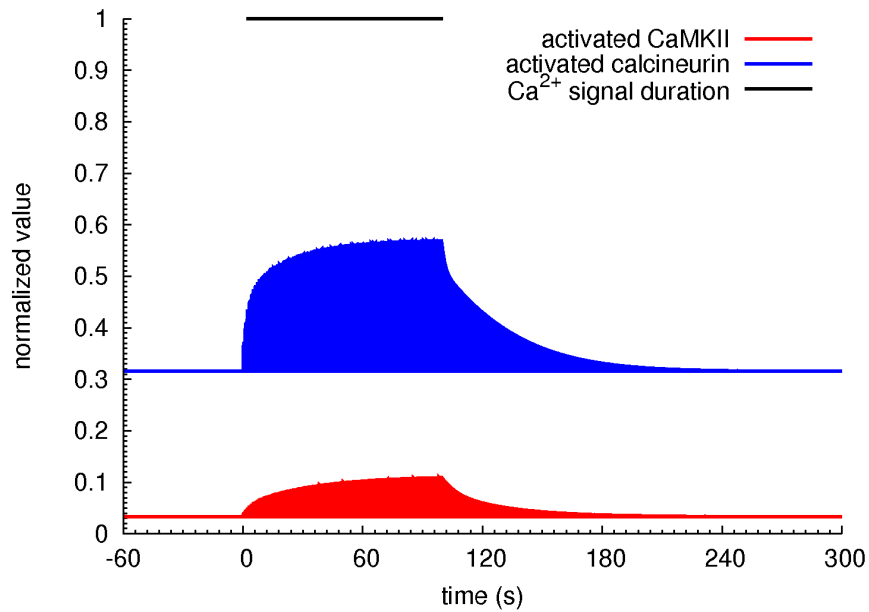


Figure 12: **The definition of 'activated area'.** The activated areas are highlighted. The time courses represent active calcineurin and CaMKII upon stimulation by a train of calcium spikes at 1 Hz. In this case, the activated area for calcineurin is 28.36, while that for CaMKII is 7.55.

### 2.3.4 *Frequency-regulated activation of calmodulin*

The frequency of calcium inputs plays a crucial role in the activation of calmodulin. The time course of calmodulin activation changed as a function of equal amplitude calcium inputs, but applied at varying frequencies (Fig. 13). In basal conditions, less than 10% of the total calmodulin was activated, and calcium inputs at low frequencies in-

duced no significant change in the activation of calmodulin. However, as the frequency increased, more calmodulin became active and the activation period was prolonged. At 50 Hz, almost 100% of the total calmodulin was in the active state, and more than half of the total calmodulin remained active for longer than 1 min. As a result, higher frequencies had no further effect. Therefore, the frequency of calcium inputs determined and stabilised the active state of calmodulin. At frequencies below 50 Hz, calmodulin was able to decode the calcium input frequency, and translated this information into the amount of active calmodulin, which was then transmitted to its targets.
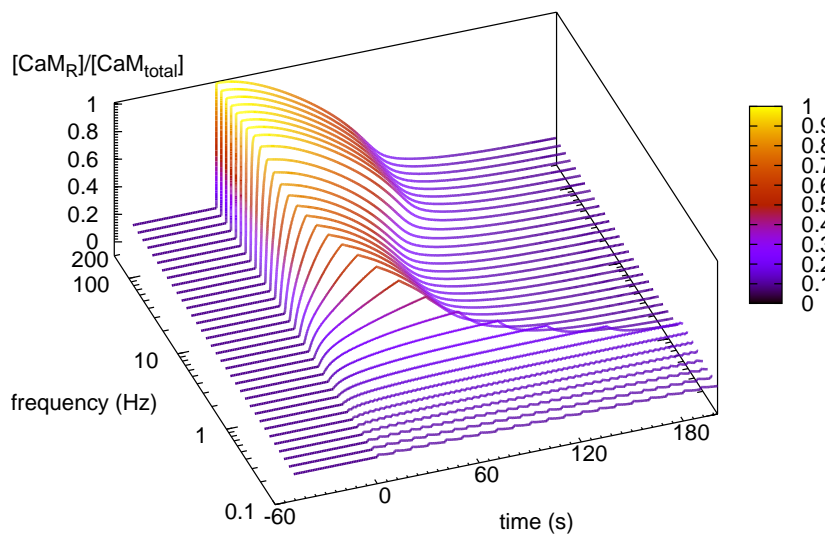


Figure 13: **Effects of calcium input frequencies on activation of calmodulin**. Dependence of calmodulin activation on calcium input frequencies. Each curve represents a time course of normalised active calmodulin, stimulated by a train of calcium inputs at a specific frequency. Although the frequency differs between curves, the number of calcium inputs and the input size remain the same (100 inputs, 43200 molecules for each input).

### 2.3.5   *Frequency-regulated calmodulin binding*

The frequency of calcium spikes defined the ratio of calmodulin bound to calcineurin versus that bound to CaMKII. As the frequency in-

creased, more calmodulin bound to CaMKII rather than to calcineurin, and for increasing periods (Fig. 14).
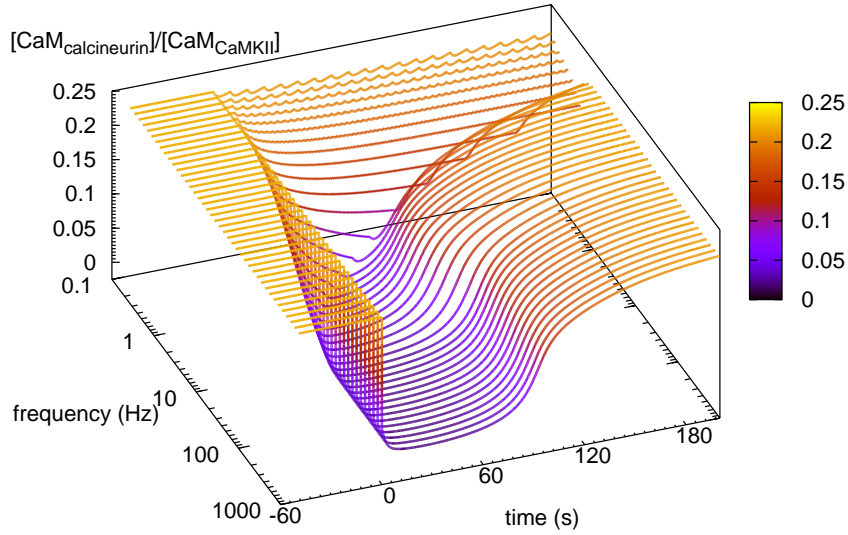


Figure 14: **The ratio of calmodulin bound to calcineurin versus that bound to CaMKII**. Each curve represents a time course of the ratio between calmodulin bound to calcineurin and that bound to CaMKII, for a train of calcium inputs at a specific frequency. For each frequency, the stimulus is composed of the same number of inputs with the same input size (100 inputs, 43200 molecules for each input).

As indicated above, calcium inputs at high frequencies steadily increased the activity of calmodulin. Because of the higher affinity of calmodulin for calcineurin compared to CaMKII, one could argue that calmodulin first binds to all the calcineurin molecules, then the additional calmodulin activates CaMKII. However, this was not the case because at the lowest ratio (about 0.02), approximately 34% of the total calcineurin was bound by calmodulin, which was far from being saturated. At the peak of calmodulin activation, about 39% of the total CaMKII was bound by calmodulin. Since the respective concentrations of CaMKII and calmodulin are 70 μM and 30 μM, this indicates the almost all the calmodulin molecules bound to CaMKII.

2.3.6  *Frequency-modulated activation of calcineurin and CaMKII*

The relative activation of calcineurin and CaMKII dictate the direction of synaptic plasticity, since their activation can induce opposing consequences on the synaptic strength. Fig. 15 and Fig. 16 show the time courses of calcineurin, CaMKII and PP1 in response to calcium inputs at two specific frequencies: 1 Hz and 50 Hz. In basal conditions, approximately 32% of the total calcineurin was active, and about 3% of the total CaMKII subunits were stimulated. This was due to the fact that less than 10% of the total calmodulin was active, and it tightly bound to calcineurin. Comparing to 1 Hz calcium stimulation, calcium input at 50 Hz triggered more significant activation of CaMKII, despite the pronounced activation of PP1 by calcineurin. At a 50 Hz frequency of calcium stimulation, calcineurin initially displayed a sharp activation, then plunged down to basal levels, prior to a second increase. This indicates that CaMKII competes with calcineurin for active calmodulin. However, high frequency calcium inputs did not prevent the activation of calcineurin. Instead, it shifted the balance from active calcineurin to active CaMKII. Thus, the information carried by calcium frequency was translated into the relative amplitude and duration of activation between these two proteins. As shown in Fig. 17, the ratio of active calcineurin versus CaMKII decreased when the frequency increased, indicating more CaMKII was active compared to calcineurin.

The information presented above is summarised in Fig. 18 (red line), which represents the ratio of calcineurin to CaMKII activated area (the calculation of 'activated area' is explained in section 2.3.3), in response to calcium inputs at 34 different frequencies. This suggests a frequency-dependent response. When calcium inputs were infrequent (e.g. 0.1 Hz), calcineurin activity was higher than that of CaMKII. However, an increase in frequency favoured a higher relative increase in CaMKII. In the 0.3-2.5 Hz input frequency range, there was a sharp drop in the ratio of stimulated calcineurin to CaMKII, indicating increased CaMKII activation. This shift of activity slowed down when the frequency further increased, and stabilised at 50 Hz, where the CaMKII activated area was more than twice that of calcineurin. Therefore, it was the frequency of calcium inputs that de-
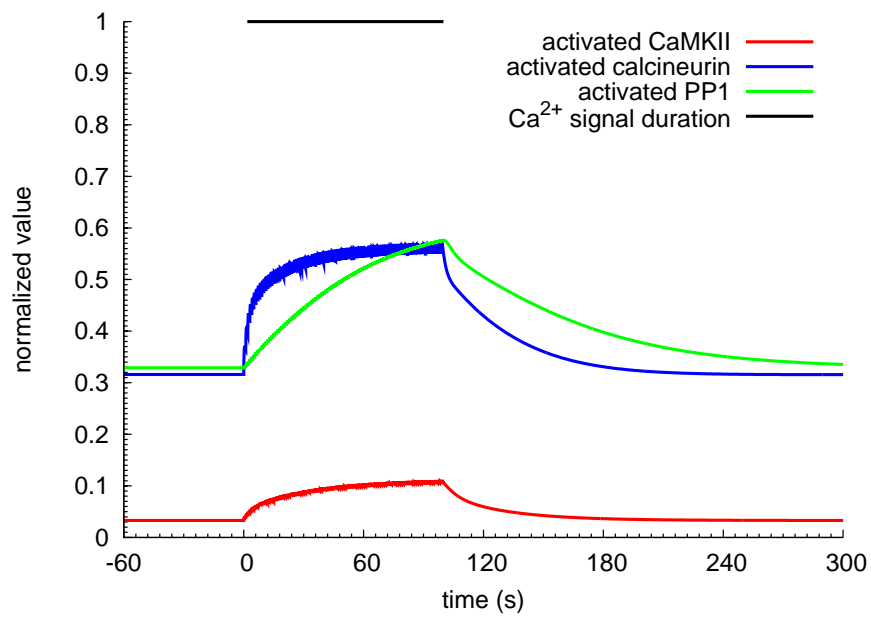
Figure 15: **Effects of a low-frequency calcium signal on activation of calcineurin and CaMKII**. Time courses of normalised activated CaMKII, calcineurin, and PP1 in response to a 100-input calcium stimulation at 1 Hz.
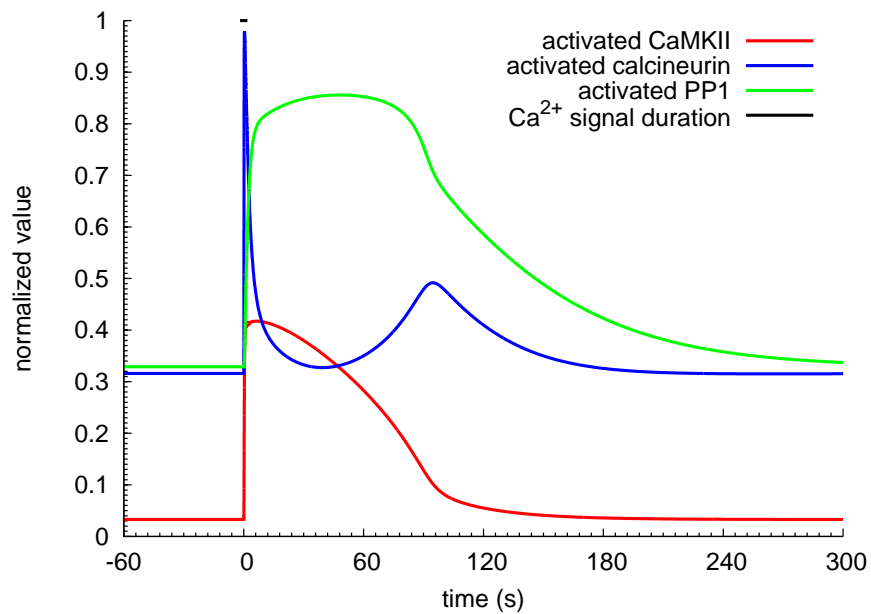


Figure 16: **Effects of a high-frequency calcium signal on activation of calcineurin and CaMKII**. Time courses of normalised activated CaMKII, calcineurin, and PP1 in response to a 100-input calcium stimulation at 50 Hz.
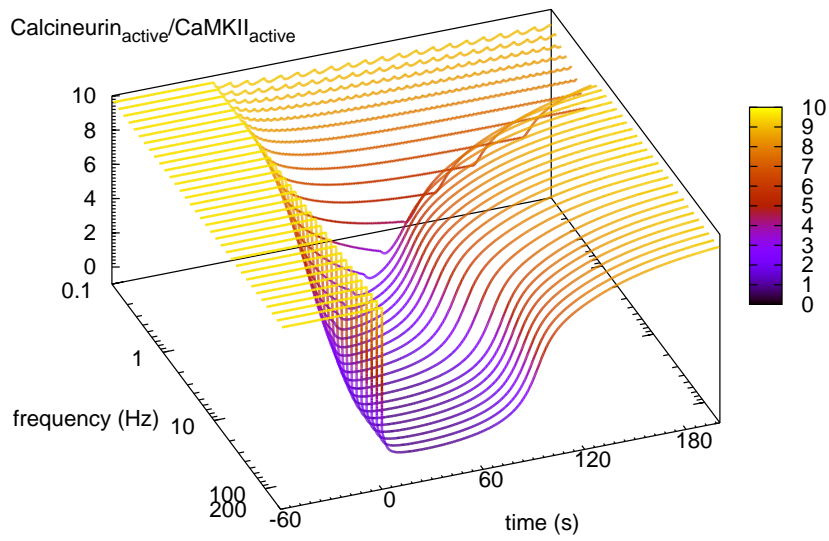
Figure 17: **Comparison of calcineurin and CaMKII activation induced by calcium inputs at different frequencies**. Dependence of the respective activation of calcineurin versus CaMKII on the frequency of calcium inputs. Each curve represents a time course of the ratio of activated calcineurin versus CaMKII, for a train of calcium inputs at a specific frequency. For each frequency, the stimulus is composed of the same number of inputs with the same input size (100 inputs, 43200 molecules for each input).

termined the relative activation of calcineurin and CaMKII, with high calcium input frequency favouring CaMKII activation.

### 2.3.7 *CaMKII autophosphorylation, a calcium input frequency decoder*

As presented above, CaMKII was significantly stimulated when the frequency of calcium inputs increased above a threshold. It has been shown that CaMKII autophosphorylation on Thr286 results in a bistability of the enzyme activity (Zhabotinsky, 2000). Moreover, Thr286 phosphorylation is one mechanism by which CaMKII decodes calcium spike frequency *in vitro* (De Koninck and Schulman, 1998). The CaMKII autophosphorylation is indeed a frequency detector (Fig. 18). When the phosphorylation was prevented in the model (*in silico* mutation by setting the autophosphorylation rate as zero), the activation of CaMKII at high frequencies became less pronounced than in the wild type, and it hardly overcame the activation of calcineurin. In addition, the differences in response between the mutated and wild-type CaMKII become wider with increasing frequency of calcium spikes. In addition, when the frequency of calcium inputs became higher, the divergence of responses between the mutated and wild-type CaMKII became wider, which shows that the autophosphorylation of CaMKII influences mostly its response to calcium inputs at higher frequencies. This can also be interpreted as CaMKII autophosphorylation being mainly triggered at higher frequencies of calcium inputs.

The autophosphorylation of a CaMKII subunit on Thr286 requires that both this subunit and one adjacent neighbour are simultaneously active (Reviewed in Rosenberg *et al.*, 2005). This requirement is the foundation of frequency-dependent autophosphorylation, since it establishes a threshold for activated calmodulin, beyond which CaMKII can be highly activated. Assuming there are only a few active calmodulin molecules able to bind CaMKII subunits, the low probability of two calmodulin molecules binding two adjacent subunits means very few subunits could be phosphorylated. Moreover, the phosphatase, which possesses a higher affinity for calmodulin, prevents the build up of this phosphorylation.

The autophosphorylation of CaMKII also causes calmodulin trapping. Autophosphorylation on Thr286 markedly increases the affin-
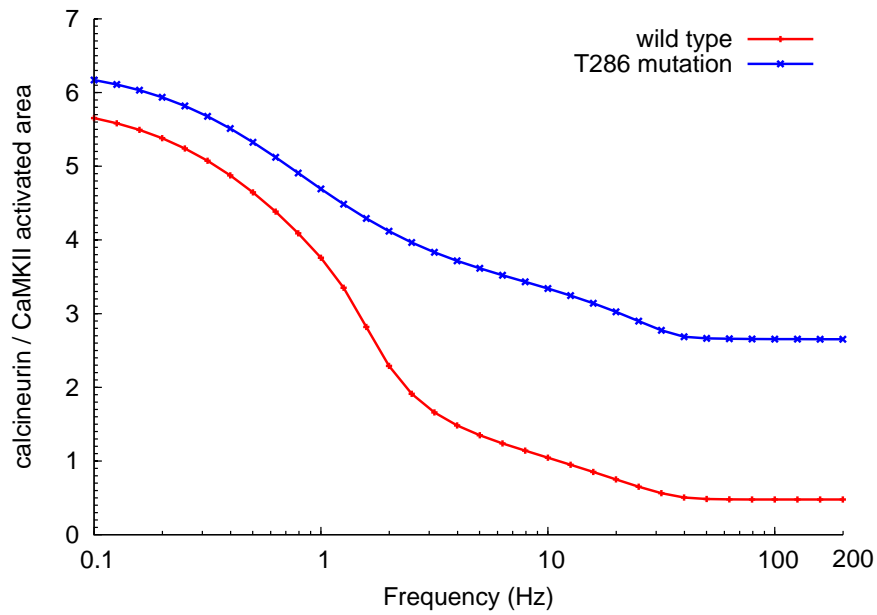
Figure 18: **Effect of CaMKII autophosphorylation on the relative activa-
tion of calcineurin and CaMKII**. Ratio of calcineurin to CaMKII
activated area for the wild type (red line) and a CaMKII autophos-
phorylation mutant (at residue Thr286) (blue line). Each point
represents the ratio of activated areas, upon the stimulation by
a train of calcium inputs at a specific frequency (for the detailed
calculation of "activated area", see the methods section). Stimula-
tion at each frequency is composed of 100 calcium inputs with
the same input size (43200 molecules).

ity between CaMKII and calmodulin (Meyer *et al.*, 1992), and locks
CaMKII in the active state long after the end of calcium elevation.
Therefore, the autophosphorylation facilitates CaMKII in the competi-
tion with other calmodulin-binding proteins. Thus, CaMKII responds
to higher frequency signals with a positive feedback. This is clearly
shown in the simulations where mutated CaMKII attracted less cal-
modulin during high-frequency stimulation than wild-type CaMKII.

### 2.3.8    *Total amount of calcium ions*

If the calcium input frequency is crucial for the activation of cal-
cineurin and CaMKII, would there be a role for the absolute amount
of calcium ions? To answer this question, I initially varied the total
amount of calcium input by changing the number of inputs used in
a stimulus, while maintaining the input amplitude as previously de-
scribed (2.3.2). At a given frequency, CaMKII activation was propor-
tional to the number of inputs (Fig. 19). Moreover, increased number
of inputs resulted in increased CaMKII activity at low-frequency stim-
uli. However, when the number of inputs reached a certain threshold
level, the increased quantity of calcium ions cannot further increase
CaMKII sensitivity, even at lower-frequency stimuli. This ruled out
a limiting role of calmodulin amount because calmodulin activation
hardly saturated at low input frequencies (Fig. 13). Irrespective of
the number of calcium inputs, the ratio of active calcineurin versus
CaMKII reached the same level, indicating that the final extent of
CaMKII activation at high calcium input frequencies was independ-
ent from the number of calcium inputs.

   As discussed by Sabatini *et al.* (2002), the amplitude of the NMDA
receptor-dependent calcium spike depends on the depolarization of
the postsynaptic membrane, the peak concentration ranging from 0.7
to 12 μM. A second approach to vary the total calcium input is there-
fore to increase the size of each input while keeping the same number
of inputs (100 inputs). For instance, the free intracellular calcium con-
centration reached 12 micromolar (corresponding to 7224 molecules)
within 10 milliseconds, and declined over approximately 200 milli-
seconds, which is in agreement with experimental measurements (Fig.
20) (Sabatini *et al.*, 2002). Akin to the increase of number in calcium
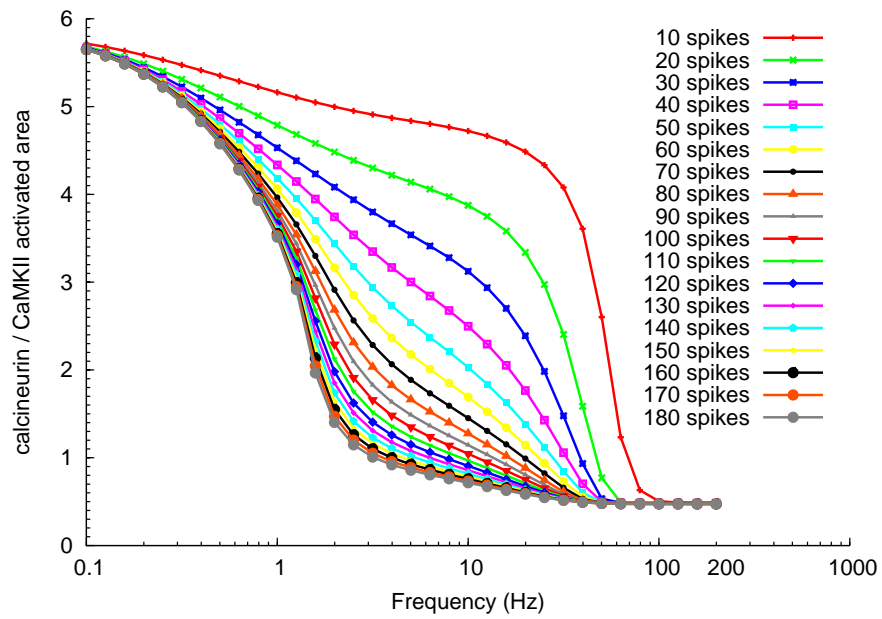
Figure 19: **Effect of calcium input number on the relative activation of calcineurin and CaMKII**. Comparison of different numbers of calcium inputs. Each point represents the ratio of calcineurin versus CaMKII activated area, when stimulated by a train of calcium inputs at a given frequency. The curves represent different numbers of calcium inputs, the amount for each input being the same (43200 molecules).

inputs, large calcium input sizes increased the proportion of active CaMKII at low frequencies, even when the frequency was as low as 0.1 Hz (Fig. 21). Once again, the final ratio of calcineurin versus CaMKII activity remained the same, indicating that the level of activated CaMKII at high-frequency stimulation is independent of the calcium input size as well. However, simulations with larger calcium input sizes reached this final ratio more rapidly than those with smaller sizes. Sabatini *et al.* (2002) argued that NMDA receptor-induced calcium influx at resting membrane potential triggers LTD, but induces LTP when coupled with postsynaptic membrane depolarization because of the large amplitude of calcium input. Combined with my simulation results, a more complete picture might be that large amplitude of calcium influx more easily induces LTP because it relies less on high spiking frequencies.
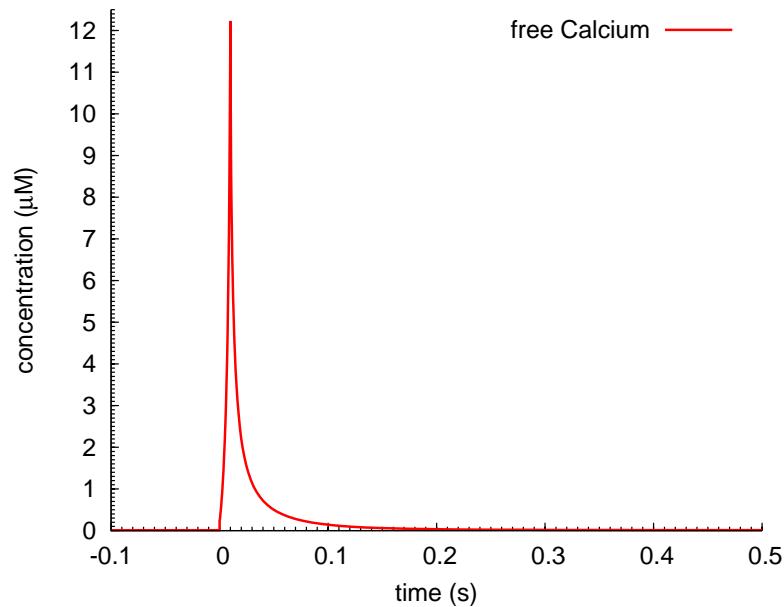


Figure 20: **Intracellular free calcium concentration increase induced by a large calcium input**. Increase of postsynaptic free calcium concentration induced by a single input. Following a single calcium input (113400 molecules), the peak amplitude, 12 micromolar (corresponding to 7224 molecules), is achieved within 10 milliseconds, followed by a rapid decay back to basal level.

Thus, high frequencies of calcium inputs provide a mechanism to produce transient but potent calcium elevations, in order to activate CaMKII. This is important when each calcium input is not

Figure 21: **Effect of calcium input size on the relative activation of calcineurin and CaMKII**. Comparison of the relative activation between calcineurin and CaMKII, stimulated by different sizes of calcium input. Each curve represents a different size of calcium input, while the labelled concentration indicates the peak level a free calcium spike reaches after this input. Each point represents the ratio of calcineurin versus CaMKII activated area, when stimulated by a train of calcium inputs at a given frequency.

large enough, or the number of calcium inputs is limited. In parallel, a large amount of calcium ions entering into the spine can lower the threshold frequency required for activating CaMKII. Therefore, the total amount of inputted calcium ions contributes to the sensitivity of the system towards decoding the frequencies, and determines above which frequency CaMKII can overcome calcineurin, and when LTP can be triggered over LTD. However, the final extent to which CaMKII can be activated seems independent from the actual quantity of calcium ions, though it may depend on other factors, such as phosphatase inhibitors, and the availability of calmodulin.

### 2.3.9  *Calmodulin availability*

Calmodulin not only activates CaMKII, but its availability also influences how CaMKII responds to calcium input frequency (Klee, 1991; Luby-Phelps *et al.*, 1995). When calmodulin concentration was increased from 30 micromolar to 45 micromolar and 60 micromolar, the amount of CaMKII activation at low frequencies of calcium stimulation increased (Fig. 22). In addition, the stabilised CaMKII activition at high calcium frequencies rose when the total calmodulin concentration increased. It therefore seems that calmodulin plays a dual role in the activation of CaMKII. Besides its ability to activate CaMKII subunits, the amount of calmodulin also limits the extent of CaMKII autophosphorylation on Thr286, in response to different frequencies. As free calmodulin is less abundant than CaMKII in the spine (Xia and Storm, 2005), the availability of calmodulin limits the chance of a CaMKII subunit having a neighbouring subunit in the active state and able to phosphorylate it. If we view autophosphorylation and calmodulin trapping as a cooperative process, calmodulin availability would determine the input frequencies that induce the onset of this process. Besides, there may be active recruitment processes for calmodulin taking place in specific locations within a spine, for instance, in the area near calcium channels in the PSD. According to our simulation results, in these regions, CaMKII activation can be induced by much lower frequencies of calcium influx, and may play an important role in modulating synaptic plasticity.
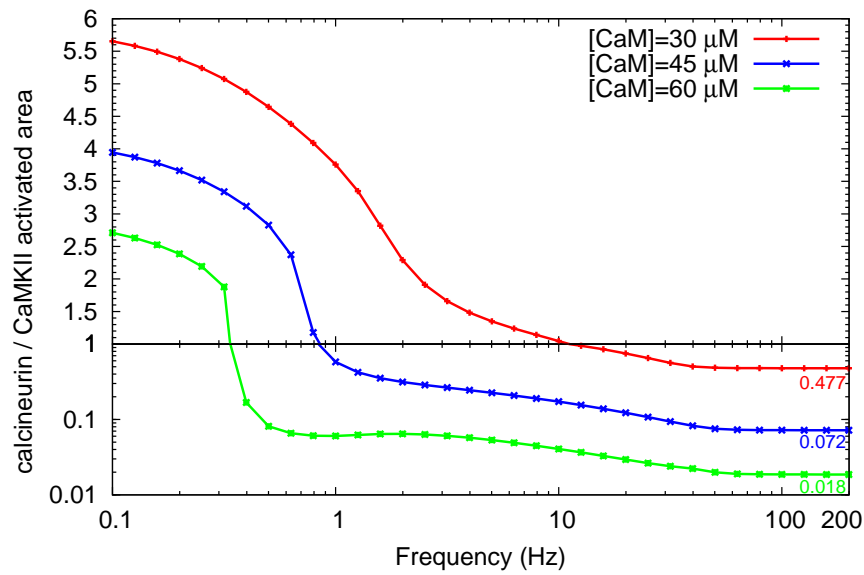
Figure 22: **Effect of calmodulin concentration on the relative activation of calcineurin and CaMKII**. Comparison of the relative activation between calcineurin and CaMKII, when different concentrations of calmodulin are available. Calmodulin concentration varies among different curves, but the number of calcium inputs and the amount of molecules for each input remain the same (100 inputs, 43200 molecules per input). On a given curve, each point shows the ratio of activated area of calcineurin versus CaMKII, when stimulated by a train of calcium inputs at a given frequency.

### 2.3.10  *PP1 inhibition by DARPP-32*

DARPP-32 interacts with PP1 through two binding domains, which contribute to both low affinity binding and inhibition (Hemmings *et al.*, 1990; Desdouits *et al.*, 1995a; Kwon *et al.*, 1997; Huang *et al.*, 1999). Upon binding both sites, the affinity between DARPP-32 and PP1 is increased to a nanomolar range (Desdouits *et al.*, 1995a; Hemmings *et al.*, 1984a). In my model, a relatively low affinity ($K_d$=100 nM) was used, representing the average inhibitory effect of different PP1 inhibitors, under basal conditions. However, when the affinity between DARPP-32 and PP1 was increased to approximately 70-fold ($K_d$=1.5 nM) (Hemmings *et al.*, 1984a), with basal DARPP-32 phosphorylation unchanged, the activation of CaMKII effectively rose during low-frequency calcium stimulation (Fig. 23). Moreover, the size of CaMKII activated area was 10 times that of calcineurin in the high-frequency range (50 Hz to 200 Hz), which was a 5-fold increase when compared with the ratio obtained in the low affinity simulation (Fig. 23). This indicates that, although CaMKII activation outpaces its phosphatase at high frequency stimulation (Fig. 16), PP1 still plays an important role in shaping CaMKII response to calcium. The potency of PP1, which is controlled by DARPP-32, not only determines the sensitivity of the CaMKII frequency response, but also the extent to which CaMKII can be activated by high frequency calcium input. This points to other avenues of controlling synaptic plasticity via other signalling pathways.
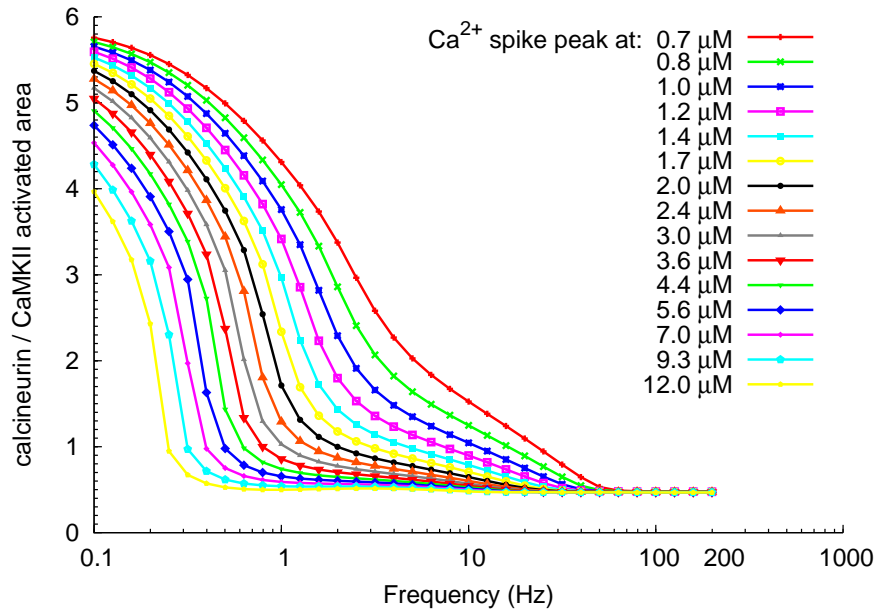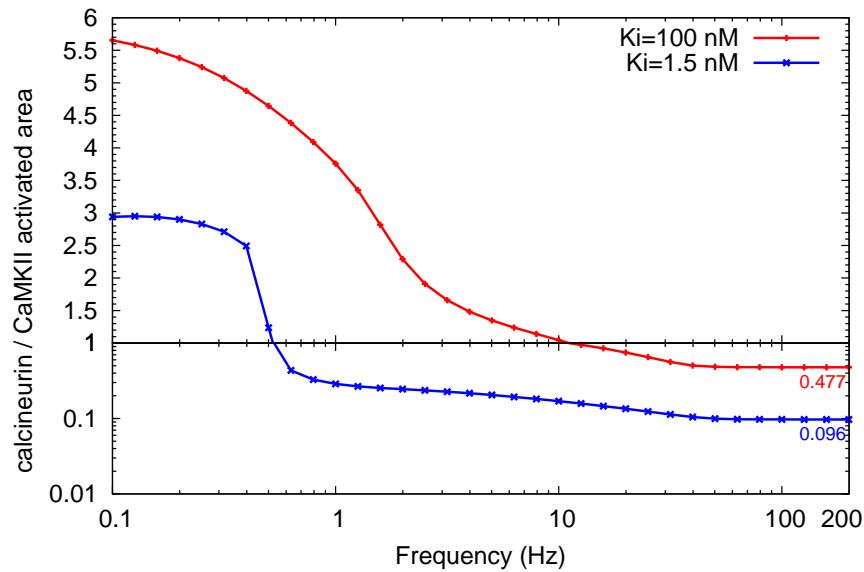
Figure 23: **Effect of increased PP1 inhibition on the relative activation of calcineurin and CaMKII** Comparison of the relative activation of calcineurin and CaMKII, between different inhibitory potentials of DARPP-32 on PP1. The constant for competitive inhibition changes between the curves, but the number of calcium inputs and the amount of molecules for each input remain the same (100 inputs, 43200 molecules per input). On a given curve, each point shows the ratio of relative activation between calcineurin and CaMKII, stimulated by a train of calcium inputs at a specific frequency.

## 2.4    DISCUSSION

The influx of calcium through the NMDA receptor is of particular importance for synaptic plasticity. However, the mechanisms underlying the dual role of calcium, triggering either LTP or LTD, are still largely unclear. In the present study, I explored how postsynaptic calcium elevation could drive different biochemical cascades by inducing different responses of calcineurin and CaMKII according to calcium input frequency, amplitude, and duration. I showed that increased calcium input frequency increases both the activation of calcineurin and CaMKII. However, changing input frequency shifts the balance of activation between the two enzymes. In addition, the activation of CaMKII can be achieved either by high-frequency calcium inputs, or at low frequencies by stimulation with large inputs.

My simulation results are in agreement with previous experimental reports. Low-frequency calcium input lasting longer induced large activation of calcineurin, demonstrated as follows. First, Mulkey and Malenka (1992) showed that the electrical induction of LTD resulting from low-frequency afferent stimulation needs to last for 30 s. Second, Yang *et al.* (1999) showed that a moderate increase in calcium for about 1 min can induce LTD. Short high frequency calcium inputs preferentially triggered the activation of CaMKII. This is also supported by experimental evidence showing that LTP is elicited by stimulation transiently raising calcium to significantly high levels (Petrozzino *et al.*, 1995) for about 2 seconds (Malenka *et al.*, 1992; Yang *et al.*, 1999). In my simulations, larger calcium input sizes allowed CaMKII activation at lower calcium input frequencies (Fig. 21). This has been demonstrated in experiments showing that paired low-frequency afferent stimulation with postsynaptic depolarization results in LTP rather than LTD (Gustafsson *et al.*, 1987). In addition, this computational model provided useful information for the range of frequencies of postsynaptic calcium spikes, which could induce LTP.

High-frequency stimulation induces short but potent elevation of the free intracellular calcium concentration, and these specific calcium transients place a specific temporal constraint for calcium decoding proteins, such as calmodulin. I demonstrated that calmodulin

activation depends on the calcium firing frequencies. With a constant total amount of calcium ions input, high frequency inputs stimulate calmodulin more efficiently.

Another decoder of calcium input frequency is CaMKII, due to its multimeric structure and intersubunit autophosphorylation. As introduced above, high-frequency calcium inputs induce the activation of calmodulin, which enhances its probability of binding to neighbouring subunits, thus inducing CaMKII autophosphorylation. Most importantly, this autophosphorylation promotes high affinity calmodulin binding (Meyer *et al.*, 1992; Hanson *et al.*, 1994) and converts this kinase into $Ca^{2+}$/calmodulin independent state (Miller and Kennedy, 1986; Mukherji and Soderling, 1994). CaMKII frequency decoding ability has been demonstrated *in vitro*. De Koninck and Schulman (1998) showed that CaMKII autophosphorylation occurs in a frequency-dependent manner and this frequency response is modulated by the amplitude and duration of each calcium pulse, which is congruent with my findings. Although the calcium input frequency shifts the balance of activated calcineurin and CaMKII, the total amount of calcium ions in the signal defines how sensitive the system is towards different calcium input frequencies. In other words, large amounts of calcium ions lower the frequency threshold that induces the autophosphorylation of CaMKII (Fig. 19 and Fig. 21). Thus, variation of calcium input frequency may be a strategy for neurons to build up transient calcium concentration when total calcium input is limited. The activation of CaMKII can equally be induced either by high frequency of calcium spikes or a large amount of calcium ions. Interestingly, the range of frequencies sensitive to the activation of signal goes from 3 to 50 Hz, corresponding roughly to the frequencies used to induce postsynaptic LTD and LTP (Mulkey and Malenka, 1992; Petrozzino *et al.*, 1995).

LTP and LTD are two widespread phenomena regulating the strength of possibly every excitatory synapse. They demonstrate how each synapse can undergo long-lasting modifications in response to synaptic activity. There are many different forms of LTP and LTD, and their underlying molecular mechanisms vary depending on the synapses and the neuronal circuits involved (Malenka and Bear, 2004). In the MSN of the striatum, dopamine afferents modulate glutamate-induced syn-

aptic plasticity through DARPP-32 inhibition of PP1, thus regulating CaMKII, and the neuronal plasticity at the heart of drug addiction (Anderson *et al.*, 2008). DARPP-32 is highly expressed in MSN, and its high reported affinity binding to PP1 means that inhibition is almost irreversible. As shown above (Fig. 23), this inhibition increases CaMKII sensitivity towards low frequency calcium firing. Hence, in MSN, the activation of dopamine D1 receptor and the DARPP-32 pathway can trigger LTP, as shown by Wolf *et al.* (2004). Furthermore, repeated *in vivo* treatments with psychostimulants increases the surface expression of AMPA receptors in the striatum (Boudreau and Wolf, 2005). However, paradoxically, a single cocaine injection in drug-naive animals exerts no effect on synaptic plasticity, while in drug-experienced animal it induces LTD (Kourrich *et al.*, 2007). It seems that, although drugs of abuse could theoretically influence short-term synaptic plasticity and induce potentiation, these psychostimulants exert their effects through a more complicated procedure involving long-term neuroadaptation. Nevertheless, the computational model presented here improved our understanding of calcium signalling involved in synaptic plasticity. The frequency of postsynaptic calcium influx regulates the induction of LTP and LTD, while the amount of calcium ions shifts the windows of frequencies required for this bidirectional regulation. Furthermore, synaptic plasticity is induced in a cell-specific manner, and is modulated by other pathways, such as the dopamine regulated PP1 inhibition in MSN. Finally, frequency adds complexity to calcium signals, thereby increasing the spectrum and accuracy of control on downstream targets.

# STRUCTURAL PLASTICITY

## 3.1  INTRODUCTION

Long-term neuroadaptation relies largely on morphological altera-
tions of neurons and modifications of synaptic connections, the so
called structural plasticity (Brown and Kolb, 2001; Robinson and Kolb,
1999a). Some of the processes regulating structural plasticity are the
same as those for the early phase synaptic plasticity. NMDA receptor
activation leads to a postsynaptic calcium elevation, which activates
kinases and GTPases, and modulates glutamate receptors. Among
these calcium effectors, accumulating evidence indicates that MAP
kinases and, in particular, ERK1/2, are crucial in regulating structural
changes such as dendritic remodelling and the density of synaptic
connections (Wu *et al.*, 2001b; Thomas and Huganir, 2004).

ERK1/2, their upstream regulators, and their downstream targets,
have been found to be highly expressed in neurons (Boulton *et al.*,
1991). ERK1/2 can directly modulate the transport of AMPA recept-
ors to the postsynaptic membrane (Zhu *et al.*, 2002), a key process in
inducing LTP (Hayashi *et al.*, 2000; Lu *et al.*, 2001; Shi *et al.*, 2001), and
in stabilising rapid morphology changes of the spine (Fischer *et al.*,
2000). Sustained activation of ERK1/2 is essential for new spine form-
ation in hippocampal neurons (Wu *et al.*, 2001b). Activated ERK1/2
can translocate to the nucleus, and regulate several key transcription
factors crucial for long-term memory. This regulation may be direct,
as in the case of Elk1 (Berman *et al.*, 1998; Davis *et al.*, 2000; San-
anbenesi *et al.*, 2002) or indirect, as for CREB, where it is mediated
through control of the mitogen- and stress-activated kinases (MSK)s
(Deak *et al.*, 1998), and ribosomal protein S6 kinases (RSK)s (Xing
*et al.*, 1996).

In neuronal cells, ERK1/2 activation can be induced by glutam-
ate signalling via elevated postsynaptic calcium level (Fiore *et al.*,
1993; Zhu *et al.*, 2002). Calcium influx activates Ras by controlling

the balance of activation between Ras guanine nucleotide exchange factor protein (Ras-GEF) and Ras GTPase activating protein (Ras-GAP) (Thomas and Huganir, 2004). Activated Ras leads to the activation of Raf, which in turn phosphorylates the dual-specificity MAP-K/ERK kinase (MEK). ERK1/2 are unique MAP kinases, because their full activation requires the phosphorylation not only of a threonine (Thr183) but also of a tyrosine (Tyr185) residue by MEK (Anderson *et al.*, 1990; Robinson and Cobb, 1997). The deactivation of ERK1/2 can be achieved by three groups of phosphatases: the dual specific phosphatases (Camps *et al.*, 2000), the serine/threonine phosphatases (Alessi *et al.*, 1995), and the tyrosine phosphatases (Pulido *et al.*, 1998; Saxena *et al.*, 1999) (PTPs). In the case of the serine/threonine phosphatases, ERK1/2 can be effectively dephosphorylated by PP2A but not by calcineurin or PP1 (Zhou *et al.*, 2002).

In the striatum, the administration of various drugs of abuse activates extracellular signal regulated kinase-2 (ERK2) through the combined stimulation of the glutamate NMDA receptor and the dopamine D1 receptor (Valjent *et al.*, 2000, 2005; Salzmann *et al.*, 2003). The consequences of such activation are the increased intracellular levels of two major second messengers, $Ca^{2+}$ and cAMP, respectively. Increased cAMP levels lead to the phosphorylation of DARPP-32 on Thr34; calcium elevation results in the activation of MAP kinase pathway, but also in the dephosphorylation of DARPP-32 on Thr34. Interestingly, acute cocaine injection to a mouse carrying either inactivated DARPP-32 or a Thr34Ala mutation results in attenuated ERK2 activation, indicating that cocaine effectively stimulates DARPP-32 phosphorylation on Thr34, and that this phosphorylation is specifically required for activation of ERK2. DARPP-32 is highly expressed in MSN and is a potent PP1 inhibitor once phosphorylated on Thr34 (Hemmings *et al.*, 1990). Therefore, phospho-Thr34 DARPP-32 might enhance ERK1/2 activity by inhibiting PP1. Since PP1 cannot directly dephosphorylate ERK1/2(Zhou *et al.*, 2002), how PP1 negatively regulates ERK1/2 is still an open question.

While the glutamate-dependent signalling pathways activate the phosphorylation of ERK1/2, it is likely that dopamine exerts its effect by inhibiting phosphatases acting on ERK1/2. The striatal-enriched tyrosine phosphatase (STEP) has been implicated as playing a key

role, linking DARPP-32 to the MAP kinase pathway (Valjent *et al.*, 2005; Girault *et al.*, 2007). It has also been established that *N*-methyl-D-aspartate receptor (NMDAR)-mediated calcium elevation activates STEP, leading to the dephosphorylation of ERK2 on the tyrosine residue (Paul *et al.*, 2003). STEP loses its phosphatase activity when phosphorylated by PKA (Paul *et al.*, 2000). Its dephosphorylation, which may involve several potential phosphatases, restores this phosphatase activity. One homolog of STEP, HePTP, can be activated by PP1, but not by calcineurin (Nika *et al.*, 2004). Therefore, it is possible that dopamine positively modulates ERK1/2 activity through DARPP-32 inhibition on PP1, and the subsequent inactivation of STEP.

Conversely, Paul *et al.* (2003) raised the possibility that calcineurin, instead of PP1, activates STEP. Indeed, after exposure to a calcineurin inhibitor, cyclosporin A, glutamate stimulation results in higher levels of tyrosine-phosphorylated ERK2 than that are observed in the control. Further, this phosphorylation level persists 30 minutes post-stimulation. Moreover, glutamate fails to activate STEP when calcineurin is inhibited. It therefore seems that DARPP-32 has no influence on STEP activity. However, it is difficult to conclude that calcineurin activates STEP directly, because it can release PP1 inhibition by dephosphorylating DARPP-32 at Thr34, thus inhibiting calcineurin decreases PP1 activity as well.

NMDA receptors can trigger postsynaptic calcium influx, activating second messenger signalling pathways, and controlling activity-dependent synaptic plasticity. NMDA receptors are tetrameric complexes composed of two NR1 and two NR2 subunits (Sheng *et al.*, 1994; Kim *et al.*, 2005). The identities of NR2 subunits, especially the relative expression levels of NR2A and NR2B, vary according to neuronal differentiation stage. In mice, NR2B-containing NMDA receptors are strongly expressed during birth, and slowly decline during adulthood. NR2A-containing NMDA receptors appear around postnatal day 7 and gradually increase during adulthood (Monyer *et al.*, 1994; Sheng *et al.*, 1994; Barria and Malinow, 2005). NR2A- and NR2B-containing receptors not only have distinct gating kinetics (Cull-Candy *et al.*, 2001), but also have opposing effects on regulating Ras-ERK1/2 signalling pathway. It has been shown that NR2B-containing NMDA receptors negatively regulate ERK1/2 activity, the

converse of the effect exerted by NR2A-containing receptors (Kim *et al.*, 2005).

Synaptic Ras GTPase activating protein (SynGAP) is a major component of the PSD (Cheng *et al.*, 2006). In cultured neurons, SynGAP inhibits ERK1/2 (Rumbaugh *et al.*, 2006). SynGAP associates with NR2B via the binding of PSD95/SAP102's PDZ domain, or via indirect connection with CaMKII (Kim *et al.*, 1998; Vazquez *et al.*, 2004; Krapivinsky *et al.*, 2004). CaMKII translocates from cytosol to the PSD, and associates with NR2B following treatments that induce autophosphorylation of CaMKII and LTP (Strack *et al.*, 1997b; Leonard *et al.*, 1999; Strack *et al.*, 2000; Meng and Zhang, 2002). Furthermore, Oh *et al.* (2004) identified four specific serine residues of SynGAP which, once phosphorylated by CaMKII, lead to increased Ras-GAP activity. Therefore, the negative regulation of NR2B-containing NMDA receptor on MAP kinase pathway may be due to the preferential coupling of SynGAP and activated CaMKII to NR2B (Kim *et al.*, 2005). Thus, PP1 can inhibit SynGAP and exert positive regulation on ERK1/2, because it dephosphorylates CaMKII, preventing it from activating SynGAP. Therefore, PP1 may have dual roles in regulating ERK1/2 activity, and would shift between roles according to neuronal differentiation stage.

In the following sections I will first address the question of which phosphatase activates STEP, PP1 or calcineurin, by using computational modelling. I will then describe experimental results conducted on primary striatal neuron cultures revealing a peculiar inhibitory effect of glutamate on ERK activity. Finally, I will present a detailed computational model that provides a tentative explanation of the opposite effects displayed by PP1 on ERK activity according to different neuronal differentiation, and in particular the type of NMDA receptors expressed.

## 3.2 EXPERIMENTAL METHODS

The methods used to model the signalling pathways and run numerical simulations are presented in 2.2. In addition to $Ca^{2+}$ perturbation, the simulation of MAP kinase model also requires the cAMP input,

which was realised by increasing the cAMP influx constant for 5 milliseconds for each spike.

Phosphatase inhibition *in silico* was achieved by increasing the concentration of phosphatase inhibitor, which processes high affinity binding to phosphatase (as listed in Table 3), 50 min prior to calcium input. Specifically, 5 $\mu$M tautomycetin was used for inhibiting PP1, while 5 $\mu$M cyclosporin A for inhibiting calcineurin.

### 3.2.1 *Cell culture and glutamate stimulation*

Primary neuronal cultures were obtained from 15-day embryonic Swiss mice. Striatum were dissected under the microscope, and the retrieved tissues was incubated with trypsin (0.001 g/mL) under 37°C water bath for 30 min. The trypsinized striatum was then quenched using DNase (0.004 g/mL) and heat-inactivated fetal bovine serum (10%) and centrifuged (900 rpm, 5 min, room temperature). The supernatant was removed, and the tissue pellet was triturated in neurobasal media. Cells were plated on tissue culture dishes (800 000 cells per 35 mm culture dish for western blot; 150 000 cells per 14 mm culture dish for immunofluorescence) for 7 or 14 days at 37°C in a humidified atmosphere consisting of 5% $CO_2$. Culture dishes had been coated with Poly-L-lysine (50 $\mu$g/mL) in an incubator at 37°C overnight, prior to cell plating.

A protein phosphatase inhibitor, either tautomycetin (5 $\mu$M for inhibiting PP1) or okadaic acid (500 nM for inhibiting PP2A) was added into the cell culture, and incubated at 37°C for 50 min prior to glutamate stimulation (using 50 $\mu$M). Incubation of the stimulated cultures was terminated at various time intervals, as indicated in the results. Control groups were treated with DMSO, instead of tautomycetin or okadaic acid, in equal concentration and incubated for equal time intervals.

Neuronal cultures grown on coverslips for immunofluorescence received the same treatment of protein phosphatase inhibitors, as indicated above. However, they were only treated with glutamate for 0 or 10 minutes before fixation.

3.2.2  *Western blotting*

After treatment by phosphatase inhibitors and glutamate stimulation, the cells were washed twice with ice-cold phosphate-buffered saline (PBS), and were lysed in sodium dodecyl sulphate (SDS) (1%) and sodium orthovanadate ($Na_3VO_4$) (1 mM), followed by sonication (2x33 s, 43 W), then heated for 5 minutes ($100°C$ ).

Each sample (containing 30 $\mu$g protein) was separated by 10% SDS-polyacrylamide gel electrophoresis (SDS-PAGE) followed by western blotting. Activated ERK1/2 and total ERK1/2 were detected by probing the blots with mouse monoclonal antibodies against diphospho-ERK1/2 (1:1000, Sigma) and ERK1/2 (1:5000, Sigma).

3.2.3  *Immunofluorescence of striatal neurons in culture*

After treatment by phosphatase inhibitors and glutamate stimulation, the cells were washed twice with PBS, then fixed with PBS containing 2% paraformaldehyde (40 min, room temperature). After three rinses in PBS, cells were treated with 0.1% Triton for 15 minutes, then washed three rinses with PBS. Later, cells were treated with blocking buffer (3% Bovine Serum Albumin (BSA) in PBS) for 1 hour at room temperature, then incubated overnight at 4°C in 1% BSA with diphospho-ERK1/2 (1:1000 Cell signalling, rabbit polyclonal) and MAP2 (1:1000 Signal, mouse monoclonal) antibodies. After three rinses with PBS, anti-mouse Alexa488-conjugated antibody and anti-mouse Cy3-conjugated antibody (1:400 Molecular Probes) were added, and cells incubated for 1 h at room temperature.

Cells were rinsed three times with PBS prior to mounting under coverslips with Vectashield with 4',6-diamidino-2-phenylindole (DAPI) labelling nucleus (Vector Laboratories).

3.3  Phosphatase regulating STEP activity

In order to decipher which phosphatase stimulates STEP, calcineurin or PP1, I compared the results obtained from two computational models with existing experimental measurements.

*Model structure and simulation plan*

The two models described here (Fig. 24), share the majority of interactions, including the dopamine activated DARPP-32 pathway and glutamate stimulated MAP kinase pathway. The only difference between the models is the activation of STEP, either by calcineurin or by PP1. All the quantitative parameters used in these two models are listed in Table 3, and the abbreviations are explained in Table 4. The models and the Python script for simulation in E-Cell, are available online (`http://www.ebi.ac.uk/~luli/thesis/mapk/step/`).
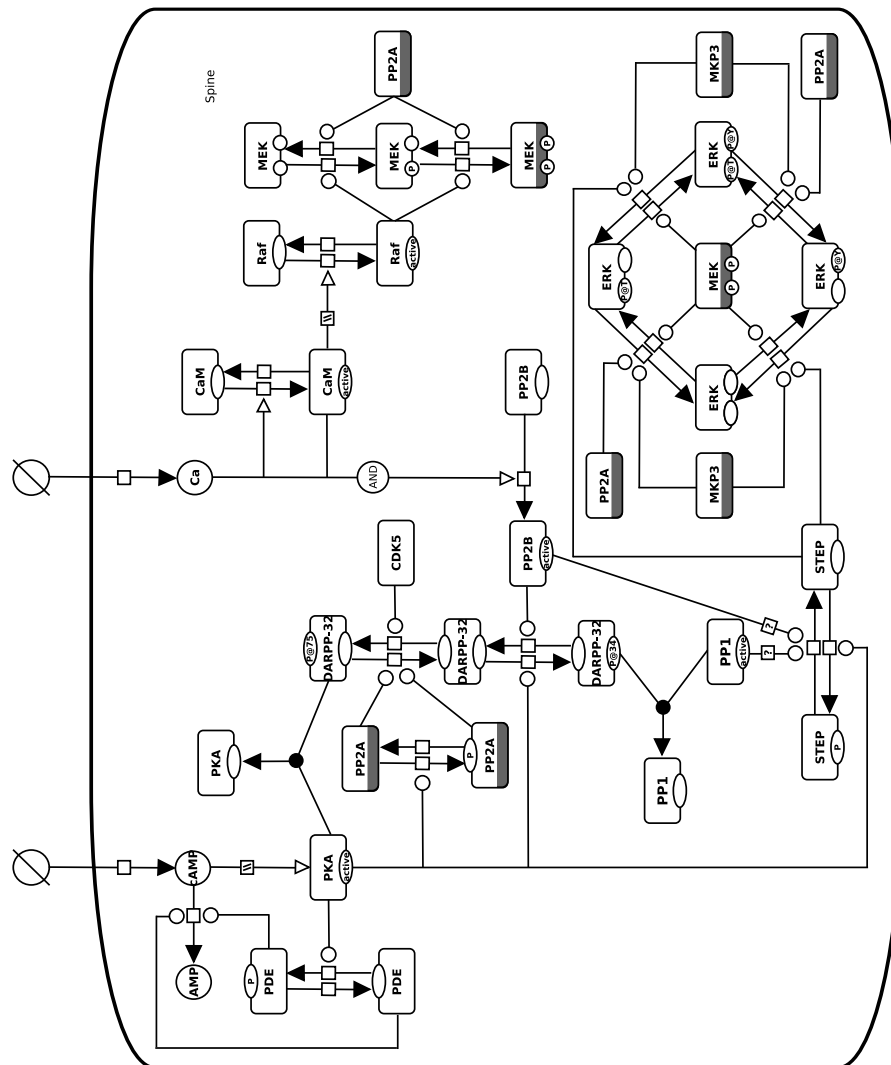
Figure 24: **Computational models of the regulation of STEP activity.** The graphical conventions are those of the Process Description language of Systems Biology Graphical Notation (SBGN) (Le Novère *et al.*, 2009). Rectangular box with rounded corners: macromolecule, circular container: simple chemical, elliptical container: state variable, "empty set": a source or sink, square on the arc: process, square containing parallel slanted lines: omitted process, square containing question mark: uncertain process, filled disc on the arc: association, filled arrow head: production, empty arrow head: stimulation, empty circle: catalysis.

Table 3: List of parameters used for simulation of the MAP kinase model that concerns PP1 or calcineurin (PP2B) activates STEP.

| Parameter | Value | Reference |
|---|---|---|
| $Ca^{2+}$ pump: | | |
| $v_{max}$ | $4 \times 10^{-3}\,Ms^{-1}$ | (cf. Markram et al., 1998)[*],[1] |
| $K_m$ | $1 \times 10^{-6}\,M$ | (Markram et al., 1998)[*] |
| $Ca^{2+}$ leak: | | |
| $k$ | $3 \times 10^{-4}\,Ms^{-1}$ | (cf. Markram et al., 1998)[*],[1] |
| $Ca^{2+}$ binding calcium buffer protein ($CBP$): | | |
| $k_{on_{CBP_{fast}}}$ | $10^9\,M^{-1}s^{-1}$ | (Markram et al., 1998)[*],[2] |
| $k_{off_{CBP_{fast}}}$ | $10^3\,s^{-1}$ | (Markram et al., 1998)[*],[2] |
| $k_{on_{CBP_{medium}}}$ | $10^8\,M^{-1}s^{-1}$ | (Markram et al., 1998)[*],[2] |
| $k_{off_{CBP_{medium}}}$ | $10^2\,s^{-1}$ | (Markram et al., 1998)[*],[2] |
| $k_{on_{CBP_{slow}}}$ | $10^7\,M^{-1}s^{-1}$ | (Markram et al., 1998)[*],[2] |
| $k_{off_{CBP_{slow}}}$ | $10\,s^{-1}$ | (Markram et al., 1998)[*],[2] |
| $k_{on_{CBP_{vslow}}}$ | $10^6\,M^{-1}s^{-1}$ | (Markram et al., 1998)[*],[2] |
| $k_{off_{CBP_{vslow}}}$ | $1\,s^{-1}$ | (Markram et al., 1998)[*],[2] |
| $CaM$ activation (Hill equation): | | |
| $K_d$ | $7 \times 10^{-6}\,M$ | (D'Alcantara et al., 2003)[*],[3] |
| $n_H$ | $4$ | (D'Alcantara et al., 2003)[*],[3] |

Table 3: continued

*CaM* inactivation:

| $k$ | $2.5\,s^{-1}$ | this study* |

*PP2B* binding $Ca^{2+}$ (Hill equation):

| $K_d$ | $2 \times 10^{-7}\,M$ | this study* |
| $n_H$ | 1.6 | this study* |

$Ca^{2+}$ ions dissociate from *PP2B*:

| $k$ | $5\,s^{-1}$ | this study* |

*PP2BCa*4 binding *CaMCa*4:

| $k_{on_{PP2B}}$ | $6 \times 10^{9}\,M^{-1}s^{-1}$ | (Meyer *et al.*, 1992)[4] |
| $k_{off_{PP2B}}$ | $6\,s^{-1}$ | (Meyer *et al.*, 1992)[4] |

*cAMP* in (constant flux):

| $k$ | $2.3 \times 10^{-7}\,Ms^{-1}$ | (estimated from Bacskai *et al.*, 1993)*,[5] |

*cAMP* pump:

| $k$ | $4\,s^{-1}$ | (estimated from Bacskai *et al.*, 1993)*,[5] |

*PKA* activation:

| $k_{on_{R2C2\_cAMP}}$ | $5.4 \times 10^{7}\,M^{-1}s^{-1}$ | (Bhalla and Iyengar, 1999)*,[6] |
| $k_{off_{R2C2\_cAMP}}$ | $33\,s^{-1}$ | (Bhalla and Iyengar, 1999)*,[6] |
| $k_{on_{cAMPR2C2\_cAMP}}$ | $5.4 \times 10^{7}\,M^{-1}s^{-1}$ | (Bhalla and Iyengar, 1999)*,[6] |
| $k_{off_{cAMPR2C2\_cAMP}}$ | $33\,s^{-1}$ | (Bhalla and Iyengar, 1999)*,[6] |
| $k_{on_{cAMP2R2C2\_cAMP}}$ | $7.5 \times 10^{7}\,M^{-1}s^{-1}$ | (Bhalla and Iyengar, 1999)*,[7] |

Table 3: continued

| | | |
|---|---|---|
| $k_{off_{cAMP2R2C2\_cAMP}}$ | $110\,s^{-1}$ | (Bhalla and Iyengar, 1999)*,[7] |
| $k_{on_{cAMP3R2C2\_cAMP}}$ | $7.5 \times 10^7\,M^{-1}s^{-1}$ | (Bhalla and Iyengar, 1999)*,[6] |
| $k_{off_{cAMP3R2C2\_cAMP}}$ | $32.5\,s^{-1}$ | (Bhalla and Iyengar, 1999)*,[6] |
| $k_{off_{cAMP4R2C\_PKA}}$ | $10\,s^{-1}$ | (Bhalla and Iyengar, 1999)* |
| $k_{on_{cAMP4R2C\_PKA}}$ | $1.8 \times 10^7\,M^{-1}s^{-1}$ | (Bhalla and Iyengar, 1999)* |
| $k_{off_{cAMP4R2\_PKA}}$ | $10\,s^{-1}$ | (Bhalla and Iyengar, 1999)* |
| $k_{on_{cAMP4R2\_PKA}}$ | $1.8 \times 10^7\,M^{-1}s^{-1}$ | (Bhalla and Iyengar, 1999)* |

*PKA* phosphorylates *PDE*:

| | | |
|---|---|---|
| $k_{on}$ | $6 \times 10^6\,M^{-1}s^{-1}$ | (Fernandez *et al.*, 2006)* |
| $k_{off}$ | $36\,s^{-1}$ | (Fernandez *et al.*, 2006)* |
| $k_{cat}$ | $9\,s^{-1}$ | (Fernandez *et al.*, 2006)* |

*PDEp* dephosphorylation:

| | | |
|---|---|---|
| $k$ | $0.1\,s^{-1}$ | (Fernandez *et al.*, 2006)* |

*PKA* phosphorylates *PP2A*:

| | | |
|---|---|---|
| $k_{on}$ | $2.4 \times 10^6\,M^{-1}s^{-1}$ | (Usui *et al.*, 1998)[8] |
| $k_{off}$ | $0.1\,s^{-1}$ | (Usui *et al.*, 1998)[8] |
| $k_{cat}$ | $0.3\,s^{-1}$ | (Usui *et al.*, 1998)[8] |

*PP2Ap* dephosphorylation:

Table 3: continued

| | | |
|---|---|---|
| $k$ | $0.08\,s^{-1}$ | in this study* |

$cAMP$ degradation:

| | | |
|---|---|---|
| $k_{on_{cAMP\_PDE}}$ | $8 \times 10^7\,M^{-1}s^{-1}$ | (Fernandez *et al.*, 2006)* |
| $k_{off_{cAMP\_PDE}}$ | $40\,s^{-1}$ | (Fernandez *et al.*, 2006)* |
| $k_{cat_{cAMP\_PDE}}$ | $10\,s^{-1}$ | (Fernandez *et al.*, 2006)* |
| $k_{on_{cAMP\_PDEp}}$ | $8 \times 10^7\,M^{-1}s^{-1}$ | (Fernandez *et al.*, 2006)* |
| $k_{off_{cAMP\_PDEp}}$ | $80\,s^{-1}$ | (Fernandez *et al.*, 2006)* |
| $k_{cat_{cAMP\_PDEp}}$ | $20\,s^{-1}$ | (Fernandez *et al.*, 2006)* |

$PKA$ phosphorylates DARPP-32 on $Thr$34:

| | | |
|---|---|---|
| $k_{on_{D\_PKA}}$ | $5.6 \times 10^6\,M^{-1}s^{-1}$ | (Hemmings *et al.*, 1984b)[9] |
| $k_{off_{D\_PKA}}$ | $10.8\,s^{-1}$ | (Hemmings *et al.*, 1984b)[9] |
| $k_{cat_{D\_PKA}}$ | $2.7\,s^{-1}$ | (Hemmings *et al.*, 1984b)[9] |
| $k_{on_{Dp75\_PKA}}$ | $5.6 \times 10^6\,M^{-1}s^{-1}$ | (estimated from Bibb *et al.*, 1999)[10] |
| $k_{off_{Dp75\_PKA}}$ | $0.3\,s^{-1}$ | (estimated from Bibb *et al.*, 1999)[10] |
| $k_{cat_{Dp75\_PKA}}$ | $0\,s^{-1}$ | (Bibb *et al.*, 1999)[10] |

$PP2B_{active}$ dephosphorylates DARPP-32 on $Thr$34:

| | | |
|---|---|---|
| $k_{on}$ | $4.1 \times 10^6\,M^{-1}s^{-1}$ | (King *et al.*, 1984)[11] |

Table 3: continued

| $k_{off}$ | $6.4\,s^{-1}$ | (King *et al.*, 1984)[11] |
|---|---|---|
| $k_{cat}$ | $0.2\,s^{-1}$ | (King *et al.*, 1984)[11] |

*CDK*5 phosphorylates DARPP-32 on *Thr*75:

| $k_{on}$ | $6.2 \times 10^6\,M^{-1}s^{-1}$ | (estimate from Hemmings *et al.*, 1984b)[9] |
|---|---|---|
| $k_{off}$ | $12\,s^{-1}$ | (estimate from Hemmings *et al.*, 1984b)[9] |
| $k_{cat}$ | $2.5\,s^{-1}$ | (estimate from Hemmings *et al.*, 1984b)[9] |

*PP*2*A* dephosphorylates DARPP-32 on *Thr*75:

| $k_{on}$ | $2.74 \times 10^6\,M^{-1}s^{-1}$ | (estimate from Hemmings *et al.*, 1990)[12] |
|---|---|---|
| $k_{off}$ | $116\,s^{-1}$ | (estimate from Hemmings *et al.*, 1990)[12] |
| $k_{cat}$ | $10\,s^{-1}$ | (estimate from Hemmings *et al.*, 1990)[12] |

*PP*2*Ap* dephosphorylates DARPP-32 on *Thr*75:

| $k_{on}$ | $2.74 \times 10^6\,M^{-1}s^{-1}$ | (estimate from Hemmings *et al.*, 1990)[12] |
|---|---|---|
| $k_{off}$ | $18.4\,s^{-1}$ | (estimate from Hemmings *et al.*, 1990)[12] |

Table 3: continued

| | | |
|---|---|---|
| $k_{cat}$ | $20\,s^{-1}$ | (estimate from Hemmings *et al.*, 1990)[12] |

DARPP-32$_{Thr34p}$ binding $PP1$:

| | | |
|---|---|---|
| $k_{on_{Dp34\_PP1}}$ | $4.0 \times 10^6\,M^{-1}s^{-1}$ | (estimate from Hemmings *et al.*, 1984a)[13] |
| $k_{off_{Dp34\_PP1}}$ | $0.06\,s^{-1}$ | (estimate from Hemmings *et al.*, 1984a)[13] |

$PP1/PP2B$ dephosphorylates $STEP$:

| | | |
|---|---|---|
| $k_{on}$ | $3 \times 10^6\,M^{-1}s^{-1}$ | (estimate from Nika *et al.*, 2004)[14] |
| $k_{off}$ | $32\,s^{-1}$ | (estimate from Nika *et al.*, 2004)[14] |
| $k_{cat}$ | $0.2\,s^{-1}$ | (estimate from Nika *et al.*, 2004)[14] |

$PKA$ phosphorylates $STEP$:

| | | |
|---|---|---|
| $k_{on}$ | $4.1 \times 10^6\,M^{-1}s^{-1}$ | (Paul *et al.*, 2000)[15] |
| $k_{off}$ | $10\,s^{-1}$ | (Paul *et al.*, 2000)[15] |
| $k_{cat}$ | $0.67\,s^{-1}$ | (Paul *et al.*, 2000)[15] |

$Raf$ activation by $CaM$:

| | | |
|---|---|---|
| $k_{cat}$ | $10\,s^{-1}$ | this study* |
| $K_m$ | $3 \times 10^{-7}\,M$ | this study* |

$Raf$ inactivation:

| | | |
|---|---|---|
| $v_{max}$ | $1 \times 10^{-6}\,Ms^{-1}$ | this study* |

Table 3: continued

| | | |
|---|---|---|
| $K_m$ | $4.5 \times 10^{-5}\,M$ | this study* |

*Raf* phosphorylates *MEK* or *MEKp*:

| | | |
|---|---|---|
| $k_{on}$ | $3.3 \times 10^6\,M^{-1}s^{-1}$ | (Sasagawa *et al.*, 2005)* |
| $k_{off}$ | $0.42\,s^{-1}$ | (Sasagawa *et al.*, 2005)* |
| $k_{cat}$ | $0.105\,s^{-1}$ | (Sasagawa *et al.*, 2005)* |

*PP2A* or *PP2Ap* dephosphorylates *MEKp* or *MEKpp*:

| | | |
|---|---|---|
| $k_{on}$ | $8 \times 10^6\,M^{-1}s^{-1}$ | (Sasagawa *et al.*, 2005)* |
| $k_{off}$ | $122\,s^{-1}$ | (Sasagawa *et al.*, 2005)* |
| $k_{cat}$ | $3\,s^{-1}$ | (Sasagawa *et al.*, 2005)* |

*MEKpp* phosphorylates *ERK*:

| | | |
|---|---|---|
| $k_{on}$ | $16.304 \times 10^6\,M^{-1}s^{-1}$ | (Ferrell and Bhatt, 1997)[16] |
| $k_{off}$ | $4.6\,s^{-1}$ | (Ferrell and Bhatt, 1997)[16] |
| $k_{cat}$ | $0.2\,s^{-1}$ | (Ferrell and Bhatt, 1997)[16] |

*MEKpp* phosphorylates $ERK_T$ or $ERK_Y$:

| | | |
|---|---|---|
| $k_{on}$ | $16.304 \times 10^6\,M^{-1}s^{-1}$ | (Ferrell and Bhatt, 1997)[16] |
| $k_{off}$ | $0.6\,s^{-1}$ | (Ferrell and Bhatt, 1997)[16] |
| $k_{cat}$ | $0.15\,s^{-1}$ | (Ferrell and Bhatt, 1997)[16] |

*MKP3* dephosphorylates $ERK_{TY}$:

| | | |
|---|---|---|
| $k_{on}$ | $15 \times 10^6\,M^{-1}s^{-1}$ | (Zhao and Zhang, 2001)[17] |

Table 3: continued

| | | |
|---|---|---|
| $k_{off}$ | $0.235\,s^{-1}$ | (Zhao and Zhang, 2001)[17] |
| $k_{cat}$ | $0.14\,s^{-1}$ | (Zhao and Zhang, 2001)[17] |

*MKP3 dephosphorylates $ERK_T$ on Thr183:*

| | | |
|---|---|---|
| $k_{on}$ | $15 \times 10^6\,M^{-1}s^{-1}$ | (Zhao and Zhang, 2001)[17] |
| $k_{off}$ | $0.46\,s^{-1}$ | (Zhao and Zhang, 2001)[17] |
| $k_{cat}$ | $0.099\,s^{-1}$ | (Zhao and Zhang, 2001)[17] |

*MKP3 dephosphorylates $ERK_Y$ on Tyr185:*

| | | |
|---|---|---|
| $k_{on}$ | $15 \times 10^6\,M^{-1}s^{-1}$ | (Zhao and Zhang, 2001)[17] |
| $k_{off}$ | $0.25\,s^{-1}$ | (Zhao and Zhang, 2001)[17] |
| $k_{cat}$ | $0.141\,s^{-1}$ | (Zhao and Zhang, 2001)[17] |

*STEP dephosphorylates $ERK_Y$ on Tyr185:*

| | | |
|---|---|---|
| $k_{on}$ | $15 \times 10^6\,M^{-1}s^{-1}$ | (Zhou et al., 2002)[18] |
| $k_{off}$ | $7.926\,s^{-1}$ | (Zhou et al., 2002)[18] |
| $k_{cat}$ | $0.774\,s^{-1}$ | (Zhou et al., 2002)[18] |

*STEP dephosphorylates $ERK_{TY}$ on Tyr185:*

| | | |
|---|---|---|
| $k_{on}$ | $15 \times 10^6\,M^{-1}s^{-1}$ | (Zhou et al., 2002)[18] |
| $k_{off}$ | $5.88\,s^{-1}$ | (Zhou et al., 2002)[18] |
| $k_{cat}$ | $1.02\,s^{-1}$ | (Zhou et al., 2002)[18] |

Table 3: continued

*PP2A* or *PP2Ap* dephosphorylates $ERK_T$ on Thr183:

| | | |
|---|---|---|
| $k_{on}$ | $8 \times 10^6 \, M^{-1}s^{-1}$ | (Zhou *et al.*, 2002)[18] |
| $k_{off}$ | $149 \, s^{-1}$ | (Zhou *et al.*, 2002)[18] |
| $k_{cat}$ | $27 \, s^{-1}$ | (Zhou *et al.*, 2002)[18] |

*PP2A* or *PP2Ap* dephosphorylates $ERK_{TY}$ on Thr183:

| | | |
|---|---|---|
| $k_{on}$ | $8 \times 10^6 \, M^{-1}s^{-1}$ | (Zhou *et al.*, 2002)[18] |
| $k_{off}$ | $175 \, s^{-1}$ | (Zhou *et al.*, 2002)[18] |
| $k_{cat}$ | $1.22 \, s^{-1}$ | (Zhou *et al.*, 2002)[18] |

Tautomycetin inhibits PP1:

| | | |
|---|---|---|
| $k_{on}$ | $2.5 \times 10^7 \, M^{-1}s^{-1}$ | estimated[19] |
| $k_{off}$ | $0.04 \, s^{-1}$ | estimated[19] |

Cyclosporin A inhibits PP2B:

| | | |
|---|---|---|
| $k_{on}$ | $1.8 \times 10^7 \, M^{-1}s^{-1}$ | estimated[20] |
| $k_{off}$ | $0.09 \, s^{-1}$ | estimated[20] |

Concentrations:

| | | |
|---|---|---|
| $[CaM]$ | $3 \times 10^{-5} \, M$ | (Kakiuchi *et al.*, 1982)[21] |
| $[Ca^{2+}]_{basal}$ | $8 \times 10^{-8} \, M$ | (Allbritton *et al.*, 1992)[22] |
| $[CBP_{fast}]$ | $8 \times 10^{-5} \, M$ | (Naoki *et al.*, 2005)* |
| $[CBP_{medium}]$ | $8 \times 10^{-5} \, M$ | (Naoki *et al.*, 2005)* |
| $[CBP_{slow}]$ | $2 \times 10^{-5} \, M$ | (Naoki *et al.*, 2005)* |

Table 3: continued

| | | |
|---|---|---|
| $[\text{CBP}_{vslow}]$ | $2 \times 10^{-5}\,M$ | (Naoki *et al.*, 2005)* |
| [PP2B] | $1.6 \times 10^{-6}\,M$ | (cf. Goto *et al.*, 1986)[23] |
| [cAMP] | $2 \times 10^{-8}\,M$ | (cf. Bacskai *et al.*, 1993)[24] |
| [R2C2] | $1 \times 10^{-6}\,M$ | (cf. Hofmann *et al.*, 1977)[25] |
| [PDE] | $0.5 \times 10^{-6}\,M$ | (Bhalla and Iyengar, 1999)* |
| [CDK5] | $2 \times 10^{-7}\,M$ | (Fernandez *et al.*, 2006)* |
| [PP2A] | $2 \times 10^{-7}\,M$ | (Fernandez *et al.*, 2006)* |
| [PP1] | $2 \times 10^{-6}\,M$ | (cf. Ingebritsen *et al.*, 1983)[26] |
| [DARPP-32] | $5 \times 10^{-5}\,M$ | (estimated from Halpain *et al.*, 1990)[27] |
| [STEPp] | $1 \times 10^{-6}\,M$ | this study* |
| [Raf] | $1.8 \times 10^{-7}\,M$ | (Bhalla and Iyengar, 1999)* |
| [MEK] | $1.2 \times 10^{-6}\,M$ | (Huang and Ferrell, 1996)*,[28] |
| [ERK] | $1.2 \times 10^{-6}\,M$ | (Huang and Ferrell, 1996)*,[28] |
| [MKP3] | $0.0033 \times 10^{-6}\,M$ | this study* |
| Compartment: | | |
| spine volume | $10^{-15}\,l$ | (cf. Nimchinsky *et al.*, 2002)[29] |

Table 3: continued

Table 3: List of parameters used for simulation of the MAP kinase model that concerns PP1 or calcineurin (PP2B) activates STEP. Asterisk indicates that this reference refers to a computational model. [1]: Parameters were estimated according to Markram *et al.* (1998), and adjusted to maintain the resting calcium level at 10 nM. [2]: Markram *et al.* (1998) estimated these parameters according to Falke *et al.* (1994). [3]: D'Alcantara *et al.* (2003) estimated these parameters according to Linse *et al.* (1991). [4,8,9,10,11,12,13,14,16,17,18]: Parameters were obtained from *in vitro* experiments. [5]: Parameters were estimated according to basal cAMP concentration in sensory neurons of marine snail *Aplysia*, measured by Bacskai *et al.* (1993).[6]: Bhalla and Iyengar (1999) estimated these parameters according to experimental data obtained by Hasler *et al.* (1992). [7]: Bhalla and Iyengar (1999) estimated these parameters according to experimental data obtained by Ogreid and Døskeland (1981). [19,20]: Parameter was estimated according to $IC_{50}$. [21]: Measurement was obtained from cerebral cortex tissue extract from rat.[22]: Data was obtained from cytosolic extract from Xenopus laevis oocytes. [23]: Measurement was obtained from dorsal striatum tissue extract from rat. [24]: Measurement was obtained from sensory neurons of marine snail *Aplysia*. [25]: Measurement was obtained from rabbit brain extract. [26]: Measurement was obtained from rabbit brain extract.[27]: Measurement was obtained from immunoblotting of striatal slices of rats. [28]: Huang and Ferrell (1996) estimated these concentrations according to concentrations of corresponding molecules in *Xenopus oocytes* by Matsuda *et al.* (1992). [29]: Measurement was based apical spine of CA1 pyramidal neuron.

Table 4: List of abbreviations used in MAP kinase model that concerns PP1 or calcineurin (PP2B) activates STEP.

| Abbreviations | Definition/Reference |
|---|---|
| CaM | calmodulin |
| | UniProt:P62158 |
| PP2B | calcineurin/protein phosphatase 2B |
| | GO:0005955 |
| cAMP | cyclic adenosine monophosphate |
| | CHEBI:17489 |
| R2C2 | cyclic AMP-dependent protein kinase complex |
| | GO:0005952 |
| PDE | cyclic nucleotide phosphodiesterase |
| | GO:0005966 |
| CDK5 | cyclin-dependent protein kinase 5 |
| | UniProt:Q03114 |
| PP1 | protein phosphatase 1 |
| | GO:0000164 |
| PP2A | protein phosphatase 2A |
| | InterPro:IPR006186 |
| DARPP-32 | dopamine- and cAMP-regulated phosphoprotein of 32 kDa |
| | UniProt:Q9UD71 |
| STEP | striatal-enriched tyrosine phosphatase |
| | UniProt:P35234 |
| Raf | RAF proto-oncogene serine/threonine-protein kinase |
| | UniProt:P11345 |
| MEK | MAPK/ERK kinase |
| | UniProt Q01986 |
| ERK | extracellular signal regulated kinases |
| | InterPro:IPR008349 |
| MKP | mitogen-activated protein kinase phosphatase |

Table 4: continued

| | UniProt:Q64346 | |
| --- | --- | --- |
| CBP | calcium binding protein | |

Table 4: List of abbreviations used in MAP kinase model that concerns PP1 or calcineurin (PP2B) activates STEP.

In both models DARPP-32 can be phosphorylated on Thr34 by cAMP-activated PKA, and on Thr75 by a basal level CDK5. Calcineurin, once activated by calcium and calmodulin, dephosphorylates DARPP-32 on Thr34. Thr75 of DARPP-32 can be dephosphorylated by PP2A. PP2A phosphatase activity increases upon its phosphorylation by PKA. PKA can also phosphorylate PDE, which in turn catalyses cAMP decomposition into adenosine monophosphate (AMP). Once DARPP-32 is phosphorylated on Thr34 , it becomes a potent inhibitor of PP1 via a competitive inhibition mechanism; whereas when phosphorylated on Thr75, it becomes an inhibitor of PKA, also via a competitive inhibition mechanism.

A direct activation of Raf by calmodulin was used as a simplification to replace reactions describing calmodulin-activated Ras guanine nucleotide releasing factor protein (Ras-GRF), the subsequently activationg of Ras, then Raf. Dual phosphorylations of both MEK and ERK were modelled in a distributive manner, indicating that the kinases release their substrate after phosphorylation of the first residue, and are required to rebind to this substrate for phosphorylating the second residue (Ferrell and Bhatt, 1997). Two threonine sites of MEK are phosphorylated by activated Raf and dephosphorylated by PP2A. The phosphorylations of threonine and tyrosine residues of ERK are catalysed by dual-phosphorylated MEK and dephosphorylated by dual-specific phosphatase mitogen-activated protein kinase phosphatase (MKP), threonine/serine phosphatase PP2A and tyrosine phosphatase STEP. STEP is inactivated by PKA but activated by PP1 or calcineurin in the respective models.

For each computational model, several simulations were designed in order to compare simulation results with published experimental data for an animal model. The simulations included: 1) a train of high frequency calcium spikes, replicating the activation of NMDA

and AMPA receptors by glutamate input (Fig. 25, 100 spikes with a frequency of 50 Hz) (Sabatini *et al.*, 2002); 2) a transient but prolonged cAMP spike, mimicking the effect of activated D1 receptor by dopamine. (Fig. 26) (Gonon, 1997); 3) the simultaneous inputs from both calcium spikes and cAMP, replicating the activation of both NMDA and dopamine D1 receptors (Fig. 27) (Valjent *et al.*, 2005) .
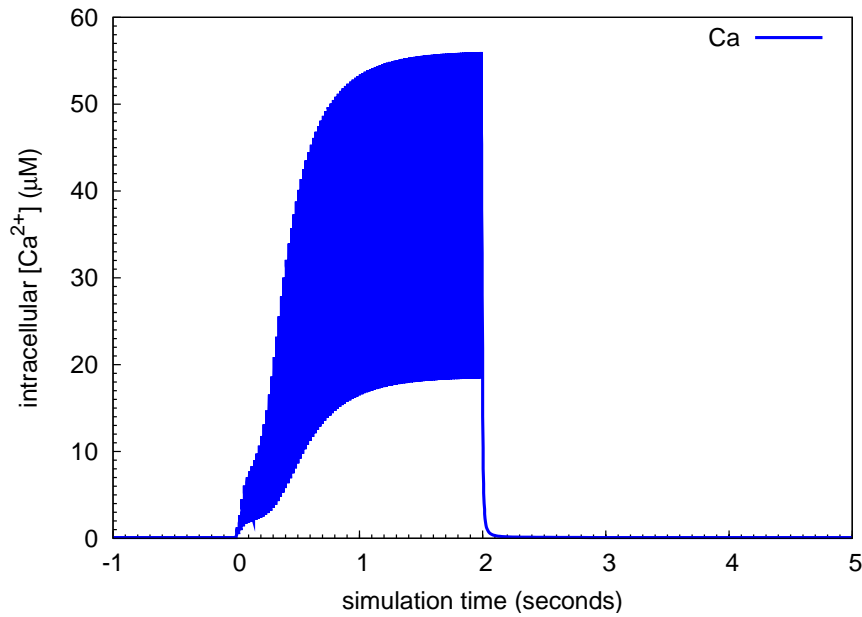


Figure 25: **A train of calcium spikes.** 100 calcium spikes are produced at 50 Hz.

*Simulation of PP1 activating STEP*

In the model where PP1 activates STEP, a train of calcium spikes led to the transient activation of ERK that reached maximum level after 5 minutes of stimulation and returned to basal activity within 1 hour, which is in agreement with published experimental data from Paul *et al.* (2003). Calcium also activated calcineurin and subsequent dephosphorylation of DARPP-32 on Thr34, resulting in reduced DARPP-32 inhibition of PP1 (Fig. 28). PP1 steadily activated STEP, and the activity of STEP peaked as much as 3 times more than its basal level, which roughly agrees with experimental measurement from Paul *et al.*
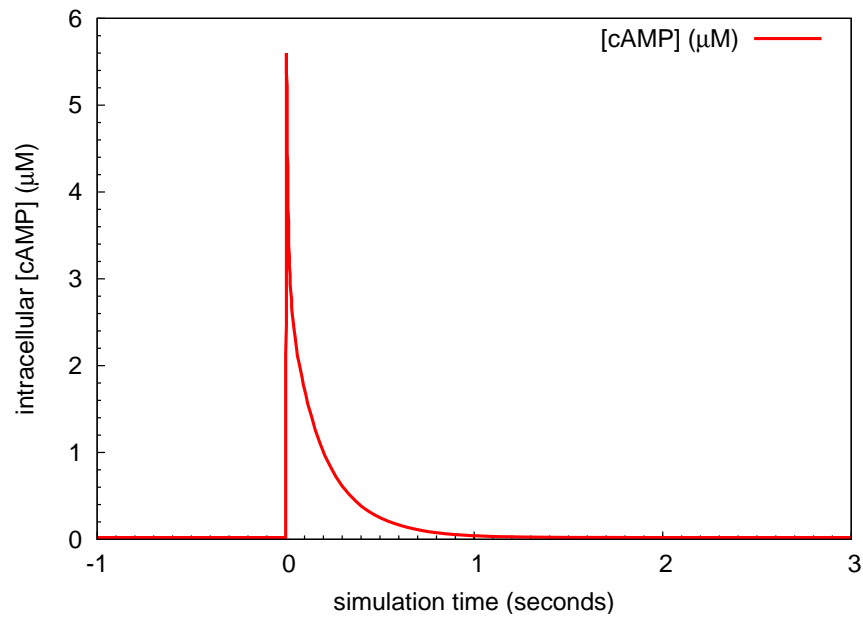
Figure 26: **A single spike of cAMP increase.**
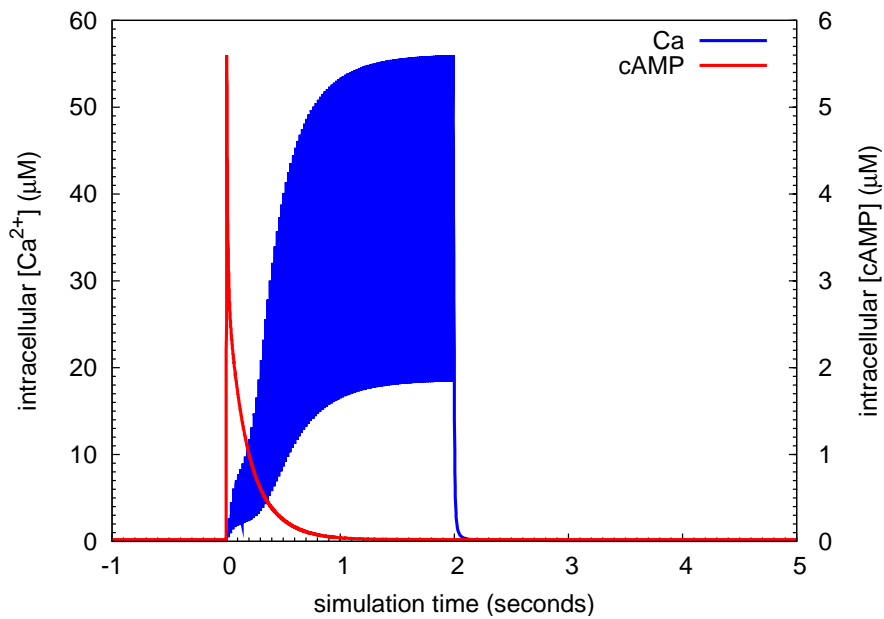


Figure 27: **Stimulation by calcium and cAMP.** 100 calcium spikes are introduced at 50 Hz, as well as a single spike of cAMP.

(2003). As a consequence, calcium-induced a transient ERK activation with the peak level only reaching about 15% of the total protein.
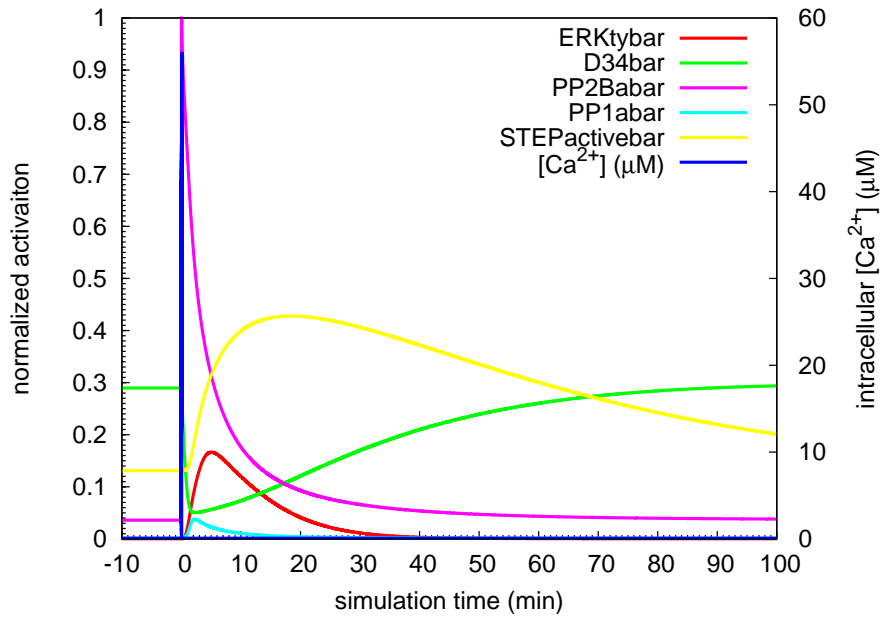


Figure 28: **Effects of a train of Ca²⁺ spikes in the model where PP1 activates STEP.** Time courses of various proteins after the simulation of 100 Ca²⁺ spikes at 50 Hz. 'bar' in the name of a protein indicates a value normalised by the total amount of that protein. Red: activated ERK. Green: phospho DARPP-32 on Thr34. Purple: activated calcineurin. Light blue: activated PP1. Yellow: activated STEP. Dark blue: intracellular Ca²⁺ concentration.

In this model, a transient cAMP pulse triggered DARPP-32 phosphorylation on Thr34 and further decreased PP1 phosphatase activity (Fig. 29). The consequence of this transient PP1 inhibition led to further reduction in STEP activity. However, since there was no upstream calcium input, there was no observable ERK activation.

The paired cAMP and calcium stimuli greatly enhanced ERK activity (Fig. 30). The maximal ERK activation reached approximately 50% of the total protein level, which was more than three-fold greater than the ERK activity induced by calcium alone. As demonstrated experimentally, increased ERK phosphorylation results from combined activation of NMDA and dopamine D1 receptor in the striatum (Valjent *et al.*, 2005), which is in agreement with our paired *in silico* stimulation results. Enhanced ERK activity was due to the positive effect of cAMP on DARPP-32 Thr34 phosphorylation, which counter-

Figure 29: **Effects of a single cAMP spike in the model where PP1 activates STEP.** Time courses of various proteins after the simulation of a single cAMP spike. 'bar' in the name of a protein indicates a value normalised by the total amount of that protein. Dark blue: intracellular cAMP elevation; other colour codes are the same as in Fig. 28.

acted the dephosphorylation effect from calcineurin, resulting from calcium. Therefore, there was no additional PP1 inhibition release from DARPP-32 and no increase in STEP phosphatase ability.



Figure 30: **Effects of a single cAMP pulse and a train of Ca²⁺ spikes in the model where PP1 activates STEP.** Time courses of various proteins after the simulation of a single cAMP pulse and a train of Ca²⁺ spikes. 'bar' in the name of a protein indicates a value normalised by the total amount of that protein. Intracellular elevation of cAMP and Ca²⁺ are not represented here. Other colour codes are the same as in Fig. 28.

In contrast, paired stimuli failed to sufficiently trigger ERK phosphorylation when DARPP-32 was 'knocked out' from the model (Fig. 31). This result had also been observed experimentally, showing that ERK activation induced by both NMDA and D1 receptors is attenuated in DARPP-32 knock-out mice (Valjent *et al.*, 2005).

In order to predict measurable outputs, PP1 or calcineurin was inhibited *in silico*, 50 minutes prior to calcium stimulation by adding 5 µM tautomycetin or 5 µM cyclosporin A correspondingly, which led to dramatically increased ERK activity in both situations when compared with calcium input alone (Fig. 32). Although, in this model, PP1 was the phosphatase activating STEP, inhibiting calcineurin led to the constant phosphorylation of DARPP-32 on Thr34, and therefore a very strong inhibition of PP1. This explains why increased ERK
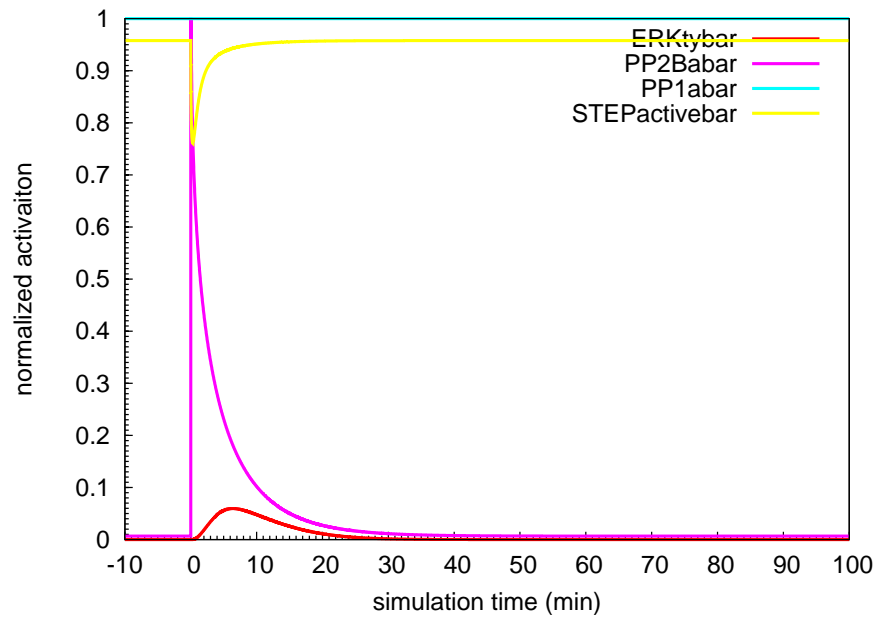
Figure 31: **Effects of a single cAMP pulse and a train of Ca²⁺ spikes in the model where PP1 activates STEP and DARPP-32 knock out.** Time courses of various proteins after the simulation of a single cAMP pulse and a train of Ca²⁺ spikes. 'bar' in the name of a protein indicates a value normalised by the total number of that protein. Intracellular elevation of cAMP and Ca²⁺ are not represented here. Other colour codes are the same as in Fig. 28.

activity, resulting from calcineurin inhibition, cannot be used in support of the hypothesis that calcineurin phosphorylates STEP (Paul *et al.*, 2003).
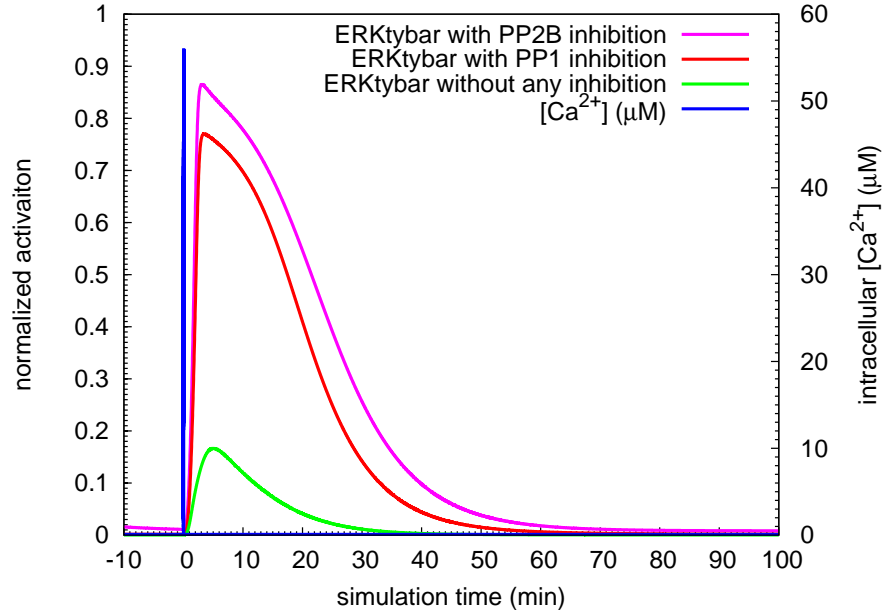


Figure 32: **ERK activity after calcineurin or PP1 inhibition followed by a train of Ca²⁺ spikes, in the model where PP1 activates STEP.** Protein phosphatase, either calcineurin or PP1, was inhibited after equilibrium and 50 minutes before Ca²⁺ input. 'bar' in the name of a protein indicates a value normalised by the total amount of ERK. Purple: ERK activation when calcineurin is inhibited. Red: ERK activation when PP1 is inhibited. Green: ERK activity with only Ca²⁺ input. Blue: intracellular Ca²⁺ concentration.

*Simulation of calcineurin activating STEP*

In the model where calcineurin activates STEP, a train of calcium spikes led to insufficient and transient activation of ERK. This is because activated calcineurin directly increased STEP activity, which in turn dephosphorylated ERK (Fig. 33).

The cAMP pulse alone was also insufficient to induce ERK activation (Fig. 34), whereas paired cAMP and calcium stimuli only slightly increased and prolonged ERK phosphorylation, when compared to a single calcium input (Fig. 35). Therefore, even the combined activa-
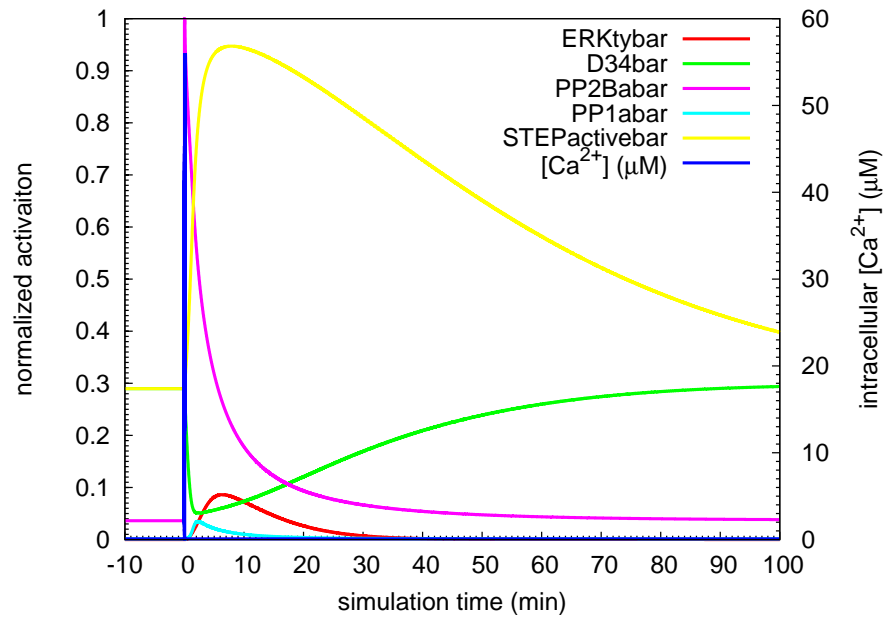
Figure 33: **Effects of a train of Ca²⁺ spikes in the model where calcineurin activates STEP.** Time courses of various proteins after the simulation of 100 Ca²⁺ spikes at 50 Hz. ′bar′ in the name of a protein indicates a value normalised by the total amount of that protein. Red: activated ERK. Green: phospho DARPP-32 on Thr34. Purple: activated calcineurin. Light blue: activated PP1. Yellow: activated STEP. Dark blue: intracellular Ca²⁺ concentration.

tion of NMDA and dopamine D1 receptors was not sufficient to activate ERK. This is not in agreement with experimental data (Valjent *et al.*, 2005).
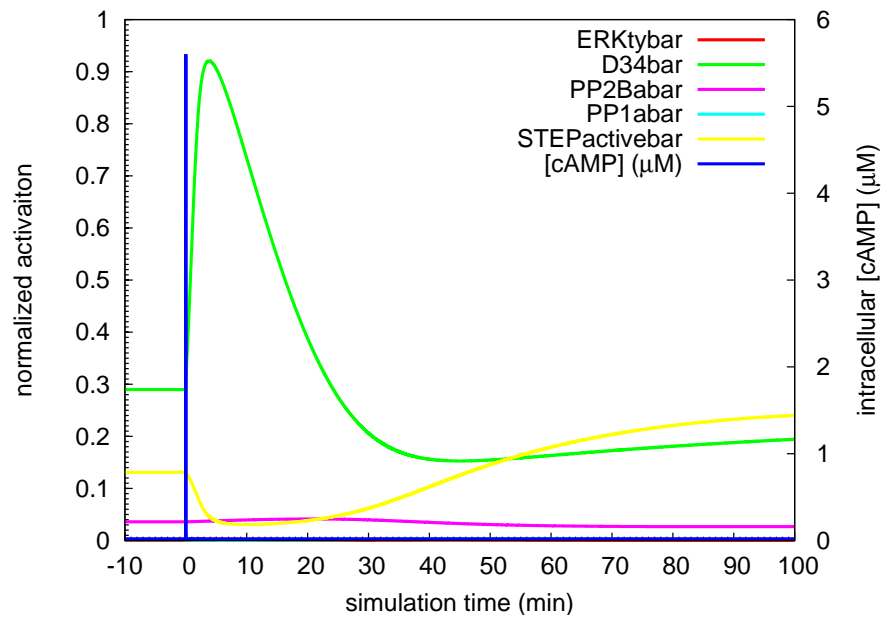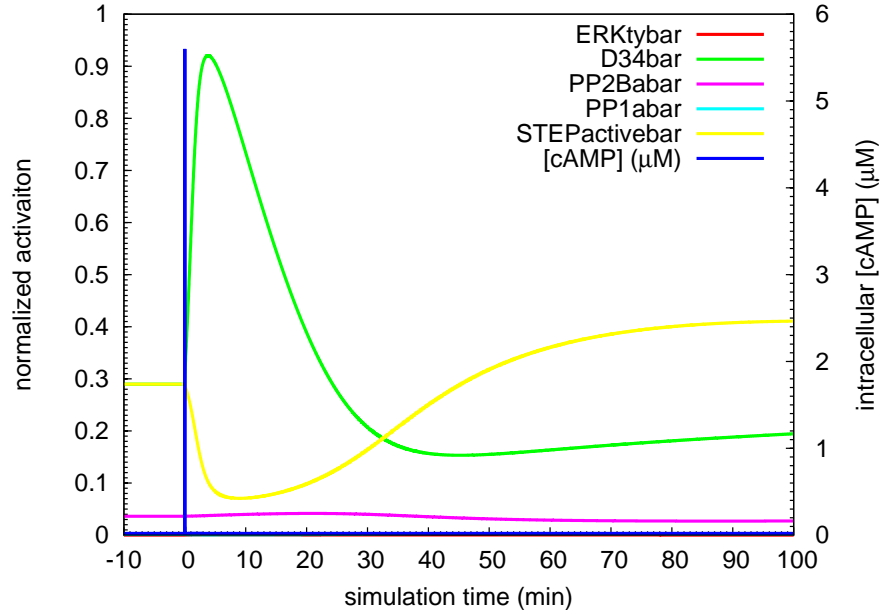


Figure 34: **Effects of a single cAMP spike in the model where calcineurin activates STEP.** Time courses of various proteins after the simulation of a single cAMP spike. 'bar' in the name of a protein indicates a value normalised by the total amount of that protein. Dark blue: intracellular cAMP elevation, other colour codes are the same as in Fig. 33.

In the protein phosphatase inhibition experiments *in silico*, only inhibition of calcineurin significantly increased ERK activity, while PP1 inhibition had no effect (Fig. 36). Since DARPP-32 did not mediate this calcium induced STEP activation, inhibiting PP1 had no effect on STEP activity.

*Summary and conclusion*

Two computational models were constructed, to represent the different regulatory effects on STEP. By comparing the simulations with existing experimental measurements for each model, I have demonstrated how different model structures, whilst utilising the same parameter set, could produce different and distinct simulation results.
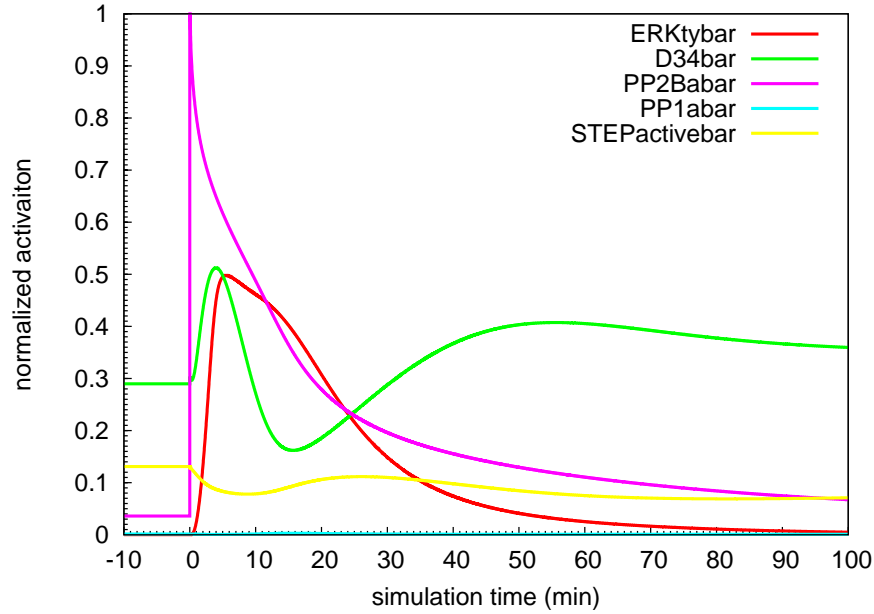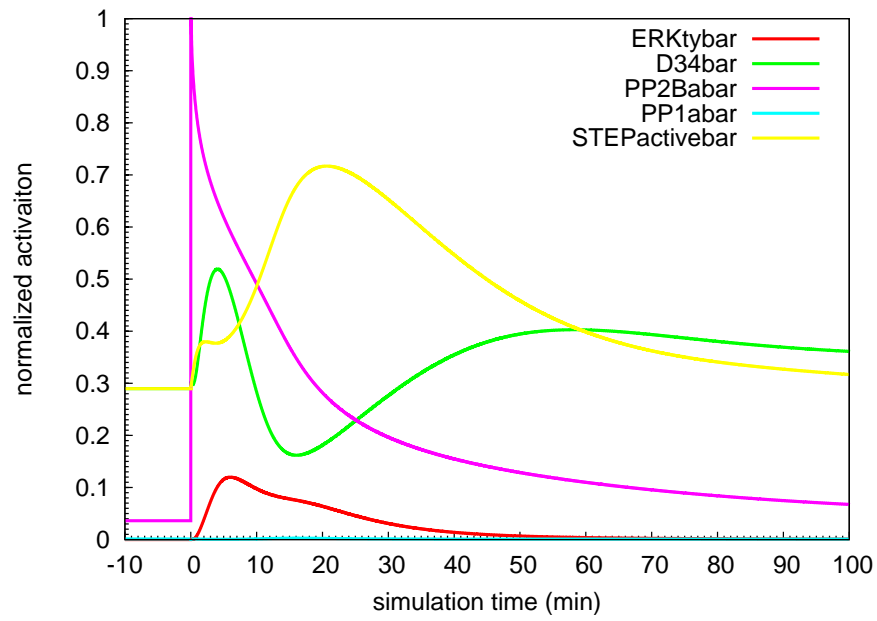
Figure 35: **Effects of a single cAMP pulse and a train of Ca²⁺ spikes in the model where calcineurin activates STEP.** Time courses of various proteins after the simulation of a single cAMP pulse and a train of Ca²⁺ spikes. 'bar' in the name of a protein indicates a value normalised by the total amount of that protein. Intracellular elevation of cAMP and Ca²⁺ are not represented here. Other colour codes are the same as in Fig. 33.
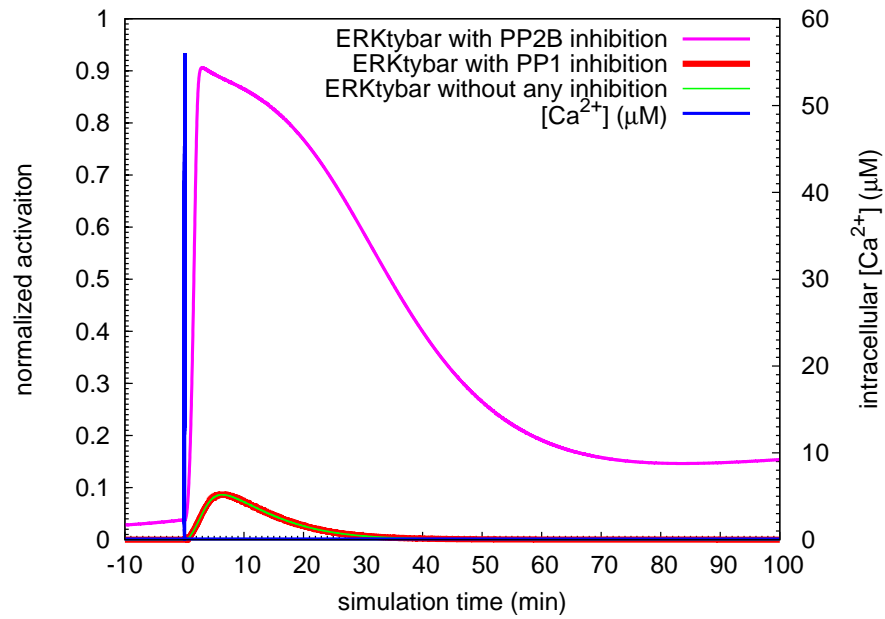
Figure 36: **The ERK activity after calcineurin or PP1 inhibition followed by a train of Ca²⁺ spikes, in the model where calcineurin activates STEP.** Protein phosphatase, either calcineurin or PP1, was inhibited after equilibrium and 50 minutes before Ca²⁺ input. 'bar' in the name indicates a value normalised by the total amount of ERK. Purple: ERK activation when calcineurin is inhibited. Red: ERK activation when PP1 is inhibited. Green: ERK activity with only Ca²⁺ input. Blue: intracellular Ca²⁺ concentration. Since the red line and green line overlapped, the red line is drawn thicker.

DARPP-32, once dephosphorylated by calcineurin, demonstrated reduced inhibition of PP1. The inhibition of calcineurin, as would be expected, increased DARPP-32 phosphorylation on Thr34, thereby increasing the inhibition of PP1. Therefore, experiments based on calcineurin inhibition are somewhat confusing, since the results reflect both the inhibition of calcineurin, and of PP1. This is illustrated in the simulations above, where calcineurin inhibition in both models resulted in increased ERK activity (Fig. 32,36).

In the model where PP1 activates STEP, ERK phosphorylation increased dramatically due to combined *in silico* stimulation from cAMP and calcium (Fig. 30). Furthermore, this activation was attenuated in simulations using a DARPP-32 knock-out (Fig. 31), which is in agreement with experimental observations (Valjent *et al.*, 2005). In contrast, the model where calcineurin activates STEP could not reproduce these phenomena (Fig. 35). Therefore, it is possible that PP1, instead of calcineurin, activates STEP, exerting an inhibitory effect on ERK activity, and that DARPP-32 plays an important role in modulating this effect.

In order to further validate my model, I decided to apply PP1 inhibition on primary striatal neuron cultures, as shown in next section. The idea was to apply specific PP1 inhibitors before glutamate stimulation, then compare ERK activity with the situation when only glutamate is applied. If PP1 adopts inhibitory regulation on ERK via activating STEP, increased ERK phosphorylation upon PP1 inhibition should been observed.

## 3.4 Experimental investigation of PP1 inhibitors on ERK activation

*ERK2 activity in 7-day neuronal cultures*

The 7-day neuronal cultures were treated with glutamate (50 $\mu$M) for varying times and analysed by immunoblotting with the antibody recognising ERK1/2 when phosphorylated on both threonine and tyrosine residues. Basal ERK2 was mainly in the dephosphorylated form. Following glutamate stimulation, ERK2 phosphorylation reached its

peak level within 2 to 5 minutes, and then decreased (Fig. 37 and Fig. 38).

The tautomycetin (TC) treatment followed by glutamate stimulation resulted in similar transient activation of ERK2 and there was no significant difference between treated and untreated sample at any time point (Fig. 37 and Fig. 38).



Figure 37: **ERK2 activity in response to PP1 inhibition and glutamate stimulation in 7-day neuronal cultures.** Activation of ERK2 after glutamate stimulation for the duration indicated on the x-axis. Green bars represent cultures only stimulated with glutamate. Red bars represent cultures incubated with tautomycetin(5 $\mu$M, 50 minutes) followed by glutamate stimulation. The data was collected from 7-day primary cultures of striatal neurons. Quantification of ERK2 activation was calculated using the ratio between phospho-ERK2 and corresponding total ERK2. Data are mean $\pm$ SEM (four repeats per group). Paired T-test indicated no significant difference between TC treated and control group, for all time points.

*ERK activity in 14-day neuronal cultures*

In contrast to 7-day cultures, 14-day primary cultures revealed a much higher basal ERK2 activity. Incubating neurons with glutamate (50 $\mu$M) for varying times resulted in a marked time-dependent decrease in
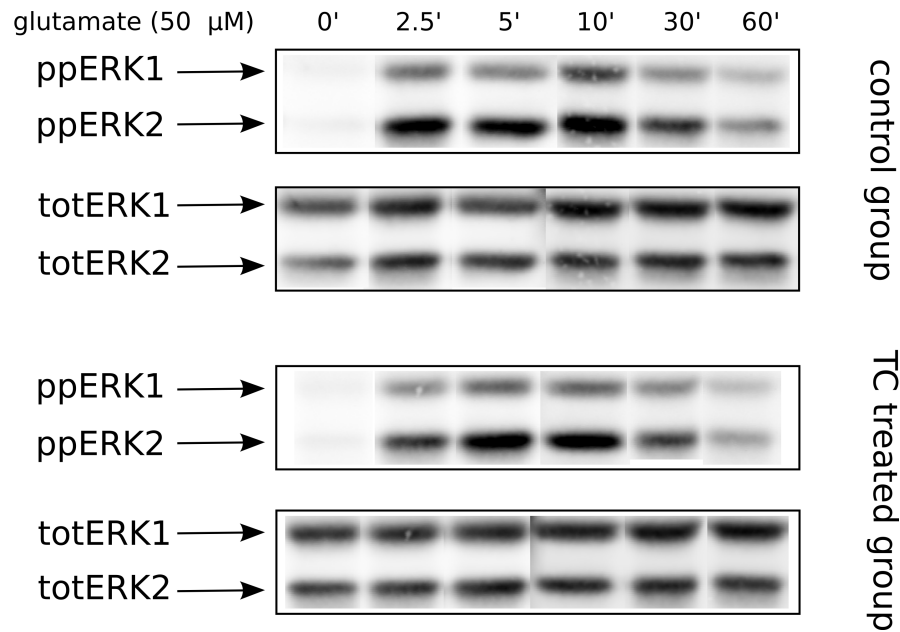
Figure 38: **Western blot image of ERK1/2 activity in response to PP1 inhibition and glutamate stimulation in 7-day neuronal cultures.** Western blot of samples extracted from 7-day culture, as described in 3.2. Control samples were compared with TC treated samples (5 $\mu$M, 50 minutes).

dual-phosphorylated ERK2, suggesting that ERK2 was rapidly inactivated following glutamate treatment (Fig. 39 and Fig. 40).

Surprisingly, PP1 inhibition by TC treatment in these neurons resulted in a much pronounced decrease in ERK2 activation, not only at basal condition but also at every glutamate treated time point compared with untreated group (Fig. 39 and Fig. 40). This result indicates that PP1 has a stimulating effect on ERK activity in 14-day cultures of striatal neurons.

TC can also inhibit PP2A nonspecifically (higher $IC_{50}$ than for inhibiting PP1). To rule out such an effect, I examined the phosphorylation status of ERK2 after PP2A inhibition by incubating cultures with okadaic acid, followed by glutamate treatment. Immunoblotting analysis shows a strong increase in dual-phosphorylated ERK2 at basal time point (0 min), as well as at all glutamate-treated time points (Fig. 41). As PP2A, a major serine/threonine phosphatase, can directly dephosphorylate ERK2 on the threonine residue, the increase in ERK activity is not surprising. These data suggests that the TC treatment does not inhibit the effect of PP2A on ERK, and that results ob-
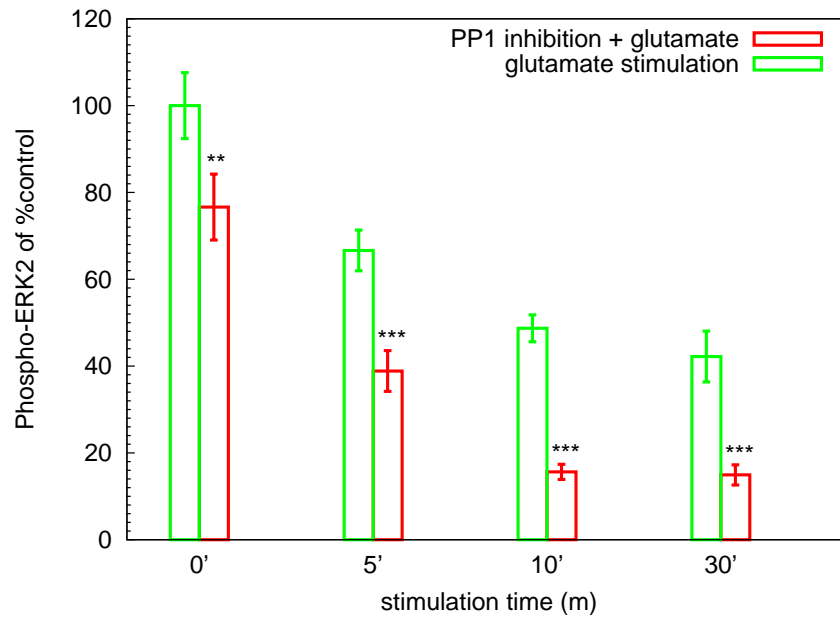
Figure 39: **ERK2 activity in response to PP1 inhibition and glutamate stimulation in 14-day cultured neurons.** Activation of ERK2 after glutamate stimulation for the duration indicated on the x-axis. Green bars represent the group only stimulated with glutamate. Red bars represent the group incubated with tautomycetin (5 $\mu$M, 50 min) followed by glutamate stimulation. The data was collected from 14-day primary striatal neuron cultures. Quantification of ERK2 activation was calculated using the ratio between phospho-ERK2 and total ERK2. Data are mean $\pm$ SEM (7 repeats per group), paired T test: **, P<0.01; ***, P<0.002
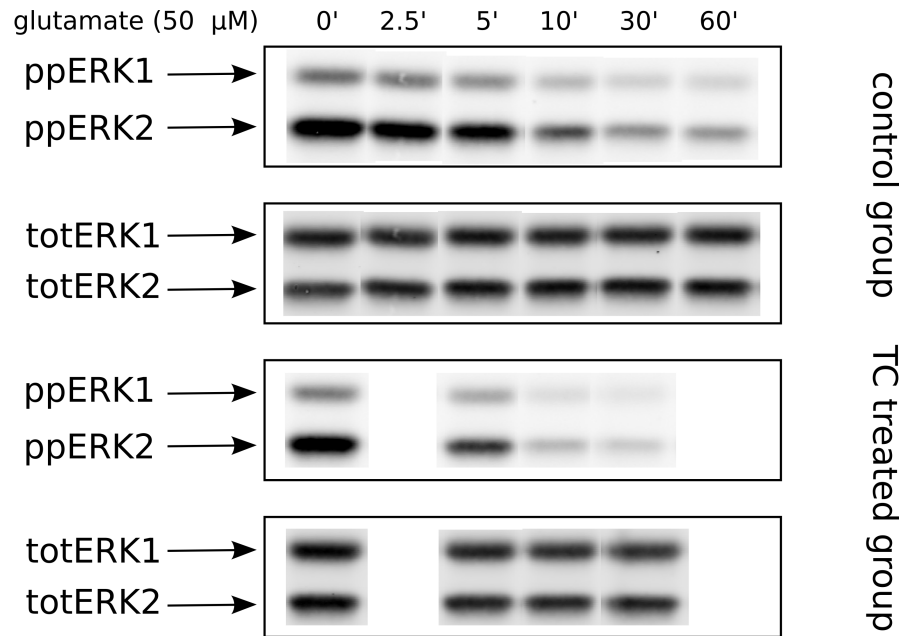
Figure 40: **Western blot image of ERK1/2 activity in response to PP1 inhibition and glutamate stimulation in 14-day neuronal cultures.** Western blot of samples extracted from 14-day culture, as described in 3.2. Control samples were compared with TC treated samples (5 $\mu$M, 50 min).

served are due to PP1 inhibition. Since, ERK2 activity still decreased over time, even after inhibition of PP2A, the glutamate-induced ERK2 dephosphorylation might be due to a glutamate-activated tyrosine phosphatase or to a glutamate-inhibited kinase, upstream of the MAP kinase pathway.

In order to confirm the results of the western blots, immunofluorescence experiments on 14-day cultured neurons were carried out. In the basal state, ERK2 was present primarily in the dual-phosphorylated form (Fig. 42). Incubation with glutamate for 10 minutes resulted in decreased ERK2 activity (Fig. 43). Neurons with TC treatment exhibited dramatically decreased ERK2 activity in the basal state (Fig. 44), and in 10-minute glutamate treated states (Fig. 45). The immunofluorescence results are summarised in Fig. 46.
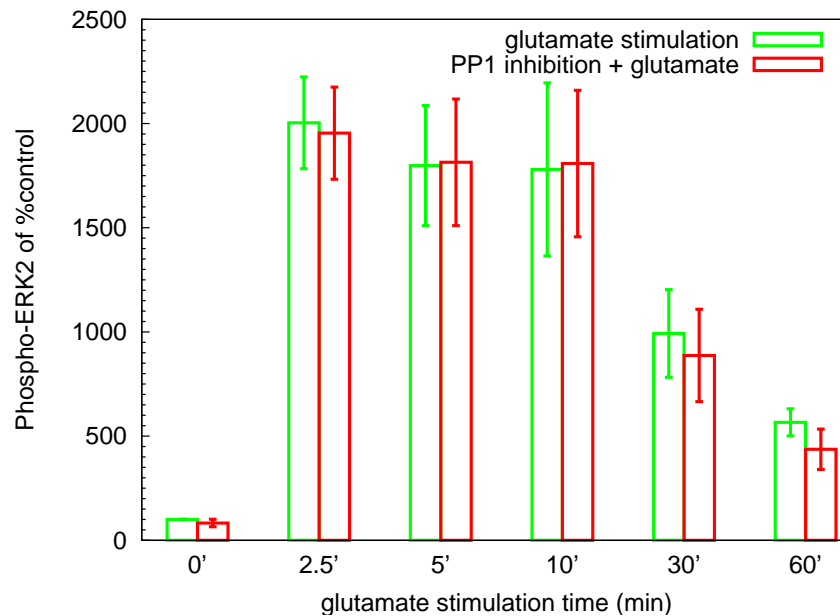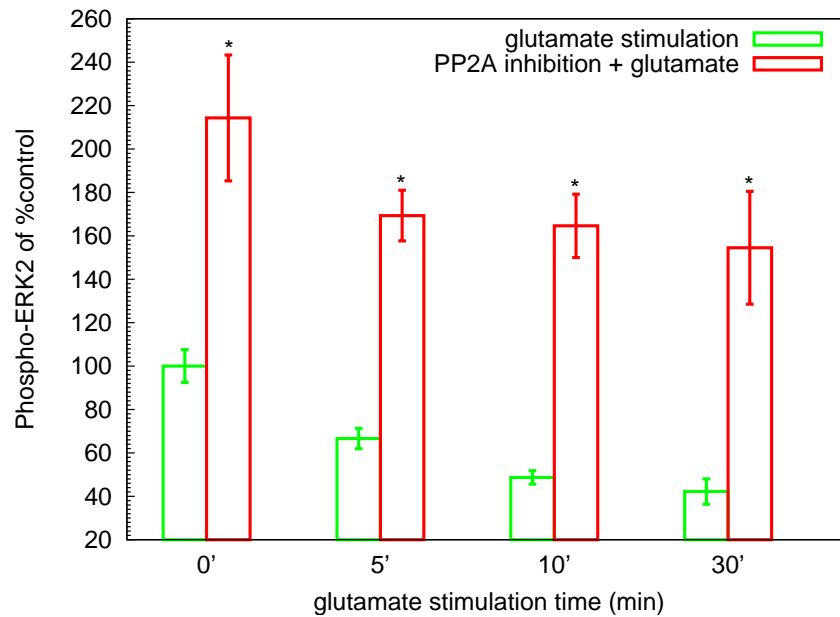
Figure 41: **ERK2 activity in response to PP2A inhibition and glutamate stimulation in 14-day neuronal cultures.** Activation of ERK2 after glutamate stimulation for the duration indicated on the x-axis. Green bars represent the group only stimulated with glutamate. Red bars represent the group incubated with okadaic acid (500 nM, 50 min) followed by glutamate stimulation. The data was collected from 14-day primary striatal neuronal cultures. Quantification of ERK2 activation was calculated using the ratio between phospho-ERK2 and total ERK2. Data are mean ± SEM (3 repeats per group), paired T test: *, P<0.05
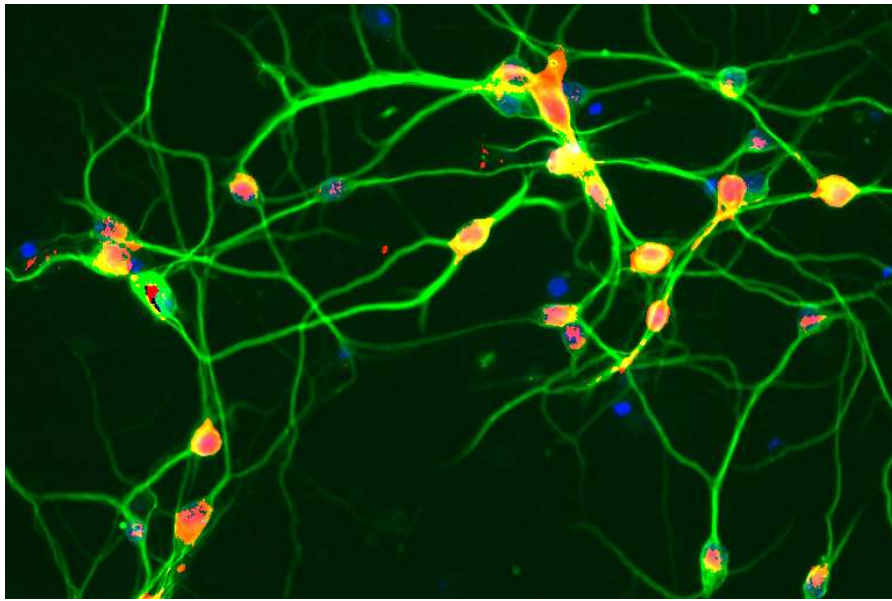
Figure 42: **Immunofluorescence image of ERK1/2 activation at basal level in 14-day neuronal cultures.** Immunofluorescence colabelling of MAPK2 (in green), activated ERK (in red), and nuclear (in blue).
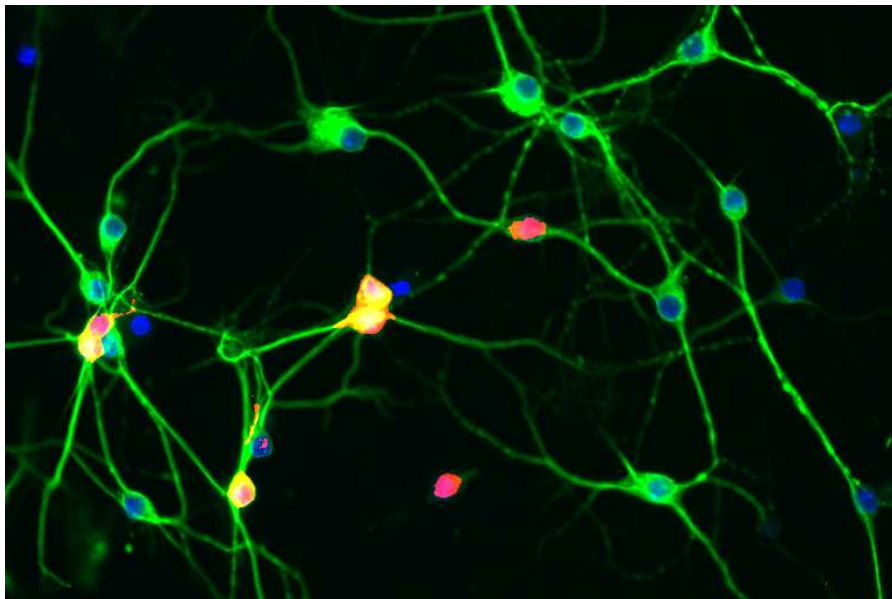


Figure 43: **Immunofluorescence image on ERK1/2 activation after 10 minutes glutamate stimulation in 14-day neuronal cultures.** Immunofluorescence colabelling of MAPK2 (in green), activated ERK (in red), and nuclear (in blue).
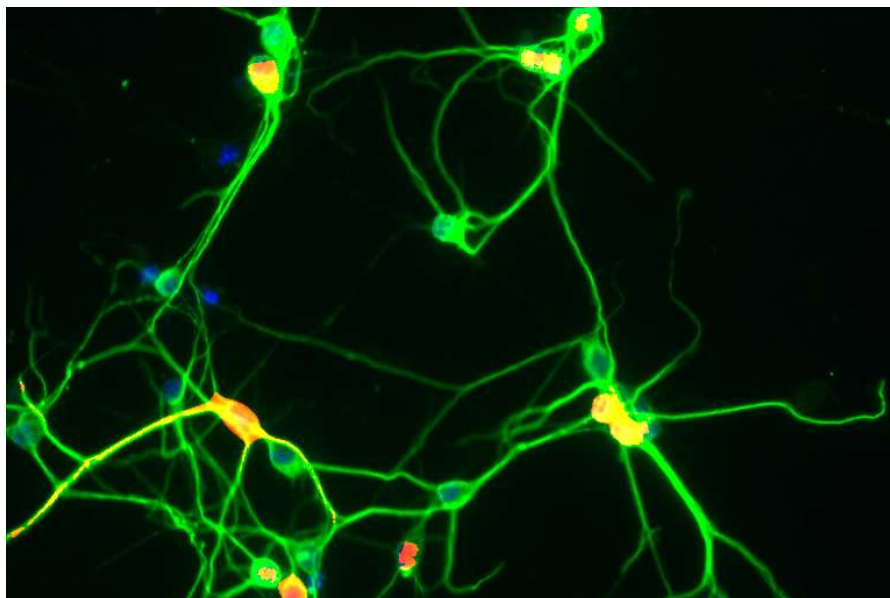
Figure 44: **Immunofluorescence image on ERK1/2 activation in response to PP1 inhibition in 14-day neuronal cultures.** Immunofluorescence colabelling of MAPK2 (in green), activated ERK (in red), and nuclear (in blue). 14-day neuronal cultures were treated with tautomycetin for 50 minutes before fixation.
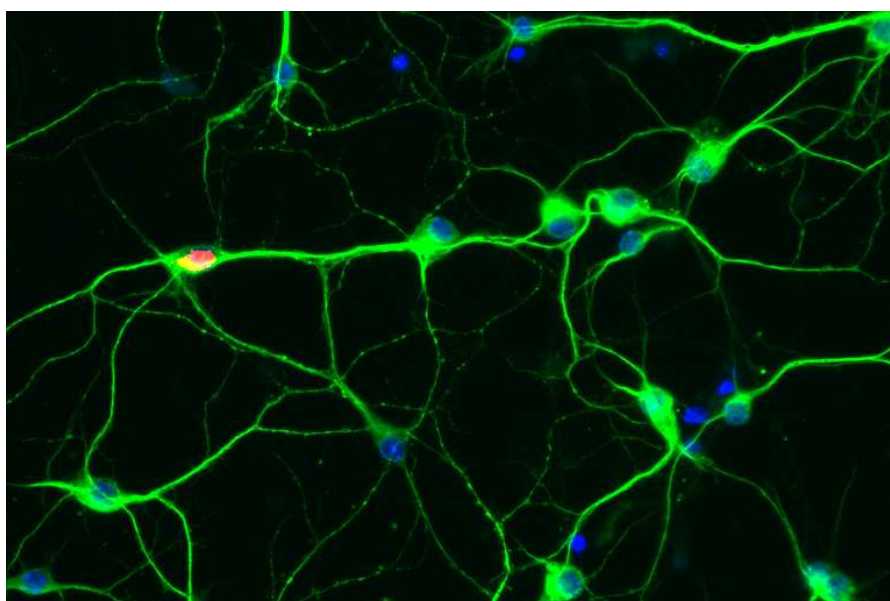


Figure 45: **Immunofluorescence image on ERK1/2 activation in response to PP1 inhibition and glutamate stimulation in 14-day neuronal cultures.** Immunofluorescence colabelling of MAPK2 (in green), activated ERK (in red), and nuclear (in blue). 14-day neuronal cultures were treated with tautomycetin for 50 minutes followed by glutamate for 10 minutes before fixation.
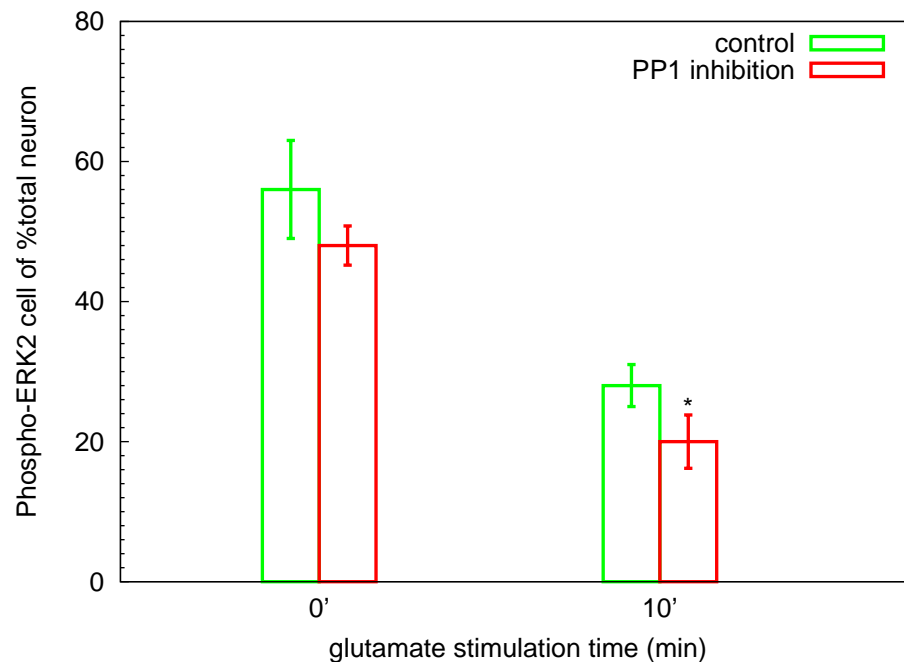
Figure 46: **Summary of immunofluorescence experiments on ERK1/2 activation**. The cells were enumerated using immunofluorescence images following PP1 inhibition and glutamate stimulation, in 14-day neuronal cultures. Green bars represent the group stimulated only with glutamate. Red bars represent the group incubated with tautomycetin (5 $\mu$M, 50 min) prior to glutamate stimulation. Data are mean $\pm$ SEM (On average, 120 neurons were counted across 6 regions per coverslip. 3 repeats per group). paired T test: *, P=0.04. A more detailed description of the procedure is given in 3.2.

*Summary and conclusion*

Experiments, conducted on primary striatal neuron cultures, displayed a switch in glutamate influence on ERK2 activity, changing from activation to inhibition, after 7 and 14 days respectively. Surprisingly, in 14-day cultures, PP1 exerted a stimulatory effect on ERK2, instead of the predicted inhibitory effect by previous work (Valjent *et al.*, 2005), and incorporated into my initial computational models. Furthermore, according to the immunofluorescence results above, the phosphorylation of ERK2 predominantly occurred in neuronal cells. Thus, some non-neuronal contribution cannot be the explanation for glutamate induced ERK2 dephosphorylation.

A possible explanation to these contradictory results might be the different neuronal differentiation states. This is evidenced, firstly, by the differential effects observed of glutamate on ERK2 activity, which varied with the culture duration. This may indicate a developing glutamate signalling pathway. Secondly, previous *in vivo* work with DARPP-32 knock-out mice demonstrated that PP1 indirectly exerts a negative effect on MAP kinase pathway (Valjent *et al.*, 2005). The results obtained here were *in vitro* from primary cultured neurons, which may not be as mature as the neurons in a normal functioning brain. Would it be possible that, during neuronal differentiation, the effect of PP1 on ERK changes?

As highlighted previously (section 3.1), NR2A- and NR2B-containing NMDA receptors have opposite effects on ERK activity. The inhibitory effect exerted by NR2B-containing NMDA receptor is due to the activation, by CaMKII, of SynGAP, a synaptic-specific Ras-GAP protein. Since PP1 deactivates CaMKII, it prevents CaMKII's negative regulation on the MAP kinase pathway. In short, 14-day cultured striatum neurons may not be mature, and may predominantly express NR2B-containing NMDA receptors. Therefore, in these neurons, PP1 would act as a positive regulator of ERK activation.

## 3.5    Dual influence of PP1 on ERK activity

*Model structure and simulation plan*

Based on my experimental results, as described above, and their possible explanation, a preliminary model was constructed (Fig. 47). In this model, the ratio of NR2A- and NR2B-containing NMDA receptors determines the amplitude and duration of calcium influx through NMDA receptors, because of their distinct gating and pharmacological properties (Cull-Candy *et al.*, 2001; Naoki *et al.*, 2005). NR2B-containing NMDA receptor also serves as a scaffold protein, coupling SynGAP and CaMKII, and thereby facilitating the phosphorylation of SynGAP by activated CaMKII. CaMKII is activated by binding calmodulin, then autophosphorylates on Thr286, increasing its affinity for calmodulin. The activation of the MAP kinase pathway is initiated by calmodulin activating Ras-GRF, which in turn catalyses RasGDP phosphorylation to generate RasGTP. RasGTP binds and activates Raf, which then activates MEK, thereby stimulating ERK. ERK can be dephosphorylated by dual-specific phosphatase MKP, threonine/serine phosphatase PP2A and tyrosine phosphatase STEP. In this model, PP1 displays two modulations of the MAP kinase pathway: on the one hand, PP1 stimulates STEP, deactivating ERK; on the other hand, PP1 dephosphorylates CaMKII, inhibiting SynGAP, thereby stimulating ERK. As this model is the expanded version of the MAP kinase model described before (3.3), only the additional quantitative parameters are listed in Table 5, and additional abbreviations are explained in Table 6. This model and the Python script for simulation in E-Cell are available online (`http://www.ebi.ac.uk/~luli/thesis/mapk/dual/`).

In the following section, I present results obtained from two different models, where either NR2B- or NR2A-containing NMDA receptor is predominantly expressed. All other parameters remain exactly the same. Several simulation experiments were designed to replicate the stimuli used in experiments on primary cultures. The *in silico* stimulations for each model include: 1) a train of low-frequency calcium pulses, applied as a background signal, to replicate basal spontaneous glutamate activity. This mimics a relatively high ERK basal activ-

ity, corresponding to that observed experimentally in 14-day cultured neurons; 2) a group of calcium spikes at high frequency, in order to model the effect of glutamate stimulation; 3) the PP1 inhibitor, tautomycetin, introduced 50 minutes before the high frequency calcium inputs, to duplicate protein phosphatase inhibition experiments.

By using a computational modelling approach, I tested to ascertain whether the type of NMDA receptors expressed could cause a switch in the roles of PP1 on ERK activity.

Figure 47: **Computational model of the dual effect of PP1 on ERK activity.** PP1 inhibitory and stimulatory effects on ERK1/2 are depicted in green and red respectively. For clarity, the DARPP-32 pathway and other phosphatases of ERK1/2, except STEP, are not included in this diagram. The graphical conventions are those of the Process Description language of Systems Biology Graphical Notation (SBGN) (Le Novère *et al.*, 2009). Rectangular box with rounded corners: macromolecule, circular container: simple chemical, elliptical container: state variable, "empty set": a source or sink, rectangle with cut-corners: complex, square on the arc: process, filled disc on the arc: association, filled arrow head: production, empty arrow head: stimulation, empty circle: catalysis.
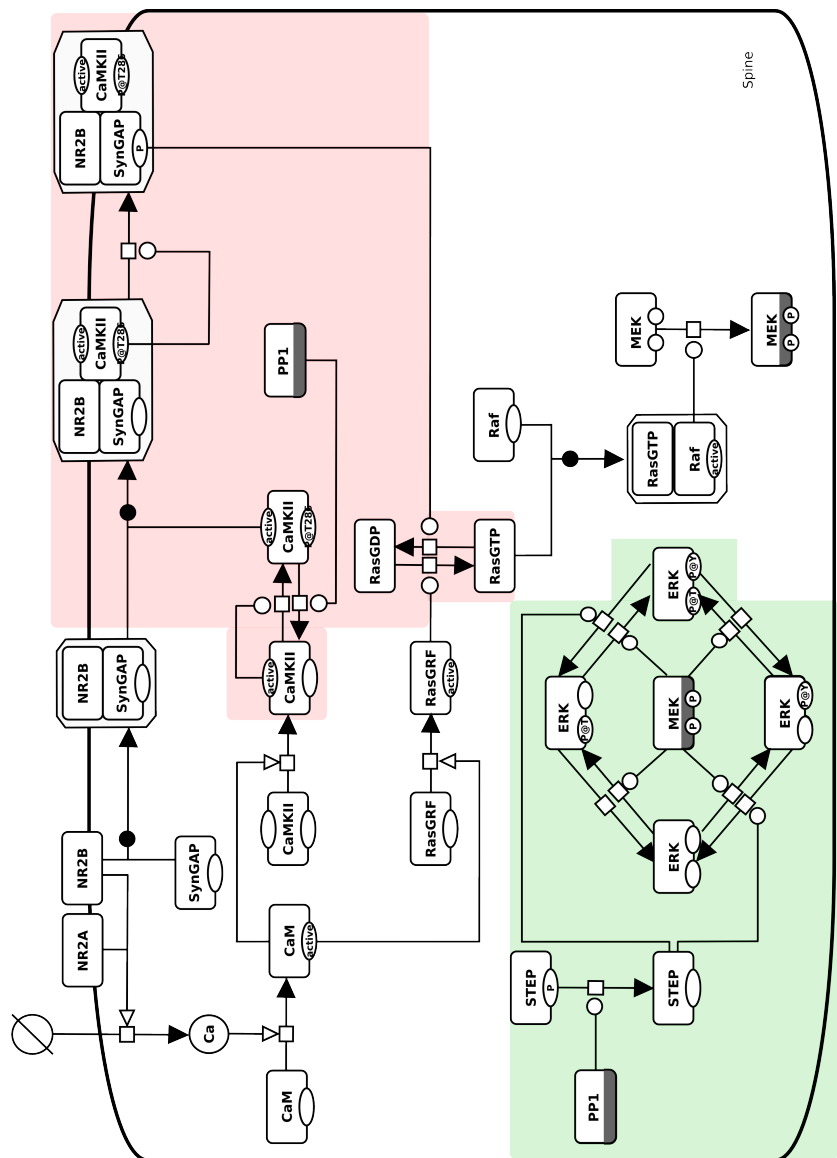
Table 5: List of parameters used for simulation of the expanded MAP kinase model that simulates the dual regulatory roles of PP1 on ERK1/2. Only additional parameters that differ from those in Table 3 on page 65 are listed.

| Parameter | Value | Reference |
|---|---|---|
| *SynGAP* binding *NR2B*: | | |
| $k_{on}$ | $6 \times 10^8 \, M^{-1}s^{-1}$ | this study* |
| $k_{off}$ | $1 \, s^{-1}$ | this study* |
| *CaMCa4* binding *CaMKII*: | | |
| $k_{on_{CaMKII}}$ | $3.2 \times 10^6 \, M^{-1}s^{-1}$ | (Tzortzopoulos *et al.*, 2004)[1] |
| $k_{off_{CaMKII}}$ | $0.343 \, s^{-1}$ | (Tzortzopoulos *et al.*, 2004)[1] |
| $k_{on_{CaMKIIp}}$ | $3.2 \times 10^6 \, M^{-1}s^{-1}$ | (Tzortzopoulos *et al.*, 2004)[1] |
| $k_{off_{CaMKIIp}}$ | $0.001 \, s^{-1}$ | (Meyer *et al.*, 1992)[2] |
| *CaMKII* autophosphorylation on *Thr*286: | | |
| $k_{Thr286p}$ | $6.3 \, s^{-1}$ | (Lučić *et al.*, 2008)[3] |
| *CaMKIIp* binding *NR2B*: | | |
| $k_{on}$ | $2.76 \times 10^8 \, M^{-1}s^{-1}$ | this study* |
| $k_{off}$ | $1 \, s^{-1}$ | this study* |
| *CaMKIIp_NR2B* phosphorylates *SynGAP_NR2B*: | | |
| $k$ | $1.0 \, s^{-1}$ | this study* |
| *SynGAPp_NR2B* dephosphorylation: | | |
| $k$ | $0.02 \, s^{-1}$ | this study* |
| *PP1* dephosphorylates *CaMKII*: | | |
| $k_{on_{CaMKIIp_pP1}}$ | $3.0 \times 10^6 \, M^{-1}s^{-1}$ | this study* |
| $k_{off_{CaMKIIp_pP1}}$ | $0.5 \, s^{-1}$ | this study* |
| $k_{cat_{CaMIIp_pP1}}$ | $2.0 \, s^{-1}$ | (Zhabotinsky, 2000)* |

Table 5: continued

*CaMCa*4 activates *RasGEF*:

| | | |
|---|---|---|
| $k_{on}$ | $3 \times 10^7 \, M^{-1}s^{-1}$ | this study[*] |
| $k_{off}$ | $0.6 \, s^{-1}$ | this study[*] |

*RasGDP* activation by *CaMCa4_RasGEF*:

| | | |
|---|---|---|
| $k_{cat}$ | $2 \, s^{-1}$ | (estimate from Sasagawa *et al.*, 2005)[*] |
| $K_m$ | $2 \times 10^{-8} \, M$ | (estimate from Sasagawa *et al.*, 2005)[*] |

*RasGTP* dephosphorylation by *SynGAP*:

| | | |
|---|---|---|
| $k_{on}$ | $5 \times 10^6 \, M^{-1}s^{-1}$ | (Sasagawa *et al.*, 2005)[*],[4] |
| $k_{off}$ | $4 \, s^{-1}$ | (Sasagawa *et al.*, 2005)[*],[4] |
| $k_{cat}$ | $10 \, s^{-1}$ | (Sasagawa *et al.*, 2005)[*],[4] |

*RasGTP* autodephosphorylation:

| | | |
|---|---|---|
| $v_{max}$ | $1 \times 10^{-8} \, Ms^{-1}$ | this study[*] |
| $K_m$ | $1 \times 10^{-6} \, M$ | this study[*] |

*RasGTP* activates *Raf* :

| | | |
|---|---|---|
| $k_{on}$ | $6 \times 10^7 \, M^{-1}s^{-1}$ | (Sasagawa *et al.*, 2005)[*] |
| $k_{off}$ | $0.5 \, s^{-1}$ | (Sasagawa *et al.*, 2005)[*] |

*Raf* inactivation:

| | | |
|---|---|---|
| $v_{max}$ | $1 \times 10^{-8} \, Ms^{-1}$ | this study[*] |
| $K_m$ | $1 \times 10^{-6} \, M$ | this study[*] |

$Ca^{2+}$ input :

| | | |
|---|---|---|
| $k$ | $5 \times 10^{-3} - 20 \times 10^{-3} \, Ms^{-1}$ | $-rI/2FV$ |

Numbers:

Table 5: continued

| | | |
|---|---|---|
| $F$ | $9.6485 \times 10^4\, Cmol^{-1}$ | Faraday's constant |
| total NR2 subunits | 40 | (cf. Racca *et al.*, 2000)[5] |
| $I$ | $5 - 20\, pA$ | (Naoki *et al.*, 2005)*,[6], dependeing on NMDA receptor composition. |
| $r$ | 0.2 | (Naoki *et al.*, 2005)*,[6], the fraction of current I carried by $Ca^{2+}$. |
| Concentrations: | | |
| [CaMKII] | $7 \times 10^{-5}\, M$ | (cf. Petersen *et al.*, 2003)[7] |
| [SynGAP] | $5 \times 10^{-6}\, M$ | (cf. Cheng *et al.*, 2006)[8] |
| [RasGEF] | $1.8 \times 10^{-7}\, M$ | this study* |
| [RasGDP] | $1.8 \times 10^{-7}\, M$ | (Bhalla and Iyengar, 1999)* |

Table 5: List of parameters used for simulation of the expanded MAP kinase model that simulates the dual regulatory roles of PP1 on ERK1/2. Only additional parameters that differ from those in Table 3 on page 65 are listed. Asterisk indicates that the reference refers to a computational model. [1,2,3]: Parameters were obtained from *in vitro* experiments. [4]: Sasagawa *et al.* (2005) estimated these parameters according to Gideon *et al.* (1992). [5]: Data was obtained from synaptic immunogold labelling for NMDARs of rats pyramidal neuron. [6]: Naoki *et al.* (2005) estimated these parameters according to Nimchinsky *et al.* (2004); Piña-Crespo and Gibb (2002). [7]: Measurement was obtained from immunogold labelling on isolated PSD extract from rats forbrain. [8]: Data was obtained from PSD fractions prepared from rat forebrains and cerebellums.

| Abbreviations | Definition/Reference |
| --- | --- |
| CaMKII | calcium/calmodulin-dependent protein kinase II GO:0005954 |
| SynGAP | synaptic Ras GTPase activating protein UniProt:Q9QUH6 |
| RasGEF | Ras guanine nucleotide exchange factor InterPro:IPR008937 |
| Ras | Ras small GTPase InterPro:IPR020849 |

Table 6: List of abbreviations used in expanded MAP kinase model that concerns dual regulatory roles of PP1 on ERK1/2. Only additional abbreviations that differ from those in Table 4 on page 76 are listed.

*Distinct ERK activity induced by different compositions of NMDA receptors*

High frequency calcium inputs caused a decrease of ERK activity when NR2B-containing NMDA receptors were highly expressed (Fig. 48), akin to the glutamate induced ERK dephosphorylation in 14-day neuronal cultures (Fig. 39). This model further supports the hypothesis that reduced ERK phosphorylation may be due to the activation of CaMKII, and the subsequent activation of SynGAP (Fig. 48). In contrast, where NMDA receptors were predominantly composed of NR2A subunits, glutamate stimulated ERK activity. This is the result of the insufficiency NR2B subunits to couple CaMKII with SynGAP (Fig. 49). The low ERK activation peak in this figure is due to the basal activity of STEP.

*Distinct responses induced by different compositions of NMDA receptors after PP1 inhibition*

When PP1 was inhibited in the model where NMDA receptors are predominantly composed of NR2B, PP1 inhibition resulted in a reduction of basal ERK activity. Upon high frequency calcium stimulation,
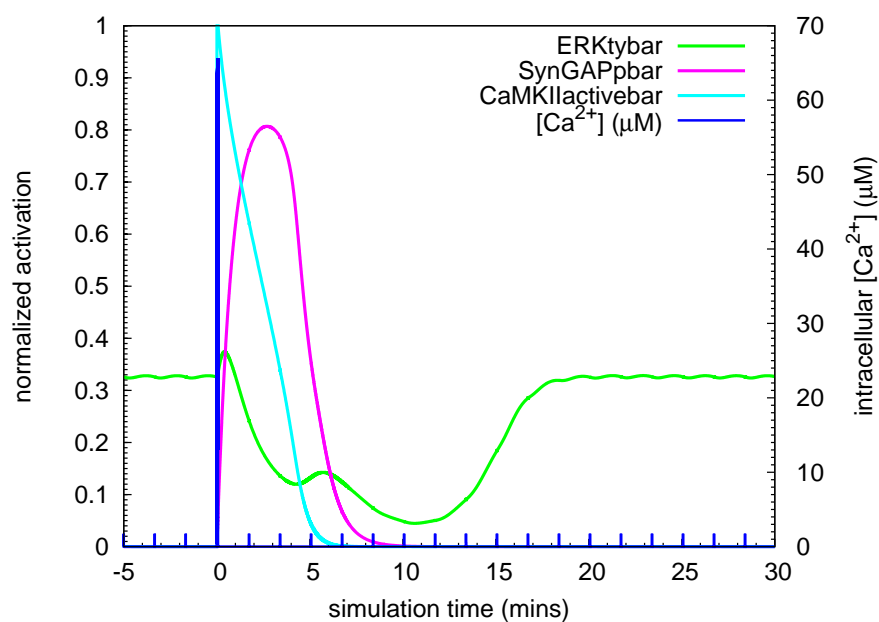
Figure 48: **Effects of Ca²⁺ stimulation in the model where NR2B subunits constitute 90% of the total NR2 subunits.** Time courses of indicated proteins after simulation of high frequency Ca²⁺ input, in a low frequency Ca²⁺ spike background. In this model, NR2B-containing NMDA receptors were composed of 90% of the total NMDA receptors. 'bar' in the name of a protein indicates a value normalised by the total amount of this protein. Green, activated ERK; Purple, phosphorylated SynGAP; Light blue, activated CaMKII; Dark blue, intracellular Ca²⁺.
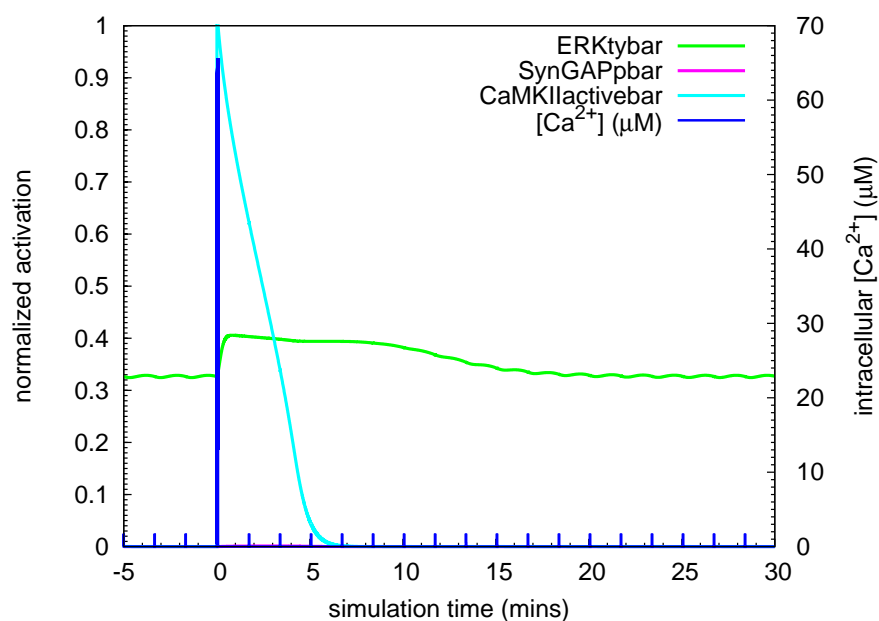
Figure 49: **Effects of Ca²⁺ stimulation in the model where NR2A subsunits constitute 90% of the total NR2 subunits.** Time courses of indicated proteins after simulation of high frequency Ca²⁺ input, in a low frequency Ca²⁺ spike background. In this model, NR2A-containing NMDA receptors were composed of 90% of the total NMDA receptors. 'bar' in the name of a protein indicates a value normalised by the total amount of this protein. Colour codes are the same as in Fig. 48.

dual phosphorylated ERK displayed a sharp but transient rise, which then fell steeply at a rate that was faster than without PP1 inhibition (Fig. 50). Thus, this model reproduces ERK activity as observed in 14-day cultures, and suggests a mechanism whereby PP1 could play a role to enhance ERK activity. The inhibition of PP1 switched on the sustained activation of CaMKII, which was then translated into the persistent activation of SynGAP via NR2B coupling (Fig. 51), thereby resulting in the inhibition of the Ras-ERK pathway. On the other hand, when NMDA receptors were predominantly composed of NR2A, the inhibition of PP1 significantly increased ERK activity following a high frequency calcium stimulation, because of the decreased STEP phosphatase activity (Fig. 52). Therefore, in the latter model, PP1 plays an inhibitory role on ERK activity. Overall, these two models, by switching the composition of NR2 subunits of NMDA receptor, suggest two opposing roles for PP1 in the regulation of the Ras-ERK pathway.
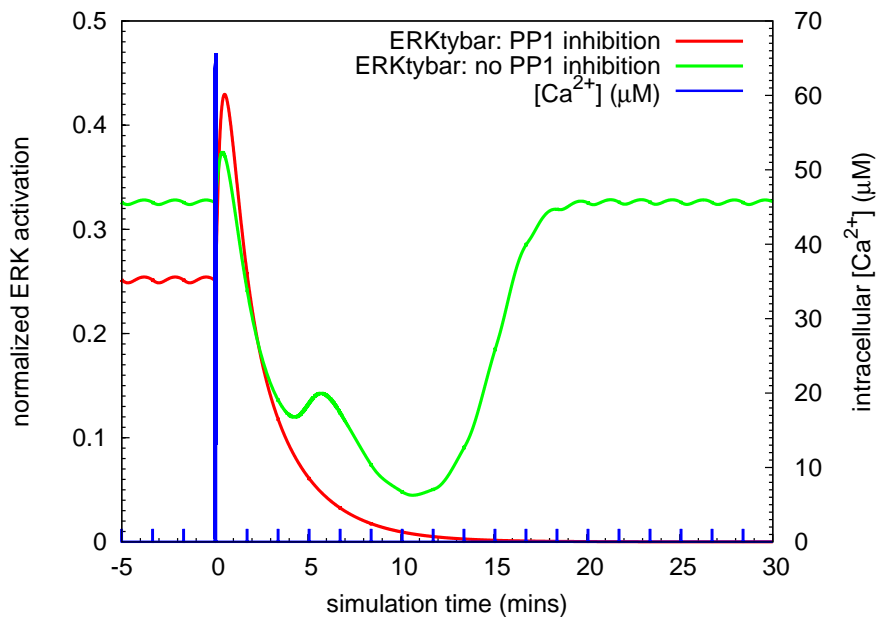


Figure 50: **ERK activity after Ca²⁺ stimulation in the model where NR2B subunits constitute 90% of the total NR2 subunits.** Comparison of ERK activities between PP1 inhibited (red line) and PP1 not inhibited (green line) situations after Ca²⁺ stimulation. In this model, NR2B- containing NMDA receptors were composed of 90% of the total NMDA receptors. 'bar' in the name indicates a value normalised by the total amount of ERK. Dark blue line represents intracellular Ca²⁺ concentration.
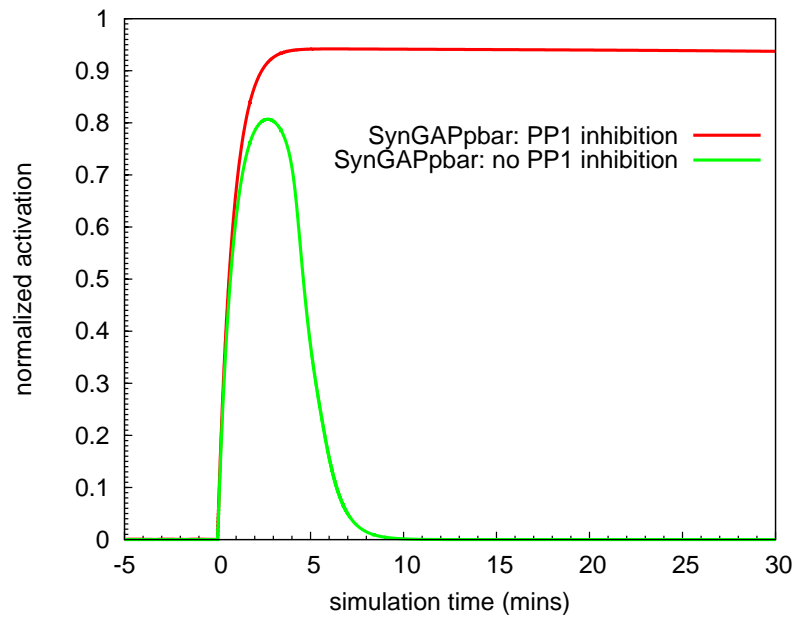
Figure 51: **SynGAP activity after Ca²⁺ stimulation in the model where NR2B subsunits constitute 90% of the total NR2 subunits.** Comparison of SynGAP activities between PP1 inhibited (red line) and PP1 not inhibited (green line) situations after Ca²⁺ stimulation. In this model, NR2B- containing NMDA receptors were composed of 90% of the total NMDA receptors. 'bar' in the name indicates a value normalised by the total amount of SynGAP.
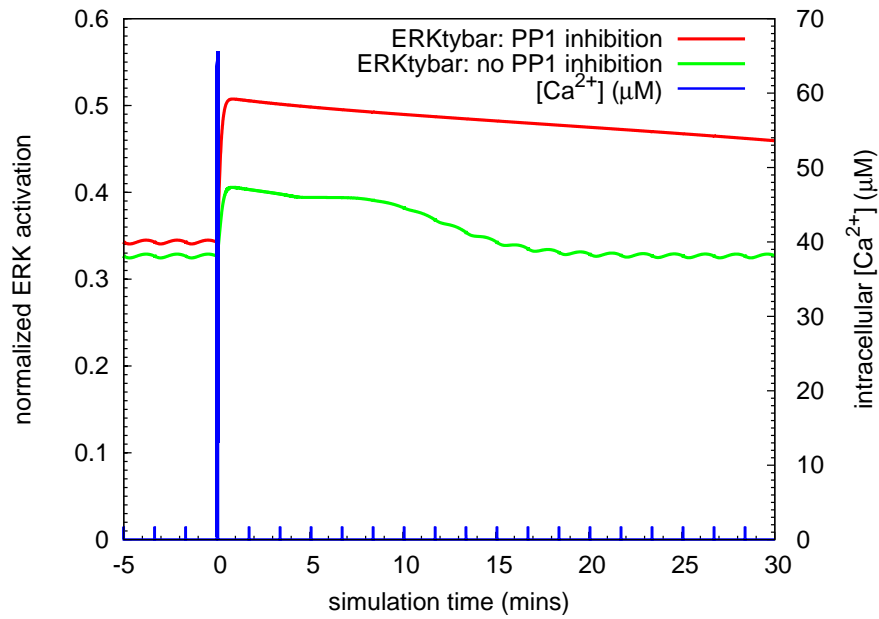
Figure 52: **ERK activity after Ca²⁺ stimulation in the model where NR2A subunits constitute 90% of the total NR2 subunits.** Comparison of ERK activities between PP1 inhibited (red line) and PP1 not inhibited (green line) situations after Ca²⁺ stimulation. In this model, NR2A- containing NMDA receptors were composed of 90% of the total NMDA receptors. 'bar' in the name indicates a value normalised by the total amount of ERK. Dark blue line represents intracellular Ca²⁺ concentration.

*Summary and conclusion*

A preliminary model, containing two opposing regulatory roles of
PP1 on the Ras-ERK pathway, has been constructed. Simulation res-
ults with two different compositions of NMDA receptors in NR2 sub-
units indicate that the role of PP1 can be dynamically balanced by
the type of NMDA receptor expressed. In immature neurons, high
expression levels of NR2B subunits effectively couple SynGAP with
CaMKII, providing a positive control on the Ras-ERK pathway me-
diated by PP1; whereas in mature neurons, high expression levels of
NR2A subunits shift the role of PP1 to that of a negative regulator of
ERK.

The time courses of calcium-induced ERK dephosphorylation (without
the inhibition of PP1) obtained in the simulation do not exactly corres-
pond to experimental results at 30 minutes (Fig. 48 and Fig. 39). Nev-
ertheless, simulation and experiments roughly agree. Most import-
antly, the distinct ERK responses to glutamate stimulation and the
even more dramatic difference in response to PP1 inhibition, between
the two NMDA receptor compositions, provide a plausible explana-
tion for the dual roles of PP1 on ERK activity (Fig. 50 and Fig. 52).

## 3.6   DISCUSSION

The MAP kinase pathway mediates persistent structural changes in
MSN (Wu *et al.*, 2001b; Park *et al.*, 2003), acting as an important
crosstalk between cortico-striatal glutamate input and mesencephalic
dopamine signal (Girault *et al.*, 2007), thus underlying drug-induced
neuroadaptation. The amplitude and duration of ERK activation are
important for regulating its targets. ERK activation relies on one dual-
specific kinase, MEK, but its inactivation can be achieved through
three classes of phosphatases, suggesting that diverse signals could
be integrated at the level of these phosphatases. Moreover, this regu-
latory integration through phosphatase may be cell-specific.

In MSN, the predominant striatal cell type, ERK activation results
from the combined stimulation of glutamate NMDA receptors and
dopamine D1 receptors (Valjent *et al.*, 2000, 2005; Salzmann *et al.*,
2003). This integration is mediated by DARPP-32, a potent PP1 inhib-

itor. Thus many studies have focused on the possible PP1 inhibitory effect on STEP, a tyrosine phosphatase deactivating ERK in the MSN.

The present study addresses the roles of PP1 on regulating glutamate NMDA receptor-dependent modulation of ERK signalling pathway in the striatum. By comparing the simulations of alternative models, where either calcineurin or PP1 directly stimulates STEP, with existing experimental data, I have demonstrated that it is possible that PP1 directly stimulates STEP, exerting an inhibitory effect on ERK activity in MSN. However, PP1 can also stimulate ERK via inhibiting Ras-GAP activity, when NR2B-containing NMDA receptors are predominantly expressed. Therefore, dopamine regulated PP1 activity may exhibit opposite effects on MAP kinase pathway according to the state of neuronal differentiation, and in particular the composition of NMDA receptors.

Brain function relies on the chemical communication between neurons via synapses. The molecular composition of synapses changes over time, resulting in distinct intracellular signalling cascades between mature and nascent synapses (Petralia *et al.*, 2005). One important aspect is the opposite effects of NMDA receptor activation on AMPA receptors, and therefore on synaptic weights (reviewed in Hall and Ghosh, 2008). In mature synapses, the activation and insertion of AMPA receptors are stimulated by the activation of NMDA receptors; whereas, in developing synapses, NMDA receptors negatively regulate AMPA receptor function. ERK plays a key role in mediating this regulation. As Zhu *et al.* (2002) demonstrated, CaMKII mediated AMPA receptor delivery to the synapse is enabled by the activation of Ras-ERK pathway. In developing synapses, NMDA signalling, through NR2B-containing receptors, permits the activation of SynGAP by CaMKII, thus inhibiting Ras-ERK pathway, and negatively regulating AMPA receptor recruitment to the postsynaptic membrane. On the contrary, in mature synapses, NMDA receptor signalling, via NR2A-containing receptors, induces the activation of ERK and positively regulates AMPA receptor insertion.

The model presented here, dealing with the changes of composition of NMDA receptors, provides a reusable and extendable base that can be used to investigate the consequences of neuronal differentiation and their effect on synaptic plasticity. In addition, this mo-

del sheds light on possible interactions between signalling cascades, particularly the two opposing regulatory effects of the dopamine signalling pathway to glutamate-mediated ERK activity.

The experiments conducted here on primary striatal neuron cultures after 7-day or 14-day show a switch of glutamate influence on ERK, from activation to inhibition. If immaturity is the explanation for NMDA receptor mediated inhibition on ERK for the 14-day cultures, we can propose an explanation for the glutamate-induced ERK activation in 7-day cultures. Kim *et al.* (2005) found a transition of NR2B function during neuronal development. Initially NR2B is critical for ERK activation. However, at a certain developmental stage, NR2B starts to mediate the downregulation of ERK activity (Kim *et al.*, 2005). Indeed, NR2B-containing NMDA receptor, by itself, is sufficient for NMDA-induced ERK activation. However, the role it plays on regulating ERK largely depends on the proteins it associates with, and this varies with the developmental stage. Since the experiments presented here were performed using primary neuronal cultures, it is possible that the level of spontaneous neuronal activity is artificially high after 14-day cultures, and the mechanisms required to downregulate glutamate receptors are evoked. NR2B mediated SynGAP activation might be initiated as a tuning procedure. Another possible explanation would be that the interplay between dopamine and glutamate systems can be dynamically adjusted: with chronically high glutamate activity, dopamine would have an inhibitory effect on glutamate-induced ERK activity, via the inhibition of PP1's positive effect on ERK pathway (via CaMKII and SynGAP); with activity-dependent glutamate input, dopamine would have a stimulating effect on glutamate induced ERK through the inhibition of PP1's inhibitory effect on mitogen-activated protein kinase (MAPK) pathway (through STEP).

The molecular interactions incorporated in this model are all obtained from published experimental evidence in MSN. However, in order to verify my model, further experiments are required. First of all, NR2B antagonists (such as ifenprodil or Ro25-6981) could be applied to 14-day neuronal cultures, which would allow me to judge whether NR2B plays an inhibitory role on ERK at this stage. Secondly, more mature neurons should be put in cultures. The results of glutam-

ate stimulation with or without PP1 inhibition would permit valida-
tion of my hypothesis that the neuronal differentiation stage shifts
the directionality of PP1's effect on ERK. However, healthy synaptic
connections do not only depend on the length of the culture, but
also on the culture system used. It is possible that the coordination
between glutamatergic input and neurotrophin factors from cortical
cells may be required for the maturation of MSN (Ivkovic and Ehrlich,
1999; Morrison and Mason, 1998; Poo, 2001). Therefore, co-culture
may need to be considered. Thirdly, spontaneous neuronal activity
induced high activation of ERK should be inhibited, for instance us-
ing tetrodotoxin.

DARPP-32 mediated PP1 inhibition, and the subsequent regulation
of ERK activity, are key parts of the molecular mechanisms underly-
ing dopamine controlled neuroplasticity (Girault *et al.*, 2007). This
regulation is dynamically adjusted depending on the type of NMDA
receptor and its associated proteins. Furthermore, dopamine can also
exert its effect after DARPP-32 translocation in the nucleus. Drugs
of abuse cause DARPP-32 phosphorylation on Thr34, as well as de-
phosphorylation on Ser97, which results in a strong inhibition of PP1
in the nucleus (Stipanovich *et al.*, 2008). Some interesting questions
to address in the future are: How do dopamine and glutamate sig-
nals regulate ERK activity and translocation into the nucleus, and
how does this nuclear PP1 inhibition further influence ERK and its
targets? However, before addressing these questions, a preliminary
issue to be considered is whether or not the same population of ERK
is active at the synaptic level and travels all the way to the nucleus,
or are there different pools of ERK? If the trafficking of upstream
molecules of MAP kinase pathway from the spine to the cell body is
involved (Harvey *et al.*, 2008) and plays an important role in regulat-
ing ERK nuclear translocation, then dopamine regulation upstream
of the ERK pathway may be more important than the synaptic regula-
tion of ERK activity itself. A computational model based on multiple
compartments should be able to provide possible answers to these
questions in the future.

# DISCUSSION

## 4.1 Dopamine modulation on synaptic plasticity in nucleus accumbens

Evidence suggests that drugs of abuse exert their addictive effects through modulating synaptic plasticity in reward-related neuronal circuits (Hyman *et al.*, 2006; Kauer and Malenka, 2007). Within these circuits, NAc plays an important role, since glutamate transmission in NAc is responsible for drug-seeking behaviour (Kalivas, 2004; Self *et al.*, 2004).

The GABAergic MSN, the predominant neuron type in NAc, is innervated by glutamate projections from limbic and cortical regions and by the dopamine inputs from the ventral mesencephalon. Therefore, through MSN, dopamine can directly affect glutamate transmission via the activation of second messenger pathways.

In MSN, both NMDA receptor-dependent LTP (Pennartz *et al.*, 1993; Mulder *et al.*, 1997; Schramm *et al.*, 2002; Li and Kauer, 2004), and NMDA receptor-dependent LTD (Thomas *et al.*, 2001) have been observed. Dopamine plays a crucial role in regulating these two forms of corticalstriatal plasticities (Centonze *et al.*, 1999; Calabresi *et al.*, 1992; Choi and Lovinger, 1997). Briefly, dopamine, through D1- and D2-like receptors, affects the intracellular cAMP level, modulating PKA activity. A major relevant substrate for PKA is the DARPP-32. This is a potent PP1 inhibitor once phosphorylated on threonine 34.

In this thesis, I have shown that the bidirectional alteration of short-term synaptic plasticity was regulated by the frequency of postsynaptic calcium inputs. I further proposed that dopamine, via the cAMP-PKA-DARPP-32 pathway, not only shifted CaMKII activation towards low-frequency calcium spikes, but also extended its activation level at high frequencies, thus potentiating glutamatergic synapses. This finding is supported by experiments showing that DARPP-32 inhibition of PP1 is required for inducing NMDA receptor-dependent LTP

in MSN (Calabresi *et al.*, 2000). In rat striatal slices, the induction of LTP requires co-occurrence of excitatory inputs with dopamine D1 receptor activation (Wickens *et al.*, 1996; Kerr and Wickens, 2001). However, regulating the potency of PP1 is just one mechanism by which dopamine modulates corticostriatal synaptic plasticity.

A crucial property of MSN in NAc and the dorsal striatum is that the basal hyperpolarized membrane potential ("down" state) can be periodically driven to a more depolarized state ("up" state), by excitatory input from cerebral cortex and thalamus (Wilson and Kawaguchi, 1996). When the synaptic input is weak, dopamine, via the activation of D1 receptor, increases $K^+$ channel current, suppressing excitability; whereas when MSN is in "up" state, dopamine, through D1 receptor, sustains this depolarized state by enhancing L-type $Ca^{2+}$ channel currents (Nicola *et al.*, 2000). This way, dopamine increases the signal-to-noise ratio and magnifies the strongest active input (Schultz, 2002). In addition, acute stimulation of D1 receptor increases GluR1-containing AMPA receptor externalization through a PKA-dependent mechanism (Wolf *et al.*, 2004). These observations, together with my findings, lead to the hypothesis that the transient activation of D1 receptor, if happening in conjunction with excitatory synaptic transmission, can enhance the effect of glutamate input, facilitating LTP in MSN.

Contrary to the D1 receptor, the D2 receptor exerts the opposite effect on cAMP, and inhibits LTP (Calabresi *et al.*, 1997). However, D1 and D2 receptors are both required for the induction of LTD in MSN, despite the fact that their activations are induced in different cellular subtypes (Calabresi *et al.*, 2000). A proposed scheme is that dopamine stimulates nitric oxide (NO) production via D1 receptors in the striatal NO synthesis-positive interneurons (a minority neuron type in the striatum) (Morris *et al.*, 1997). NO elevates intracellular cyclic guanosine monophosphate (cGMP) levels through soluble guanylyl cyclase (sGC), and cGMP in turn activates cyclic GMP-dependent protein kinase (PKG). This NO-cGMP-PKG pathway may cooperate with postsynaptic D2 receptors to induce LTD (Centonze *et al.*, 2001; Calabresi *et al.*, 1999). PKG phosphorylates DARPP-32 on Thr34, inhibiting PP1 (Hemmings *et al.*, 1984b). Furthermore, this PKG induced PP1 inhibition is necessary for LTD induction (Calabresi *et al.*, 2000). Why is DARPP-32 phosphorylation on Thr34 required for inducing both

LTP and LTD? What are the other roles played by PKA and PKG in striatal synaptic plasticity, besides their different catalytic efficiencies on phosphorylating DARPP-32? These questions may be addressed by an extension of the current model to include cGMP second messenger pathway, and to verify whether an inactivated cAMP pathway combined with the increased cGMP level could trigger distinct dynamic behaviour of CaMKII activation.

## 4.2  DRUGS OF ABUSE INDUCED STRUCTURAL PLASTICITY IN NUCLEUS ACCUMBENS

Learning can result in altered morphology structure of neurons and synapses (Moser *et al.*, 1994; Stewart and Rusakov, 1995; Leuner *et al.*, 2003), thereby affecting synaptic efficacy (Horner, 1993; Rusakov *et al.*, 1996; Nimchinsky *et al.*, 2002). Drugs of abuse can produce persistent changes in the brain, and share many cellular and molecular mechanisms with learning. Repeated exposure to amphetamine and cocaine increases spine density and dendritic branching on the MSN of the NAc (Robinson and Kolb, 1997, 1999a; Robinson *et al.*, 2001; Heijtz *et al.*, 2003; Kolb *et al.*, 2003; Li *et al.*, 2003; Norrholm *et al.*, 2003). These changes are persistent and can last up to three months after withdrawal of the drug (Kolb *et al.*, 2003; Robinson and Kolb, 1999a; Robinson *et al.*, 2001). Particularly on the MSN of the NAc, drugs of abuse increase the number of spines with multiple heads (Robinson and Kolb, 1997, 1999a). Research suggests that these MSNs are primarily influenced by addictive drugs, because both dopamine and glutamate signals are received by these neurons, and both are important for persistent experience-dependent plasticity (Robinson and Kolb, 2004; Kalivas, 1995; Wolf, 1998; Hyman and Malenka, 2001; Lamprecht and LeDoux, 2004).

Sustained structural plasticity requires the activation of ERK1/2 (Wu *et al.*, 2001b). Acute amphetamine treatment has been shown to elicit the activation of MAP kinase and neuritic growth (Park *et al.*, 2003). ERK1/2 activity can also be induced by acute cocaine injection and underlies early behavioural responses (Valjent *et al.*, 2000). One of the best studied transcription factors underlying learning and memory, CREB, is an indirect target of ERK1/2 in the nucleus, indic-

ating that ERK1/2 can transduce drug induced temporal alterations into regulation of gene expression and protein synthesis. This results in long-term changes of the dendritic structure.

In this thesis, I have shown how the activation of ERK1/2 could serve as a convergence point between cortico-striatal glutamate inputs and mesencephalic dopamine signals. In mature MSN, the convergence of dopamine induced cAMP and the glutamate triggered $Ca^{2+}$ leads to increased and prolonged ERK1/2 activity, which can be translated into a series of nuclear events. Hence, when glutamate and dopamine transmission happen concurrently, dopamine enhances, through D1 activation, cortically evoked excitation in post-synaptic MSN. This is accomplished not only by enhancing synaptic strength, but also by inducing long lasting events such as ERK1/2 mediated dendritic remodelling.

Drugs of abuse exert their effects by amplifying the function of the dopamine reward system. For instance, dramatic increases in extracellular dopamine levels (Giros *et al.*, 1996) lead to prolonged excitation in dopamine neurons (Jones *et al.*, 2000; Ungless *et al.*, 2001). This results in enhanced glutamate signalling pathway activity in MSN and sustained structural plasticity, thereby producing substantial behavioural changes (West *et al.*, 1997).

However, different drugs exert different effects on the dendritic structure, in different regions. Amphetamine and cocaine influence dendritic structure mainly on the distal portion of dendritic tree of the MSN (Robinson and Kolb, 1999a). Amphetamine has little effect on basilar dendrites of the prefrontal cortex pyramidal cells, while cocaine alters dendritic structure on both apical and basilar dendrites (Robinson and Kolb, 1997). Morphine markedly decreases spine density and branching in the NAc, in contrast to other drugs of abuse (Robinson and Kolb, 1999b; Robinson *et al.*, 2002). To date, little is known about how different patterns of synaptic reorganisation affect the function of a neural circuit, and how altered functions contribute to drug induced behavioural outcomes. This poses an important challenge not only for wet lab experiments, but also for computational modelling. Large scale quantitative models based on the whole dendritic tree, which take into account the distribution of spines, the detailed signalling network, and the communication between neigh-

bouring spines, would provide valuable insight into what really happens in the addicted brain. In fact, such a model is currently being developed by a co-worker, where my work is adapted into the molecular network within each spine on MSN.

Drug addictions are complex and involve adaptations in multiple neuronal circuits that develop with different time courses (Kauer and Malenka, 2007). The work presented here sheds light on some biochemical cascades involved in striatal neuroadaptation, and provides computational models that can be reused and extended to study other aspects of this neuroadaptation.

## 4.3    EXPERIENCE-DEPENDENT ADAPTATION

An interesting finding of this work is the developing regulatory role played by glutamate, on ERK1/2 activity, which changed from stimulation in 7-day to inhibition in 14-day cultured MSN, and finally to stimulation in mature MSN.

Using a computational approach, I propose that this glutamate-dependent dynamic regulation is due to a compositional change of the NMDA receptor, and in particular the signalling molecules assembled by the NR2B and NR2A subunits at different neuronal differentiation stages. In fact, either NR2A- or NR2B-containing NMDA receptors are able to induce ERK1/2 activation. However, as the neuron develops, NR2B is coupled to an inhibitor of Ras-ERK1/2 pathway (Kim *et al.*, 2005). Therefore, glutamate controlled ERK1/2 activity is closely correlated with the relative expression of NR2A and NR2B subunits.

Not only do the components and their organisations change during neuron development (Petralia *et al.*, 2005), the molecular mechanisms underlying some major postsynaptic events also differ. For example, the insertion of AMPA receptors into the postsynaptic membrane is regulated differently in mature and developing neurons. AMPA receptors can be recruited to nascent synapses without the activation of NMDA receptor (Colonnese *et al.*, 2003; Groc *et al.*, 2006). In addition, NMDA receptors then negatively regulate AMPA receptor recruitment, the inverse of the situation that occurs in mature neuron (reviewed in Hall and Ghosh, 2008).

It is not clear, though, what are the reasons behind these functional changes. It might be an experience-expectant development, by which "neurons incorporate environmental stimuli to its normal pattern of development" (cited from Andersen, 2003). In this sense, during a certain period of neuronal differentiation stage, the intense glutamate input may induce adaptation in glutamatergic synapses, by adjusting the components of NMDA receptor. Thus, glutamate activates AMPA receptors, which trigger the activation of NMDA receptors that in turn positively regulate the insertion of AMPA receptors to postsynaptic membrane, strengthening glutamate transmission.

Another example, albeit far remote from the topic of this thesis, relates visual experience and NMDA receptor development in kitten visual cortex. NMDA receptors are important for eye-specific geniculocortical axon segregation during visual cortex development in kittens (Fox *et al.*, 1991). In a normal developing animal, this function is gradually attenuated as segregation concludes. However, when this segregation has been delayed by rearing the animal in darkness, the loss of NMDA receptor function is inhibited. This indicates that some critical steps in development are not programmed at the level of the genes, but caused via experience.

Adaptation occurs not only during development; LTP is a kind of adaptation, whereas dendritic structural changes due to long term drug exposure are of another kind. However, if a disruption happens during a critical development stage, it may have a greater impact than the same event occurring later in life. In mature MSN, dopamine, via inhibition of PP1, exerts a positive regulation on MAP kinase pathway. On the other hand, in developing MSN, dopamine, via the same PP1 inhibition, negatively modulates MAP kinase activity. There are emerging studies, based on human and animal models, suggesting that the effects of drugs of abuse on the developing brain are different from their effects on mature neuronal systems (Stanwood and Levitt, 2004). Developing brains are extremely plastic and vulnerable, thus prenatal cocaine exposure can lead to more permanent cellular responsiveness, and severe developmental delay (Andersen, 2003; Singer *et al.*, 2002). Although drug induced adaptation in early life may result from a far more complicated mechanism, my research on opposing dopamine

effects on MAP kinase pathway can still give some insight into how dopamine switches its role during neuron differentiation.

## 4.4   Simulation approach and parameter estimation

As described in previous chapters, the main modelling approach used in this thesis is based on deterministic simulations of continuous ODE systems, and reactions are assumed to happen in a closed, homogeneous compartment whose volume remains constant. Whilst not without limitations, such an approach and assumption can provide a good approximation of the behaviour of a large scale complex system. However, there remain many challenges for the future development of this approach.

*Parameter estimation and measurement*

The minimum requirements for modelling biochemical reactions are the concentrations of species and the kinetic constants of reactions. However, only a small fraction of these parameters were directly measured *in vivo*, the majority being obtained from experiments on purified biochemical entities. Clearly, it is even harder to obtain concentrations and reaction rates from a subcellular region, for example the dendritic spine itself. In most situations, modellers need to estimate multiple parameters from the experimental data of a single time course. This brings challenges for modelling, for instance, how to integrate measurements from different experiments, and how to constrain the parameter space and obtain reasonable estimations.

One future objective would be to work on multidimensional parameter estimations for large scale kinetic models. There are already many optimisation algorithms that are available or have been implemented (reviewed in Mendes and Kell, 1998). Some of these are based on a local search around the given initial estimations, for example the Levenberg-Marquardt algorithm (Levenberg, 1944; Marquardt, 1963) and the downhill simplex method (Nelder and Mead, 1965). Others apply a global algorithm that continually updates the sequence of the lower and upper bounds of estimated parameters (Esposito and Floudas, 2000), and some adapt the hybrid generic algorithm that first

identifies the initial guesses and then locally optimises the parameters (Wolf and Moros, 1997; Balland *et al.*, 2000; Wang and Kim, 2001; Teh and Rangaiah, 2002).

Another exciting area with potential application of this problem is real-time imaging, based on fluorescence resonance energy transfer (FRET) (Tsien *et al.*, 1993). A reporter based on FRET between fluorescent proteins can be observed in specific subcellular regions of an intact cell without buffering signalling molecules. Quantitative analysis of FRET images can reveal kinase activity in living cells (Zhang *et al.*, 2001; Ting *et al.*, 2001; Sato *et al.*, 2002). Based on the principle of FRET, Violin *et al.* (2003) designed a genetically encoded fluorescent reporter that can reversibly respond to protein kinase C (PKC) activity, and they revealed a calcium controlled oscillatory phosphorylation of PKC to histamine stimulation in Hela cells. A characteristic of spine signalling is the high spatial and temporal resolution. By using FRET, Harvey *et al.* (2008) showed, in a single dendritic spine of pyramidal neuron, Ras activation triggered by LTP and the spread of Ras activity to neighbouring spines. These data can be used by parameter searching algorithms discussed above in order to constrain parameter space and obtain reasonable parameters for computational models.

*Multi-compartment and stochastic simulations*

Major signalling proteins in a spine are assembled near the postsynaptic membrane, forming a PSD (Collins *et al.*, 2006). PSD is a highly dynamic structure. For example, during the induction of LTP, Thr286 phosphorylated CaMKII travels into the PSD, binding to the NMDA receptor (Strack *et al.*, 1997b; Shen and Meyer, 1999; Strack *et al.*, 2000; Bayer *et al.*, 2001). Insertion of new AMPA receptors in the postsynaptic membrane is another major step of LTP (Hayashi *et al.*, 2000; Lu *et al.*, 2001; Shi *et al.*, 2001). In addition, many active proteins diffuse out of the PSD to deliver the information carried by neurotransmitters to other parts of the spine, to neighbouring spines, or to the nucleus. The spine is therefore not a homogeneous compartment, since the PSD is a specific domain with distinct protein distribution. Nevertheless, PSD is also open, allowing signalling molecules to diffuse within the rest of the spine.

Hence, in computational models, should the PSD be considered as a subcellular compartment? A problem with this approach concerns the estimation of flux rates for molecules trafficking in and out of the PSD. It is crucial, since the speeds of trafficking can significantly influence the occurrence of other signalling events. It is also difficult to assess the volume of the PSD. Besides, does the shape of PSD remain constant? Moreover, the PSD consists mainly of proteins, causing massive molecular crowding and non-brownian diffusions, which invalidates mass-action law approaches.

Another approach is to consider the formation of PSD as a sequence of molecules binding to key scaffold proteins, such as PSD95, Shank, AKAP79/150 (A-kinase-associated protein of molecular weight 70 and 150 kDa), and MUPP1 (Kim and Sheng, 2004; Scannevin and Huganir, 2000; Sheng and Sala, 2001; Krapivinsky *et al.*, 2004). Still, this strategy requires many estimations about binding and dissociation rates that are usually not available from biochemical experiments. Furthermore, we still know little about the organisations of these scaffolds, and it seems that many more are waiting to be discovered (Kennedy *et al.*, 2005).

As explained above, the major signal transduction events in spine happen within a spatially limited region, the PSD, where molecules are present in a relatively low copy number. Therefore, random fluctuations would affect interactions in this region (Tölle and Le Novère, 2006). Hybrid systems that combine stochastic simulation for PSD-specific reactions with deterministic simulation for other reactions that involve larger populations can be applied. This arrangement will help address several questions in the future: what is the effect of signal transduction noise in regulating neuronal network? Are there any strategies that neurons adopt in order to filter out this noise?

*Varying volumes*

There is a strong correlation between synaptic plasticity and spine morphology. LTP induced enlargement of the spine head and shortening of spine neck have been reported in many experiments (review in Yuste and Bonhoeffer (2001); Lamprecht and LeDoux (2004)). Changes in spine morphology can contribute to enhanced synaptic

transmission due to increased glutamate receptor surface expression (Takumi *et al.*, 1999; Matsuzaki *et al.*, 2001). However, an immediate challenge for computational models based on dendritic spine is the treatment of inconstant volumes for the compartments, which change as a function of time and activity. This alters the concentrations of molecules, and subsequently influences reaction rates. Moreover, these observations weaken the assumption that the spine is a closed compartment that allows signalling molecules, for instance calcium, to undergo fast concentration changes during LTP induction (Nimchinsky *et al.*, 2002). It might still be true transiently in some microdomains nearby the receptor, however the widened spine neck can facilitate calcium diffusion into the dendritic shaft (Volfovsky *et al.*, 1999; Majewska *et al.*, 2000), and to the neighbouring spines. It might be a daunting task to model spine morphology changes, however, it will help us to predict the functional importance behind those changes.

Although building biologically realistic models is challenging and demanding, the development of computational models provides an opportunity to combine different pieces of knowledge together and to reveal the mechanisms underlying neuronal function. Each trial to reach a realistic representation and the associated quantitative analysis is valuable. As Kennedy *et al.* (2005) argued: "Rather than attempting to design experiments to distinguish between mediation and modulation, it will be more useful to ask questions about the quantitative contribution of each pathway to a change in synaptic strength."

# BIBLIOGRAPHY

J.-H. Ahn, T. McAvoy, S. V. Rakhilin, A. Nishi, P. Greengard, and A. C. Nairn. Protein kinase A activates protein phosphatase 2A by phosphorylation of the B56delta subunit. *Proc Natl Acad Sci U S A*, 104(8):2979–2984, 2007a. doi:10.1073/pnas.0611532104. (Cited on page 13.)

J.-H. Ahn, J. Y. Sung, T. McAvoy, A. Nishi, V. Janssens, J. Goris, P. Greengard, and A. C. Nairn. The B″/PR72 subunit mediates Ca2+-dependent dephosphorylation of DARPP-32 by protein phosphatase 2A. *Proc Natl Acad Sci U S A*, 104(23):9876–9881, 2007b. doi:10.1073/pnas.0703589104. (Cited on page 13.)

D. R. Alessi, N. Gomez, G. Moorhead, T. Lewis, S. M. Keyse, and P. Cohen. Inactivation of p42 MAP kinase by protein phosphatase 2A and a protein tyrosine phosphatase, but not CL100, in various cell lines. *Curr Biol*, 5(3):283–295, 1995. (Cited on page 58.)

G. E. Alexander and M. D. Crutcher. Functional architecture of basal ganglia circuits: neural substrates of parallel processing. *Trends Neurosci*, 13(7):266–271, 1990. (Cited on page 10.)

N. L. Allbritton, T. Meyer, and L. Stryer. Range of messenger action of calcium ion and inositol 1,4,5-trisphosphate. *Science*, 258(5089):1812–1815, 1992. (Cited on pages 33 and 73.)

S. L. Andersen. Trajectories of brain development: point of vulnerability or window of opportunity? *Neurosci Biobehav Rev*, 27(1-2):3–18, 2003. (Cited on page 120.)

N. G. Anderson, J. L. Maller, N. K. Tonks, and T. W. Sturgill. Requirement for integration of signals from two distinct phosphorylation pathways for activation of MAP kinase. *Nature*, 343(6259):651–653, 1990. doi:10.1038/343651a0. (Cited on page 58.)

S. M. Anderson, K. R. Famous, G. Sadri-Vakili, V. Kumaresan, H. D. Schmidt, C. E. Bass, E. F. Terwilliger, J.-H. J. Cha, and R. C. Pierce.

CaMKII: a biochemical bridge linking accumbens dopamine and glutamate systems in cocaine seeking. *Nat Neurosci*, 11(3):344–353, 2008. doi:10.1038/nn2054. (Cited on page 56.)

N. Arimura and K. Kaibuchi. Neuronal polarity: from extracellular signals to intracellular mechanisms. *Nat Rev Neurosci*, 8(3):194–205, 2007. doi:10.1038/nrn2056. (Cited on page 8.)

A. Artola and W. Singer. Long-term depression of excitatory synaptic transmission and its relationship to long-term potentiation. *Trends Neurosci*, 16(11):480–487, 1993. (Cited on page 18.)

Y. S. Babu, C. E. Bugg, and W. J. Cook. Structure of calmodulin refined at 2.2 A resolution. *J Mol Biol*, 204(1):191–204, 1988. (Cited on page 19.)

Y. S. Babu, J. S. Sack, T. J. Greenhough, C. E. Bugg, A. R. Means, and W. J. Cook. Three-dimensional structure of calmodulin. *Nature*, 315(6014):37–40, 1985. (Cited on page 19.)

B. J. Bacskai, B. Hochner, M. Mahaut-Smith, S. R. Adams, B. K. Kaang, E. R. Kandel, and R. Y. Tsien. Spatially resolved dynamics of cAMP and protein kinase A subunits in Aplysia sensory neurons. *Science*, 260(5105):222–226, 1993. (Cited on pages 33, 34, 66, 74, and 75.)

C. Bagni, L. Mannucci, C. G. Dotti, and F. Amaldi. Chemical stimulation of synaptosomes modulates alpha -Ca2+/calmodulin-dependent protein kinase II mRNA association to polysomes. *J Neurosci*, 20(10):RC76, 2000. (Cited on page 6.)

L. Balland, L. Estel, J. M. Cosmao, and N. Mouhab. A genetic algorithm with decimal coding for the estimation of kinetic and energetic parameters. *Chemometrics and Intelligent Laboratory Systems*, 50(1):121 – 135, 2000. ISSN 0169-7439. doi:DOI:10.1016/S0169-7439(99)00057-X. (Cited on page 122.)

A. P. Barnes and F. Polleux. Establishment of axon-dendrite polarity in developing neurons. *Annu Rev Neurosci*, 32:347–381, 2009. doi:10.1146/annurev.neuro.31.060407.125536. (Cited on page 8.)

A. P. Barnes, D. Solecki, and F. Polleux. New insights into the molecular mechanisms specifying neuronal polarity in vivo. *Curr Opin*

*Neurobiol*, 18(1):44–52, 2008. doi:10.1016/j.conb.2008.05.003. (Cited on page 8.)

A. Barria and R. Malinow. NMDA receptor subunit composition controls synaptic plasticity by regulating binding to CaMKII. *Neuron*, 48(2):289–301, 2005. doi:10.1016/j.neuron.2005.08.034. (Cited on page 59.)

K. U. Bayer, P. D. Koninck, A. S. Leonard, J. W. Hell, and H. Schulman. Interaction with the NMDA receptor locks CaMKII in an active conformation. *Nature*, 411(6839):801–805, 2001. doi:10.1038/35081080. (Cited on page 122.)

P. M. Bayley, W. A. Findlay, and S. R. Martin. Target recognition by calmodulin: dissecting the kinetics and affinity of interaction using short peptide sequences. *Protein Sci*, 5(7):1215–1228, 1996. doi:10.1002/pro.5560050701. (Cited on pages 26 and 34.)

J. D. Berke and S. E. Hyman. Addiction, dopamine, and the molecular mechanisms of memory. *Neuron*, 25(3):515–532, 2000. (Cited on page 1.)

D. E. Berman, S. Hazvi, K. Rosenblum, R. Seger, and Y. Dudai. Specific and differential activation of mitogen-activated protein kinase cascades by unfamiliar taste in the insular cortex of the behaving rat. *J Neurosci*, 18(23):10037–10044, 1998. (Cited on page 57.)

A. Berthet and E. Bezard. Dopamine receptors and L-dopa-induced dyskinesia. *Parkinsonism Relat Disord*, 15 Suppl 4:S8–12, 2009. doi: 10.1016/S1353-8020(09)70827-2. (Cited on page 10.)

J. Bertran-Gonzalez, C. Bosch, M. Maroteaux, M. Matamales, D. Hervé, E. Valjent, and J.-A. Girault. Opposing patterns of signaling activation in dopamine D1 and D2 receptor-expressing striatal neurons in response to cocaine and haloperidol. *J Neurosci*, 28(22):5671–5685, 2008. doi:10.1523/JNEUROSCI.1039-08.2008. (Cited on page 10.)

U. S. Bhalla. Biochemical signaling networks decode temporal patterns of synaptic input. *J Comput Neurosci*, 13(1):49–62, 2002. (Cited on page 20.)

U. S. Bhalla. Temporal computation by synaptic signaling pathways. *J Chem Neuroanat*, 26(2):81–86, 2003. (Cited on page 14.)

U. S. Bhalla. Signaling in small subcellular volumes. I. Stochastic and diffusion effects on individual pathways. *Biophysical Journal*, 87(2):733–744, 2004a. (Cited on page 17.)

U. S. Bhalla. Signaling in small subcellular volumes. II. Stochastic and diffusion effects on synaptic network properties. *Biophysical Journal*, 87(2):745–753, 2004b. (Cited on page 17.)

U. S. Bhalla and R. Iyengar. Emergent properties of networks of biological signaling pathways. *Science*, 283(5400):381–387, 1999. (Cited on pages 15, 66, 67, 74, 75, and 104.)

J. A. Bibb, G. L. Snyder, A. Nishi, Z. Yan, L. Meijer, A. A. Fienberg, L. H. Tsai, Y. T. Kwon, J. A. Girault, A. J. Czernik, R. L. Huganir, H. C. Hemmings, A. C. Nairn, and P. Greengard. Phosphorylation of DARPP-32 by Cdk5 modulates dopamine signalling in neurons. *Nature*, 402(6762):669–671, 1999. doi:10.1038/45251. (Cited on pages 11 and 68.)

J. A. Blendy and R. Maldonado. Genetic analysis of drug addiction: the role of cAMP response element binding protein. *J Mol Med*, 76(2):104–110, 1998. (Cited on page 8.)

T. V. Bliss and G. L. Collingridge. A synaptic model of memory: long-term potentiation in the hippocampus. *Nature*, 361(6407):31–39, 1993. doi:10.1038/361031a0. (Cited on pages 3, 14, and 18.)

A. B. Bortz, M. H. Kalos, and J. L. Lebowitz. A new algorithm for Monte Carlo simulation of Ising spin systems. *Journal of Computational Physics*, 17:10–18, 1975. (Cited on page 17.)

A. C. Boudreau and M. E. Wolf. Behavioral sensitization to cocaine is associated with increased AMPA receptor surface expression in the nucleus accumbens. *J Neurosci*, 25(40):9144–9151, 2005. doi:10.1523/JNEUROSCI.2252-05.2005. (Cited on page 56.)

T. G. Boulton, S. H. Nye, D. J. Robbins, N. Y. Ip, E. Radziejewska, S. D. Morgenbesser, R. A. DePinho, N. Panayotatos, M. H. Cobb, and G. D. Yancopoulos. ERKs: a family of protein-serine/threonine

kinases that are activated and tyrosine phosphorylated in response to insulin and NGF. *Cell*, 65(4):663–675, 1991. (Cited on page 57.)

D. S. Bredt and R. A. Nicoll. AMPA receptor trafficking at excitatory synapses. *Neuron*, 40(2):361–379, 2003. (Cited on page 3.)

G. E. Briggs and J. B. S. Haldane. A note on the kinetics of enzyme action. *Biochemical Journal*, 19:338–339, 1925. (Cited on page 24.)

R. W. Brown and B. Kolb. Nicotine sensitization increases dendritic length and spine density in the nucleus accumbens and cingulate cortex. *Brain Res*, 899(1-2):94–100, 2001. (Cited on page 57.)

P. Calabresi, P. Gubellini, D. Centonze, B. Picconi, G. Bernardi, K. Chergui, P. Svenningsson, A. A. Fienberg, and P. Greengard. Dopamine and cAMP-regulated phosphoprotein 32 kDa controls both striatal long-term depression and long-term potentiation, opposing forms of synaptic plasticity. *J Neurosci*, 20(22):8443–8451, 2000. (Cited on pages 13 and 116.)

P. Calabresi, P. Gubellini, D. Centonze, G. Sancesario, M. Morello, M. Giorgi, A. Pisani, and G. Bernardi. A critical role of the nitric oxide/cGMP pathway in corticostriatal long-term depression. *J Neurosci*, 19(7):2489–2499, 1999. (Cited on page 116.)

P. Calabresi, R. Maj, A. Pisani, N. B. Mercuri, and G. Bernardi. Long-term synaptic depression in the striatum: physiological and pharmacological characterization. *J Neurosci*, 12(11):4224–4233, 1992. (Cited on page 115.)

P. Calabresi, A. Saiardi, A. Pisani, J. H. Baik, D. Centonze, N. B. Mercuri, G. Bernardi, and E. Borrelli. Abnormal synaptic plasticity in the striatum of mice lacking dopamine D2 receptors. *J Neurosci*, 17(12):4536–4544, 1997. (Cited on page 116.)

M. Camps, A. Nichols, and S. Arkinstall. Dual specificity phosphatases: a gene family for control of MAP kinase function. *FASEB J*, 14(1):6–16, 2000. (Cited on page 58.)

W. A. Carlezon, R. S. Duman, and E. J. Nestler. The many faces of CREB. *Trends Neurosci*, 28(8):436–445, 2005. doi:10.1016/j.tins.2005.06.005. (Cited on page 8.)

A. Carlsson. The occurrence, distribution and physiological role of catecholamines in the nervous system. *Pharmacol Rev*, 11(2, Part 2):490–493, 1959. (Cited on page 10.)

D. Centonze, P. Gubellini, B. Picconi, P. Calabresi, P. Giacomini, and G. Bernardi. Unilateral dopamine denervation blocks corticostriatal LTP. *J Neurophysiol*, 82(6):3575–3579, 1999. (Cited on page 115.)

D. Centonze, B. Picconi, P. Gubellini, G. Bernardi, and P. Calabresi. Dopaminergic control of synaptic plasticity in the dorsal striatum. *Eur J Neurosci*, 13(6):1071–1077, 2001. (Cited on pages 14 and 116.)

D. Cheng, C. C. Hoogenraad, J. Rush, E. Ramm, M. A. Schlager, D. M. Duong, P. Xu, S. R. Wijayawardana, J. Hanfelt, T. Nakagawa, M. Sheng, and J. Peng. Relative and absolute quantification of postsynaptic density proteome isolated from rat forebrain and cerebellum. *Mol Cell Proteomics*, 5(6):1158–1170, 2006. doi: 10.1074/mcp.D500009-MCP200. (Cited on pages 60 and 104.)

G. D. Chiara. A motivational learning hypothesis of the role of mesolimbic dopamine in compulsive drug use. *J Psychopharmacol*, 12(1):54–67, 1998. (Cited on page 1.)

S. Choi and D. M. Lovinger. Decreased probability of neurotransmitter release underlies striatal long-term depression and postnatal development of corticostriatal synapses. *Proc Natl Acad Sci U S A*, 94(6):2665–2670, 1997. (Cited on page 115.)

M. O. Collins, H. Husi, L. Yu, J. M. Brandon, C. N. G. Anderson, W. P. Blackstock, J. S. Choudhary, and S. G. N. Grant. Molecular characterization and comparison of the components and multiprotein complexes in the postsynaptic proteome. *J Neurochem*, 97 Suppl 1:16–23, 2006. doi:10.1111/j.1471-4159.2005.03507.x. (Cited on page 122.)

M. T. Colonnese, J. Shi, and M. Constantine-Paton. Chronic NMDA receptor blockade from birth delays the maturation of NMDA currents, but does not affect AMPA/kainate currents. *J Neurophysiol*, 89(1):57–68, 2003. doi:10.1152/jn.00049.2002. (Cited on page 119.)

J. C. Corvol, J. M. Studler, J. S. Schonn, J. A. Girault, and D. Hervé. Galpha(olf) is necessary for coupling D1 and A2a receptors to adenylyl cyclase in the striatum. *J Neurochem*, 76(5):1585–1588, 2001. (Cited on page 11.)

T. H. Crouch and C. B. Klee. Positive cooperative binding of calcium to bovine brain calmodulin. *Biochemistry*, 19(16):3692–3698, 1980. (Cited on page 19.)

S. Cull-Candy, S. Brickley, and M. Farrant. NMDA receptor subunits: diversity, development and disease. *Curr Opin Neurobiol*, 11(3):327–335, 2001. (Cited on pages 59 and 99.)

P. D'Alcantara, S. N. Schiffmann, and S. Swillens. Bidirectional synaptic plasticity as a consequence of interdependent Ca2+-controlled phosphorylation and dephosphorylation pathways. *Eur J Neurosci*, 17(12):2521–2528, 2003. (Cited on pages 20, 65, and 75.)

S. Davis, P. Vanhoutte, C. Pages, J. Caboche, and S. Laroche. The MAPK/ERK cascade targets both Elk-1 and cAMP response element-binding protein to control long-term potentiation-dependent gene expression in the dentate gyrus in vivo. *J Neurosci*, 20(12):4563–4572, 2000. (Cited on page 57.)

P. De Koninck and H. Schulman. Sensitivity of CaM kinase II to the frequency of Ca2+ oscillations. *Science*, 279(5348):227–230, 1998. (Cited on pages 19, 44, and 55.)

M. Deak, A. D. Clifton, L. M. Lucocq, and D. R. Alessi. Mitogen- and stress-activated protein kinase-1 (MSK1) is directly activated by MAPK and SAPK2/p38, and may mediate activation of CREB. *EMBO J*, 17(15):4426–4441, 1998. doi:10.1093/emboj/17.15.4426. (Cited on page 57.)

F. Desdouits, J. J. Cheetham, H. B. Huang, Y. G. Kwon, E. F. da Cruz e Silva, P. Denefle, M. E. Ehrlich, A. C. Nairn, P. Greengard, and J. A. Girault. Mechanism of inhibition of protein phosphatase 1 by DARPP-32: studies with recombinant DARPP-32 and synthetic peptides. *Biochem Biophys Res Commun*, 206(2):652–658, 1995a. (Cited on pages 11, 33, and 52.)

F. Desdouits, D. Cohen, A. C. Nairn, P. Greengard, and J. A. Girault. Phosphorylation of DARPP-32, a dopamine- and cAMP-regulated phosphoprotein, by casein kinase I in vitro and in vivo. *J Biol Chem*, 270(15):8772–8778, 1995b. (Cited on page 11.)

F. Desdouits, J. C. Siciliano, A. C. Nairn, P. Greengard, and J. A. Girault. Dephosphorylation of Ser-137 in DARPP-32 by protein phosphatases 2A and 2C: different roles in vitro and in striatonigral neurons. *Biochem J*, 330 ( Pt 1):211–216, 1998. (Cited on page 11.)

R. E. Dolmetsch, U. Pajvani, K. Fife, J. M. Spotts, and M. E. Greenberg. Signaling to the nucleus by an L-type calcium channel-calmodulin complex through the MAP kinase pathway.sal. *Science*, 294(5541):333–339, 2001. doi:10.1126/science.1063395. (Cited on page 8.)

J. Dormand and P. Prince. A family of embedded Runge-Kutta formulae. *Journal of Computational and Applied Mathematics*, 6(1):19–26, 1980. (Cited on page 23.)

S. M. Dudek and M. F. Bear. Homosynaptic long-term depression in area CA1 of hippocampus and effects of N-methyl-D-aspartate receptor blockade. *Proc Natl Acad Sci U S A*, 89(10):4363–4367, 1992. (Cited on page 18.)

A. Dunaevsky, A. Tashiro, A. Majewska, C. Mason, and R. Yuste. Developmental regulation of spine motility in the mammalian central nervous system. *Proc Natl Acad Sci U S A*, 96(23):13438–13443, 1999. (Cited on page 5.)

F. Engert and T. Bonhoeffer. Dendritic spine changes associated with hippocampal long-term synaptic plasticity. *Nature*, 399(6731):66–70, 1999. doi:10.1038/19978. (Cited on page 5.)

W. R. Esposito and C. A. Floudas. Global Optimization for the Parameter Estimation of Differential-Algebraic Systems. *Industrial and Engineering Chemistry Research*, 39:1291–1310, 2000. (Cited on page 121.)

J. A. Esteban, S.-H. Shi, C. Wilson, M. Nuriya, R. L. Huganir, and R. Malinow. PKA phosphorylation of AMPA receptor subunits

controls synaptic trafficking underlying plasticity. *Nat Neurosci*, 6(2):136–143, 2003. doi:10.1038/nn997. (Cited on pages 6 and 11.)

N. J. Eungdamrong and R. Iyengar. Computational approaches for modeling regulatory cellular networks. *Trends Cell Biol*, 14(12):661–669, 2004. doi:10.1016/j.tcb.2004.10.007. (Cited on page 15.)

B. J. Everitt and T. W. Robbins. Neural systems of reinforcement for drug addiction: from actions to habits to compulsion. *Nat Neurosci*, 8(11):1481–1489, 2005. doi:10.1038/nn1579. (Cited on page 1.)

J. J. Falke, S. K. Drake, A. L. Hazard, and O. B. Peersen. Molecular tuning of ion binding to calcium signaling proteins. *Q Rev Biophys*, 27(3):219–290, 1994. (Cited on pages 34 and 75.)

C. P. Fall, E. S. Marland, J. M. agner, and J. J. Tyson. *Computational Cell Biology*. Springer, 2002. (Cited on page 16.)

E. Fernandez, R. Schiappa, J.-A. Girault, and N. L. Novère. DARPP-32 Is a Robust Integrator of Dopamine and Glutamate Signals. *PLoS Comput Biol*, 2(12):e176, 2006. doi:10.1371/journal.pcbi.0020176. (Cited on pages 15, 67, 68, and 74.)

J. E. Ferrell and R. R. Bhatt. Mechanistic studies of the dual phosphorylation of mitogen-activated protein kinase. *J Biol Chem*, 272(30):19008–19016, 1997. (Cited on pages 71 and 77.)

J. C. Fiala, B. Allwardt, and K. M. Harris. Dendritic spines do not split during hippocampal LTP or maturation. *Nat Neurosci*, 5(4):297–298, 2002. doi:10.1038/nn830. (Cited on page 5.)

A. A. Fienberg, N. Hiroi, P. G. Mermelstein, W. Song, G. L. Snyder, A. Nishi, A. Cheramy, J. P. O'Callaghan, D. B. Miller, D. G. Cole, R. Corbett, C. N. Haile, D. C. Cooper, S. P. Onn, A. A. Grace, C. C. Ouimet, F. J. White, S. E. Hyman, D. J. Surmeier, J. Girault, E. J. Nestler, and P. Greengard. DARPP-32: regulator of the efficacy of dopaminergic neurotransmission. *Science*, 281(5378):838–842, 1998. (Cited on page 13.)

E. Fifková and C. L. Anderson. Stimulation-induced changes in dimensions of stalks of dendritic spines in the dentate molecular layer. *Exp Neurol*, 74(2):621–627, 1981. (Cited on page 5.)

C. C. Fink, B. Slepchenko, I. I. Moraru, J. Watras, J. C. Schaff, and L. M. Loew. An image-based model of calcium waves in differentiated neuroblastoma cells. *Biophys J*, 79(1):163–183, 2000. doi:10.1016/S0006-3495(00)76281-3. (Cited on page 16.)

R. S. Fiore, T. H. Murphy, J. S. Sanghera, S. L. Pelech, and J. M. Baraban. Activation of p42 mitogen-activated protein kinase by glutamate receptor stimulation in rat primary cortical cultures. *J Neurochem*, 61(5):1626–1633, 1993. (Cited on page 57.)

M. Fischer, S. Kaech, D. Knutti, and A. Matus. Rapid actin-based plasticity in dendritic spines. *Neuron*, 20(5):847–854, 1998. (Cited on page 5.)

M. Fischer, S. Kaech, U. Wagner, H. Brinkhaus, and A. Matus. Glutamate receptors regulate actin-based plasticity in dendritic spines. *Nat Neurosci*, 3(9):887–894, 2000. doi:10.1038/78791. (Cited on pages 6 and 57.)

J. Flores-Hernández, C. Cepeda, E. Hernández-Echeagaray, C. R. Calvert, E. S. Jokel, A. A. Fienberg, P. Greengard, and M. S. Levine. Dopamine enhancement of NMDA currents in dissociated medium-sized striatal neurons: role of D1 receptors and DARPP-32. *J Neurophysiol*, 88(6):3010–3020, 2002. doi:10.1152/jn.00361.2002. (Cited on page 13.)

K. Fox, N. Daw, H. Sato, and D. Czepita. Dark-rearing delays the loss of NMDA-receptor function in kitten visual cortex. *Nature*, 350(6316):342–344, 1991. doi:10.1038/350342a0. (Cited on page 120.)

K. M. Franks, T. M. Bartol, and T. J. Sejnowski. An mcell model of calcium dynamics and frequency-dependence of calmodulin activation in dendritic spines. *Neurocomputing*, 38-40:9 – 16, 2001. ISSN 0925-2312. doi:DOI:10.1016/S0925-2312(01)00415-5. (Cited on page 20.)

K. M. Franks, T. M. Bartol, and T. J. Sejnowski. A Monte Carlo model reveals independent signaling at central glutamatergic synapses. *Biophys J*, 83(5):2333–2348, 2002. doi:10.1016/S0006-3495(02)75248-X. (Cited on page 17.)

K. M. Franks, C. F. Stevens, and T. J. Sejnowski. Independent sources of quantal variability at single glutamatergic synapses. *J Neurosci*, 23(8):3186–3195, 2003. (Cited on page 17.)

Y. Fukazawa, Y. Saitoh, F. Ozawa, Y. Ohta, K. Mizuno, and K. Inokuchi. Hippocampal LTP is accompanied by enhanced F-actin content within the dendritic spine that is essential for late LTP maintenance in vivo. *Neuron*, 38(3):447–460, 2003. (Cited on page 6.)

Y. Geinisman, R. W. Berry, J. F. Disterhoft, J. M. Power, and E. A. V. der Zee. Associative learning elicits the formation of multiple-synapse boutons. *J Neurosci*, 21(15):5568–5573, 2001. (Cited on page 5.)

P. C. Georges, N. M. Hadzimichalis, E. S. Sweet, and B. L. Firestein. The yin-yang of dendrite morphology: unity of actin and microtubules. *Mol Neurobiol*, 38(3):270–284, 2008. doi:10.1007/s12035-008-8046-8. (Cited on page 8.)

P. Gideon, J. John, M. Frech, A. Lautwein, R. Clark, J. E. Scheffler, and A. Wittinghofer. Mutational and kinetic analyses of the gtpase-activating protein (gap)-p21 interaction: the c-terminal domain of gap is not sufficient for full activity. *Mol Cell Biol*, 12(5):2050–2056, 1992. (Cited on page 104.)

D. T. Gillespie. A general method for numerically simulating the stochastic time evolution of coupled chemical reactions. *Journal of Computational Physics*, 22(4):403–434, 1976. (Cited on page 17.)

D. T. Gillespie. Exact stochastic simulation of coupled chemical reactions. *The Journal of Physical Chemistry*, 81(25):2340–2361, 1977. (Cited on page 17.)

J. A. Girault, H. C. Hemmings, K. R. Williams, A. C. Nairn, and P. Greengard. Phosphorylation of DARPP-32, a dopamine- and cAMP-regulated phosphoprotein, by casein kinase II. *J Biol Chem*, 264(36):21748–21759, 1989. (Cited on page 11.)

J.-A. Girault, E. Valjent, J. Caboche, and D. Hervé. ERK2: a logical AND gate critical for drug-induced plasticity? *Curr Opin Pharmacol*, 7(1):77–85, 2007. doi:10.1016/j.coph.2006.08.012. (Cited on pages 59, 111, and 114.)

B. Giros, M. Jaber, S. R. Jones, R. M. Wightman, and M. G. Caron. Hyperlocomotion and indifference to cocaine and amphetamine in mice lacking the dopamine transporter. *Nature*, 379(6566):606–612, 1996. doi:10.1038/379606a0. (Cited on page 118.)

F. Gonon. Prolonged and extrasynaptic excitatory action of dopamine mediated by D1 receptors in the rat striatum in vivo. *J Neurosci*, 17(15):5972–5978, 1997. (Cited on page 78.)

S. Goto, Y. Matsukado, Y. Mihara, N. Inoue, and E. Miyamoto. The distribution of calcineurin in rat brain by light and electron microscopic immunohistochemistry and enzyme-immunoassay. *Brain Res*, 397(1):161–172, 1986. (Cited on pages 33 and 74.)

P. Greengard. The neurobiology of dopamine signaling. *Biosci Rep*, 21(3):247–269, 2001a. (Cited on page 11.)

P. Greengard. The neurobiology of slow synaptic transmission. *Science*, 294(5544):1024–1030, 2001b. doi:10.1126/science.294.5544. 1024. (Cited on page 14.)

L. Groc, B. Gustafsson, and E. Hanse. AMPA signalling in nascent glutamatergic synapses: there and not there! *Trends Neurosci*, 29(3):132–139, 2006. doi:10.1016/j.tins.2006.01.005. (Cited on page 119.)

R. D. Groth, R. L. Dunbar, and P. G. Mermelstein. Calcineurin regulation of neuronal plasticity. *Biochem Biophys Res Commun*, 311(4):1159–1171, 2003. (Cited on pages 4, 11, and 30.)

C. M. Guldberg and P. Waage. Studies Concerning Affinity. *Forhandlinger: Videnskabs-Selskabet i Christiana*, 12:35–45, 1864. (Cited on page 15.)

B. Gustafsson, H. Wigström, W. C. Abraham, and Y. Y. Huang. Long-term potentiation in the hippocampus using depolarizing current pulses as the conditioning stimulus to single volley synaptic potentials. *J Neurosci*, 7(3):774–780, 1987. (Cited on page 54.)

B. J. Hall and A. Ghosh. Regulation of AMPA receptor recruitment at developing synapses. *Trends Neurosci*, 31(2):82–89, 2008. doi: 10.1016/j.tins.2007.11.010. (Cited on pages 112 and 119.)

S. Halpain, J. A. Girault, and P. Greengard. Activation of NMDA receptors induces dephosphorylation of DARPP-32 in rat striatal slices. *Nature*, 343(6256):369–372, 1990. doi:10.1038/343369a0. (Cited on pages 33 and 74.)

S. Halpain, A. Hipolito, and L. Saffer. Regulation of F-actin stability in dendritic spines by glutamate receptors and calcineurin. *J Neurosci*, 18(23):9835–9844, 1998. (Cited on page 6.)

R. M. Hanley, A. R. Means, B. E. Kemp, and S. Shenolikar. Mapping of calmodulin-binding domain of Ca2+/calmodulin-dependent protein kinase II from rat brain. *Biochem Biophys Res Commun*, 152(1):122–128, 1988. (Cited on page 19.)

P. I. Hanson, T. Meyer, L. Stryer, and H. Schulman. Dual role of calmodulin in autophosphorylation of multifunctional CaM kinase may underlie decoding of calcium signals. *Neuron*, 12(5):943–956, 1994. (Cited on pages 19, 28, and 55.)

G. E. Hardingham, Y. Fukunaga, and H. Bading. Extrasynaptic NMDARs oppose synaptic NMDARs by triggering CREB shut-off and cell death pathways. *Nat Neurosci*, 5(5):405–414, 2002. doi: 10.1038/nn835. (Cited on page 8.)

K. M. Harris, J. C. Fiala, and L. Ostroff. Structural changes at dendritic spine synapses during long-term potentiation. *Philos Trans R Soc Lond B Biol Sci*, 358(1432):745–748, 2003. doi:10.1098/rstb.2002.1254. (Cited on page 5.)

K. M. Harris, F. E. Jensen, and B. Tsao. Three-dimensional structure of dendritic spines and synapses in rat hippocampus (CA1) at postnatal day 15 and adult ages: implications for the maturation of synaptic physiology and long-term potentiation. *J Neurosci*, 12(7):2685–2705, 1992. (Cited on page 3.)

K. M. Harris and S. B. Kater. Dendritic spines: cellular specializations imparting both stability and flexibility to synaptic function. *Annu Rev Neurosci*, 17:341–371, 1994. doi:10.1146/annurev.ne.17.030194.002013. (Cited on page 5.)

C. D. Harvey, R. Yasuda, H. Zhong, and K. Svoboda. The spread of Ras activity triggered by activation of a single dendritic spine. *Science*, 321(5885):136–140, 2008. doi:10.1126/science.1159675. (Cited on pages 114 and 122.)

P. Hasler, J. J. Moore, and G. M. Kammer. Human T lymphocyte cAMP-dependent protein kinase: subcellular distributions and activity ranges of type I and type II isozymes. *FASEB J*, 6(9):2735–2741, 1992. (Cited on page 75.)

J. M. Haugh. A unified model for signal transduction reactions in cellular membranes. *Biophys J*, 82(2):591–604, 2002. doi:10.1016/S0006-3495(02)75424-6. (Cited on page 16.)

Y. Hayashi, S. H. Shi, J. A. Esteban, A. Piccini, J. C. Poncer, and R. Malinow. Driving AMPA receptors into synapses by LTP and CaMKII: requirement for GluR1 and PDZ domain interaction. *Science*, 287(5461):2262–2267, 2000. (Cited on pages 3, 57, and 122.)

R. D. Heijtz, B. Kolb, and H. Forssberg. Can a therapeutic dose of amphetamine during pre-adolescence modify the pattern of synaptic organization in the brain? *Eur J Neurosci*, 18(12):3394–3399, 2003. (Cited on page 117.)

H. C. Hemmings, P. Greengard, H. Y. Tung, and P. Cohen. DARPP-32, a dopamine-regulated neuronal phosphoprotein, is a potent inhibitor of protein phosphatase-1. *Nature*, 310(5977):503–505, 1984a. (Cited on pages 11, 20, 30, 52, and 70.)

H. C. Hemmings, A. C. Nairn, J. I. Elliott, and P. Greengard. Synthetic peptide analogs of DARPP-32 (Mr 32,000 dopamine- and cAMP-regulated phosphoprotein), an inhibitor of protein phosphatase-1. Phosphorylation, dephosphorylation, and inhibitory activity. *J Biol Chem*, 265(33):20369–20376, 1990. (Cited on pages 11, 52, 58, 69, and 70.)

H. C. Hemmings, A. C. Nairn, and P. Greengard. DARPP-32, a dopamine- and adenosine 3':5'-monophosphate-regulated neuronal phosphoprotein. II. Comparison of the kinetics of phosphorylation of DARPP-32 and phosphatase inhibitor 1. *J Biol Chem*, 259(23):14491–14497, 1984b. (Cited on pages 33, 68, 69, and 116.)

F. Hofmann, P. J. Bechtel, and E. G. Krebs. Concentrations of cyclic AMP-dependent protein kinase subunits in various tissues. *J Biol Chem*, 252(4):1441–1447, 1977. (Cited on page 74.)

C. H. Horner. Plasticity of the dendritic spine. *Prog Neurobiol*, 41(3):281–321, 1993. (Cited on page 117.)

C. Y. Huang and J. E. Ferrell. Ultrasensitivity in the mitogen-activated protein kinase cascade. *Proc Natl Acad Sci U S A*, 93(19):10078–10083, 1996. (Cited on pages 74 and 75.)

H. B. Huang, A. Horiuchi, T. Watanabe, S. R. Shih, H. J. Tsay, H. C. Li, P. Greengard, and A. C. Nairn. Characterization of the inhibition of protein phosphatase-1 by DARPP-32 and inhibitor-2. *J Biol Chem*, 274(12):7870–7878, 1999. (Cited on pages 11 and 52.)

S. E. Hyman. Addiction: a disease of learning and memory. *Am J Psychiatry*, 162(8):1414–1422, 2005. doi:10.1176/appi.ajp.162.8.1414. (Cited on page 1.)

S. E. Hyman and R. C. Malenka. Addiction and the brain: the neurobiology of compulsion and its persistence. *Nat Rev Neurosci*, 2(10):695–703, 2001. doi:10.1038/35094560. (Cited on pages 1 and 117.)

S. E. Hyman, R. C. Malenka, and E. J. Nestler. Neural mechanisms of addiction: the role of reward-related learning and memory. *Annu Rev Neurosci*, 29:565–598, 2006. doi:10.1146/annurev.neuro.29.051605.113009. (Cited on pages 1 and 115.)

T. S. Ingebritsen, A. A. Stewart, and P. Cohen. The protein phosphatases involved in cellular regulation. 6. Measurement of type-1 and type-2 protein phosphatases in extracts of mammalian tissues; an assessment of their physiological roles. *Eur J Biochem*, 132(2):297–307, 1983. (Cited on pages 33 and 74.)

R. Ito, T. W. Robbins, and B. J. Everitt. Differential control over cocaine-seeking behavior by nucleus accumbens core and shell. *Nat Neurosci*, 7(4):389–397, 2004. doi:10.1038/nn1217. (Cited on page 1.)

S. Ivkovic and M. E. Ehrlich. Expression of the striatal DARPP-32/ARPP-21 phenotype in GABAergic neurons requires neuro-

trophins in vivo and in vitro. *J Neurosci*, 19(13):5409–5419, 1999. (Cited on page 114.)

S. Jones, J. L. Kornblum, and J. A. Kauer. Amphetamine blocks long-term synaptic depression in the ventral tegmental area. *J Neurosci*, 20(15):5575–5580, 2000. (Cited on page 118.)

S. Kakiuchi, S. Yasuda, R. Yamazaki, Y. Teshima, K. Kanda, R. Kakiuchi, and K. Sobue. Quantitative determinations of calmodulin in the supernatant and particulate fractions of mammalian tissues. *J Biochem*, 92(4):1041–1048, 1982. (Cited on pages 33 and 73.)

P. W. Kalivas. Interactions between dopamine and excitatory amino acids in behavioral sensitization to psychostimulants. *Drug Alcohol Depend*, 37(2):95–100, 1995. (Cited on page 117.)

P. W. Kalivas. Glutamate systems in cocaine addiction. *Curr Opin Pharmacol*, 4(1):23–29, 2004. doi:10.1016/j.coph.2003.11.002. (Cited on page 115.)

E. R. Kandel. The molecular biology of memory storage: a dialogue between genes and synapses. *Science*, 294(5544):1030–1038, 2001. doi:10.1126/science.1067020. (Cited on pages 5 and 8.)

K. Kandler, L. C. Katz, and J. A. Kauer. Focal photolysis of caged glutamate produces long-term depression of hippocampal glutamate receptors. *Nat Neurosci*, 1(2):119–123, 1998. doi:10.1038/368. (Cited on page 3.)

J. A. Kauer and R. C. Malenka. Synaptic plasticity and addiction. *Nat Rev Neurosci*, 8(11):844–858, 2007. doi:10.1038/nrn2234. (Cited on pages 115 and 119.)

M. B. Kennedy. Signal-processing machines at the postsynaptic density. *Science*, 290(5492):750–754, 2000. (Cited on page 14.)

M. B. Kennedy, H. C. Beale, H. J. Carlisle, and L. B. Washburn. Integration of biochemical signalling in spines. *Nat Rev Neurosci*, 6(6):423–434, 2005. (Cited on pages 123 and 124.)

J. N. Kerr and J. R. Wickens. Dopamine D-1/D-5 receptor activation is required for long-term potentiation in the rat neostriatum in vitro. *J Neurophysiol*, 85(1):117–124, 2001. (Cited on page 116.)

B. N. Kholodenko and H. V. Westerhoff. The macroworld versus the microworld of biochemical regulation and control. *Trends Biochem Sci*, 20(2):52–54, 1995. (Cited on page 24.)

E. Kim and M. Sheng. PDZ domain proteins of synapses. *Nat Rev Neurosci*, 5(10):771–781, 2004. doi:10.1038/nrn1517. (Cited on page 123.)

J. H. Kim, D. Liao, L. F. Lau, and R. L. Huganir. SynGAP: a synaptic RasGAP that associates with the PSD-95/SAP90 protein family. *Neuron*, 20(4):683–691, 1998. (Cited on page 60.)

M. J. Kim, A. W. Dunah, Y. T. Wang, and M. Sheng. Differential roles of NR2A- and NR2B-containing NMDA receptors in Ras-ERK signaling and AMPA receptor trafficking. *Neuron*, 46(5):745–760, 2005. doi:10.1016/j.neuron.2005.04.031. (Cited on pages 59, 60, 113, and 119.)

M. M. King, C. Y. Huang, P. B. Chock, A. C. Nairn, H. C. Hemmings, K. F. Chan, and P. Greengard. Mammalian brain phosphoproteins as substrates for calcineurin. *J Biol Chem*, 259(13):8080–8083, 1984. (Cited on pages 11, 33, 68, and 69.)

A. Kirkwood and M. F. Bear. Homosynaptic long-term depression in the visual cortex. *J Neurosci*, 14(5 Pt 2):3404–3412, 1994. (Cited on page 20.)

C. B. Klee. Concerted regulation of protein phosphorylation and dephosphorylation by calmodulin. *Neurochem Res*, 16(9):1059–1065, 1991. (Cited on page 50.)

C. B. Klee, H. Ren, and X. Wang. Regulation of the calmodulin-stimulated protein phosphatase, calcineurin. *J Biol Chem*, 273(22):13367–13370, 1998. (Cited on page 30.)

J. A. Kleim, J. H. Freeman, R. Bruneau, B. C. Nolan, N. R. Cooper, A. Zook, and D. Walters. Synapse formation is associated with memory storage in the cerebellum. *Proc Natl Acad Sci U S A*, 99(20):13228–13231, 2002. doi:10.1073/pnas.202483399. (Cited on page 5.)

S. Knafo, Y. Grossman, E. Barkai, and G. Benshalom. Olfactory learning is associated with increased spine density along apical dendrites of pyramidal neurons in the rat piriform cortex. *Eur J Neurosci*, 13(3):633–638, 2001. (Cited on page 5.)

B. Kolb, G. Gorny, Y. Li, A.-N. Samaha, and T. E. Robinson. Amphetamine or cocaine limits the ability of later experience to promote structural plasticity in the neocortex and nucleus accumbens. *Proc Natl Acad Sci U S A*, 100(18):10523–10528, 2003. doi: 10.1073/pnas.1834271100. (Cited on page 117.)

S. J. Kolodziej, A. Hudmon, M. N. Waxham, and J. K. Stoops. Three-dimensional reconstructions of calcium/calmodulin-dependent (CaM) kinase IIalpha and truncated CaM kinase IIalpha reveal a unique organization for its structural core and functional domains. *J Biol Chem*, 275(19):14354–14359, 2000. (Cited on page 19.)

S. Kourrich, P. E. Rothwell, J. R. Klug, and M. J. Thomas. Cocaine experience controls bidirectional synaptic plasticity in the nucleus accumbens. *J Neurosci*, 27(30):7921–7928, 2007. doi:10.1523/JNEUROSCI.1859-07.2007. (Cited on page 56.)

G. Krapivinsky, I. Medina, L. Krapivinsky, S. Gapon, and D. E. Clapham. SynGAP-MUPP1-CaMKII synaptic complexes regulate p38 MAP kinase activity and NMDA receptor-dependent synaptic AMPA receptor potentiation. *Neuron*, 43(4):563–574, 2004. doi: 10.1016/j.neuron.2004.08.003. (Cited on pages 60 and 123.)

H. Kuboniwa, N. Tjandra, S. Grzesiek, H. Ren, C. B. Klee, and A. Bax. Solution structure of calcium-free calmodulin. *Nat Struct Biol*, 2(9):768–776, 1995. (Cited on page 19.)

Y. G. Kwon, H. B. Huang, F. Desdouits, J. A. Girault, P. Greengard, and A. C. Nairn. Characterization of the interaction between DARPP-32 and protein phosphatase 1 (PP-1): DARPP-32 peptides antagonize the interaction of PP-1 with binding proteins. *Proc Natl Acad Sci U S A*, 94(8):3536–3541, 1997. (Cited on pages 11 and 52.)

R. Lamprecht and J. LeDoux. Structural plasticity and memory. *Nat Rev Neurosci*, 5(1):45–54, 2004. doi:10.1038/nrn1301. (Cited on pages 5, 6, 117, and 123.)

N. Le Novère, M. Hucka, H. Mi, S. Moodie, F. Schreiber, A. Sorokin, E. Demir, K. Wegner, M. I. Aladjem, S. M. Wimalaratne, F. T. Bergman, R. Gauges, P. Ghazal, H. Kawaji, L. Li, Y. Matsuoka, A. Villéger, S. E. Boyd, L. Calzone, M. Courtot, U. Dogrusoz, T. C. Freeman, A. Funahashi, S. Ghosh, A. Jouraku, S. Kim, F. Kolpakov, A. Luna, S. Sahle, E. Schmidt, S. Watterson, G. Wu, I. Goryanin, D. B. Kell, C. Sander, H. Sauro, J. L. Snoep, K. Kohn, and H. Kitano. The Systems Biology Graphical Notation. *Nat Biotechnol*, 27(8):735–741, 2009. doi:10.1038/nbt.1558. (Cited on pages 12, 64, and 101.)

N. Le Novère, L. Li, and J.-A. Girault. DARPP-32: molecular integration of phosphorylation potential. *Cell Mol Life Sci*, 65(14):2125–2127, 2008. doi:10.1007/s00018-008-8150-y. (Cited on pages 12, 13, and 38.)

H. K. Lee, M. Barbarosie, K. Kameyama, M. F. Bear, and R. L. Huganir. Regulation of distinct AMPA receptor phosphorylation sites during bidirectional synaptic plasticity. *Nature*, 405(6789):955–959, 2000. doi:10.1038/35016089. (Cited on page 3.)

H.-K. Lee, K. Takamiya, J.-S. Han, H. Man, C.-H. Kim, G. Rumbaugh, S. Yu, L. Ding, C. He, R. S. Petralia, R. J. Wenthold, M. Gallagher, and R. L. Huganir. Phosphorylation of the AMPA receptor GluR1 subunit is required for synaptic plasticity and retention of spatial memory. *Cell*, 112(5):631–643, 2003a. (Cited on pages 3 and 6.)

K.-H. Lee, A. R. Dinner, C. Tu, G. Campi, S. Raychaudhuri, R. Varma, T. N. Sims, W. R. Burack, H. Wu, J. Wang, O. Kanagawa, M. Markiewicz, P. M. Allen, M. L. Dustin, A. K. Chakraborty, and A. S. Shaw. The immunological synapse balances T cell receptor signaling and degradation. *Science*, 302(5648):1218–1222, 2003b. doi: 10.1126/science.1086507. (Cited on page 17.)

A. S. Leonard, I. A. Lim, D. E. Hemsworth, M. C. Horne, and J. W. Hell. Calcium/calmodulin-dependent protein kinase II is associated with the N-methyl-D-aspartate receptor. *Proc Natl Acad Sci U S A*, 96(6):3239–3244, 1999. (Cited on page 60.)

B. Leuner, J. Falduto, and T. J. Shors. Associative memory formation increases the observation of dendritic spines in the hippocampus. *J Neurosci*, 23(2):659–665, 2003. (Cited on pages 5 and 117.)

K. Levenberg. A Method for the Solution of Certain Non-Linear Problems in Least Squares. *The Quarterly of Applied Mathematics*, 2:164–168, 1944. (Cited on page 121.)

Y. Li and J. A. Kauer. Repeated exposure to amphetamine disrupts dopaminergic modulation of excitatory synaptic plasticity and neurotransmission in nucleus accumbens. *Synapse*, 51(1):1–10, 2004. doi:10.1002/syn.10270. (Cited on page 115.)

Y. Li, B. Kolb, and T. E. Robinson. The location of persistent amphetamine-induced changes in the density of dendritic spines on medium spiny neurons in the nucleus accumbens and caudate-putamen. *Neuropsychopharmacology*, 28(6):1082–1085, 2003. doi: 10.1038/sj.npp.1300115. (Cited on page 117.)

S. Linse, A. Helmersson, and S. Forsén. Calcium binding to calmodulin and its globular domains. *J Biol Chem*, 266(13):8050–8054, 1991. (Cited on page 75.)

J. Lisman. A mechanism for the Hebb and the anti-Hebb processes underlying learning and memory. *Proc Natl Acad Sci U S A*, 86(23):9574–9578, 1989. (Cited on page 18.)

J. Lisman, H. Schulman, and H. Cline. The molecular basis of CaMKII function in synaptic and behavioural memory. *Nat Rev Neurosci*, 3(3):175–190, 2002. doi:10.1038/nrn753. (Cited on pages 3 and 19.)

P. M. Lledo, G. O. Hjelmstad, S. Mukherji, T. R. Soderling, R. C. Malenka, and R. A. Nicoll. Calcium/calmodulin-dependent kinase II and long-term potentiation enhance synaptic transmission by the same mechanism. *Proc Natl Acad Sci U S A*, 92(24):11175–11179, 1995. (Cited on page 18.)

W. Lu, H. Man, W. Ju, W. S. Trimble, J. F. MacDonald, and Y. T. Wang. Activation of synaptic NMDA receptors induces membrane insertion of new AMPA receptors and LTP in cultured hippocampal neurons. *Neuron*, 29(1):243–254, 2001. (Cited on pages 57 and 122.)

K. Luby-Phelps, M. Hori, J. M. Phelps, and D. Won. Ca(2+)-regulated dynamic compartmentalization of calmodulin in living smooth muscle cells. *J Biol Chem*, 270(37):21532–21538, 1995. (Cited on page 50.)

V. Lučić, G. J. Greif, and M. B. Kennedy. Detailed state model of CaMKII activation and autophosphorylation. *Eur Biophys J*, 38(1):83–98, 2008. doi:10.1007/s00249-008-0362-4. (Cited on pages 33 and 102.)

M. A. Lynch. Long-term potentiation and memory. *Physiol Rev*, 84(1):87–136, 2004. doi:10.1152/physrev.00014.2003. (Cited on pages 3 and 18.)

J. C. Magee and D. Johnston. A synaptically controlled, associative signal for Hebbian plasticity in hippocampal neurons. *Science*, 275(5297):209–213, 1997. (Cited on pages 3 and 14.)

A. Majewska, E. Brown, J. Ross, and R. Yuste. Mechanisms of calcium decay kinetics in hippocampal spines: role of spine calcium pumps and calcium diffusion through the spine neck in biochemical compartmentalization. *J Neurosci*, 20(5):1722–1734, 2000. (Cited on page 124.)

R. C. Malenka. The long-term potential of LTP. *Nat Rev Neurosci*, 4(11):923–926, 2003. doi:10.1038/nrn1258. (Cited on pages 3 and 18.)

R. C. Malenka and M. F. Bear. LTP and LTD: an embarrassment of riches. *Neuron*, 44(1):5–21, 2004. doi:10.1016/j.neuron.2004.09.012. (Cited on page 55.)

R. C. Malenka, B. Lancaster, and R. S. Zucker. Temporal limits on the rise in postsynaptic calcium required for the induction of long-term potentiation. *Neuron*, 9(1):121–128, 1992. (Cited on page 54.)

R. C. Malenka and R. A. Nicoll. Long-term potentiation–a decade of progress? *Science*, 285(5435):1870–1874, 1999. (Cited on page 19.)

M. Maletic-Savatic, R. Malinow, and K. Svoboda. Rapid dendritic morphogenesis in CA1 hippocampal dendrites induced by synaptic activity. *Science*, 283(5409):1923–1927, 1999. (Cited on pages 5 and 6.)

R. Malinow and R. C. Malenka. AMPA receptor trafficking and synaptic plasticity. *Annu Rev Neurosci*, 25:103–126, 2002. doi:10.1146/annurev.neuro.25.112701.142758. (Cited on page 3.)

H. Markram, J. Lübke, M. Frotscher, and B. Sakmann. Regulation of synaptic efficacy by coincidence of postsynaptic APs and EPSPs. *Science*, 275(5297):213–215, 1997. (Cited on pages 3 and 14.)

H. Markram, A. Roth, and F. Helmchen. Competitive calcium binding: implications for dendritic calcium signaling. *J Comput Neurosci*, 5(3):331–348, 1998. (Cited on pages 32, 34, 65, and 75.)

D. Marquardt. An Algorithm for Least-Squares Estimation of Nonlinear Parameters. *SIAM Journal on Applied Mathematics*, 11:431–441, 1963. (Cited on page 121.)

K. C. Martin, M. Barad, and E. R. Kandel. Local protein synthesis and its role in synapse-specific plasticity. *Curr Opin Neurobiol*, 10(5):587–592, 2000. (Cited on page 6.)

S. Matsuda, H. Kosako, K. Takenaka, K. Moriyama, H. Sakai, T. Akiyama, Y. Gotoh, and E. Nishida. Xenopus map kinase activator: identification and function as a key intermediate in the phosphorylation cascade. *EMBO J*, 11(3):973–982, 1992. (Cited on page 75.)

M. Matsuzaki, G. C. Ellis-Davies, T. Nemoto, Y. Miyashita, M. Iino, and H. Kasai. Dendritic spine geometry is critical for AMPA receptor expression in hippocampal CA1 pyramidal neurons. *Nat Neurosci*, 4(11):1086–1092, 2001. doi:10.1038/nn736. (Cited on page 124.)

A. Matus. Actin-based plasticity in dendritic spines. *Science*, 290(5492):754–758, 2000. (Cited on pages 5 and 8.)

E. McGlade-McCulloh, H. Yamamoto, S. E. Tan, D. A. Brickey, and T. R. Soderling. Phosphorylation and regulation of glutamate receptors by calcium/calmodulin-dependent protein kinase II. *Nature*, 362(6421):640–642, 1993. doi:10.1038/362640a0. (Cited on page 18.)

R. A. McKinney, M. Capogna, R. Dürr, B. H. Gäshwiler, and S. M. Thompson. Miniature synaptic events maintain dendritic spines via AMPA receptor activation. *Nat Neurosci*, 2(1):44–49, 1999. doi:10.1038/4548. (Cited on page 6.)

P. Mendes and D. Kell. Non-linear optimization of biochemical pathways: applications to metabolic engineering and parameter estimation. *Bioinformatics*, 14(10):869–883, 1998. (Cited on page 121.)

F. Meng and G. Zhang. Autophosphorylated calcium/calmodulin-dependent protein kinase II alpha induced by cerebral ischemia immediately targets and phosphorylates N-methyl-D-aspartate receptor subunit 2B (NR2B) in hippocampus of rats. *Neurosci Lett*, 333(1):59–63, 2002. (Cited on page 60.)

T. Meyer, P. I. Hanson, L. Stryer, and H. Schulman. Calmodulin trapping by calcium-calmodulin-dependent protein kinase. *Science*, 256(5060):1199–1202, 1992. (Cited on pages 19, 28, 32, 46, 55, 66, and 102.)

S. G. Miller and M. B. Kennedy. Regulation of brain type II Ca2+/calmodulin-dependent protein kinase by autophosphorylation: a Ca2+-triggered molecular switch. *Cell*, 44(6):861–870, 1986. (Cited on page 55.)

C. Missale, S. R. Nash, S. W. Robinson, M. Jaber, and M. G. Caron. Dopamine receptors: from structure to function. *Physiol Rev*, 78(1):189–225, 1998. (Cited on page 10.)

J. Monod, J. Wyman, and J. P. Changeux. On the Nature of Allosteric Transitions: A Plausible Model. *J Mol Biol*, 12:88–118, 1965. (Cited on page 26.)

H. Monyer, N. Burnashev, D. J. Laurie, B. Sakmann, and P. H. Seeburg. Developmental and regional expression in the rat brain and functional properties of four NMDA receptors. *Neuron*, 12(3):529–540, 1994. (Cited on page 59.)

B. J. Morris, C. S. Simpson, S. Mundell, K. Maceachern, H. M. Johnston, and A. M. Nolan. Dynamic changes in NADPH-diaphorase staining reflect activity of nitric oxide synthase: evidence for a dopaminergic regulation of striatal nitric oxide release. *Neuropharmacology*, 36(11-12):1589–1599, 1997. (Cited on page 116.)

M. E. Morrison and C. A. Mason. Granule neuron regulation of purkinje cell development: striking a balance between neurotrophin and

glutamate signaling. *J Neurosci*, 18(10):3563–3573, 1998. (Cited on page 114.)

M. B. Moser, M. Trommald, and P. Andersen. An increase in dendritic spine density on hippocampal CA1 pyramidal cells following spatial learning in adult rats suggests the formation of new synapses. *Proc Natl Acad Sci U S A*, 91(26):12673–12675, 1994. (Cited on page 117.)

S. Mukherji and T. R. Soderling. Regulation of Ca2+/calmodulin-dependent protein kinase II by inter- and intrasubunit-catalyzed autophosphorylations. *J Biol Chem*, 269(19):13744–13747, 1994. (Cited on pages 19 and 55.)

A. B. Mulder, M. P. Arts, and F. H. L. da Silva. Short- and long-term plasticity of the hippocampus to nucleus accumbens and prefrontal cortex pathways in the rat, in vivo. *Eur J Neurosci*, 9(8):1603–1611, 1997. (Cited on page 115.)

R. M. Mulkey, S. Endo, S. Shenolikar, and R. C. Malenka. Involvement of a calcineurin/inhibitor-1 phosphatase cascade in hippocampal long-term depression. *Nature*, 369(6480):486–488, 1994. doi:10.1038/369486a0. (Cited on pages 4, 18, 20, and 30.)

R. M. Mulkey, C. E. Herron, and R. C. Malenka. An essential role for protein phosphatases in hippocampal long-term depression. *Science*, 261(5124):1051–1055, 1993. (Cited on page 20.)

R. M. Mulkey and R. C. Malenka. Mechanisms underlying induction of homosynaptic long-term depression in area CA1 of the hippocampus. *Neuron*, 9(5):967–975, 1992. (Cited on pages 3, 54, and 55.)

H. Naoki, Y. Sakamira, and S. Ishii. Local signaling with molecular diffusion as a decoder of Ca2+ signals in synaptic plasticity. *Molecular Systems Biology*, 1:2005.0027:E1–E12, 2005. doi:10.1038/msb4100035. (Cited on pages 16, 20, 31, 33, 34, 73, 74, 99, and 104.)

J. A. Nelder and R. Mead. A simplex method for function minimization. *Computer Journal*, 7:308–313, 1965. (Cited on page 121.)

D. Neveu and R. S. Zucker. Postsynaptic levels of [Ca2+]i needed to trigger LTD and LTP. *Neuron*, 16(3):619–629, 1996. (Cited on page 18.)

S. M. Nicola, J. Surmeier, and R. C. Malenka. Dopaminergic modulation of neuronal excitability in the striatum and nucleus accumbens. *Annu Rev Neurosci*, 23:185–215, 2000. doi:10.1146/annurev.neuro.23.1.185. (Cited on page 116.)

K. Nika, H. Hyunh, S. Williams, S. Paul, N. Bottini, K. Taskén, P. J. Lombroso, and T. Mustelin. Haematopoietic protein tyrosine phosphatase (HePTP) phosphorylation by cAMP-dependent protein kinase in T-cells: dynamics and subcellular location. *Biochem J*, 378(Pt 2):335–342, 2004. doi:10.1042/BJ20031244. (Cited on pages 59 and 70.)

I. Nikonenko, P. Jourdain, S. Alberi, N. Toni, and D. Muller. Activity-induced changes of spine morphology. *Hippocampus*, 12(5):585–591, 2002. doi:10.1002/hipo.10095. (Cited on page 5.)

E. A. Nimchinsky, B. L. Sabatini, and K. Svoboda. Structure and function of dendritic spines. *Annu Rev Physiol*, 64:313–353, 2002. doi:10.1146/annurev.physiol.64.081501.160008. (Cited on pages 5, 23, 34, 74, 117, and 124.)

E. A. Nimchinsky, R. Yasuda, T. G. Oertner, and K. Svoboda. The number of glutamate receptors opened by synaptic stimulation in single hippocampal spines. *J Neurosci*, 24(8):2054–2064, 2004. doi:10.1523/JNEUROSCI.5066-03.2004. (Cited on page 104.)

A. Nishi, J. A. Bibb, S. Matsuyama, M. Hamada, H. Higashi, A. C. Nairn, and P. Greengard. Regulation of DARPP-32 dephosphorylation at PKA- and Cdk5-sites by NMDA and AMPA receptors: distinct roles of calcineurin and protein phosphatase-2A. *J Neurochem*, 81(4):832–841, 2002. (Cited on page 13.)

A. Nishi, J. A. Bibb, G. L. Snyder, H. Higashi, A. C. Nairn, and P. Greengard. Amplification of dopaminergic signaling by a positive feedback loop. *Proc Natl Acad Sci U S A*, 97(23):12840–12845, 2000. doi:10.1073/pnas.220410397. (Cited on page 12.)

A. Nishi, G. L. Snyder, A. C. Nairn, and P. Greengard. Role of calcineurin and protein phosphatase-2A in the regulation of DARPP-32 dephosphorylation in neostriatal neurons. *J Neurochem*, 72(5):2015–2021, 1999. (Cited on page 11.)

S. D. Norrholm, J. A. Bibb, E. J. Nestler, C. C. Ouimet, J. R. Taylor, and P. Greengard. Cocaine-induced proliferation of dendritic spines in nucleus accumbens is dependent on the activity of cyclin-dependent kinase-5. *Neuroscience*, 116(1):19–22, 2003. (Cited on page 117.)

D. Ogreid and S. O. Døskeland. The kinetics of association of cyclic AMP to the two types of binding sites associated with protein kinase II from bovine myocardium. *FEBS Lett*, 129(2):287–292, 1981. (Cited on page 75.)

J. S. Oh, P. Manzerra, and M. B. Kennedy. Regulation of the neuron-specific Ras GTPase-activating protein, synGAP, by Ca2+/calmodulin-dependent protein kinase II. *J Biol Chem*, 279(17):17980–17988, 2004. doi:10.1074/jbc.M314109200. (Cited on page 60.)

C. C. Ouimet, K. C. Langley-Gullion, and P. Greengard. Quantitative immunocytochemistry of DARPP-32-expressing neurons in the rat caudatoputamen. *Brain Res*, 808(1):8–12, 1998. (Cited on page 11.)

C. C. Ouimet, P. E. Miller, H. C. Hemmings, S. I. Walaas, and P. Greengard. DARPP-32, a dopamine- and adenosine 3':5'-monophosphate-regulated phosphoprotein enriched in dopamine-innervated brain regions. III. Immunocytochemical localization. *J Neurosci*, 4(1):111–124, 1984. (Cited on page 11.)

A. Parent and L. N. Hazrati. Functional anatomy of the basal ganglia. I. The cortico-basal ganglia-thalamo-cortical loop. *Brain Res Brain Res Rev*, 20(1):91–127, 1995. (Cited on page 1.)

Y. H. Park, L. Kantor, B. Guptaroy, M. Zhang, K. K. W. Wang, and M. E. Gnegy. Repeated amphetamine treatment induces neurite outgrowth and enhanced amphetamine-stimulated dopamine release in rat pheochromocytoma cells (PC12 cells) via a protein

kinase C- and mitogen activated protein kinase-dependent mechanism. *J Neurochem*, 87(6):1546–1557, 2003. (Cited on pages 111 and 117.)

S. Paul, A. C. Nairn, P. Wang, and P. J. Lombroso. NMDA-mediated activation of the tyrosine phosphatase STEP regulates the duration of ERK signaling. *Nat Neurosci*, 6(1):34–42, 2003. doi:10.1038/nn989. (Cited on pages 59, 78, and 84.)

S. Paul, G. L. Snyder, H. Yokakura, M. R. Picciotto, A. C. Nairn, and P. J. Lombroso. The Dopamine/D1 receptor mediates the phosphorylation and inactivation of the protein tyrosine phosphatase STEP via a PKA-dependent pathway. *J Neurosci*, 20(15):5630–5638, 2000. (Cited on pages 59 and 70.)

M. E. Payne, Y. L. Fong, T. Ono, R. J. Colbran, B. E. Kemp, T. R. Soderling, and A. R. Means. Calcium/calmodulin-dependent protein kinase II. Characterization of distinct calmodulin binding and inhibitory domains. *J Biol Chem*, 263(15):7190–7195, 1988. (Cited on page 19.)

O. B. Peersen, T. S. Madsen, and J. J. Falke. Intermolecular tuning of calmodulin by target peptides and proteins: differential effects on Ca2+ binding and implications for kinase activation. *Protein Sci*, 6(4):794–807, 1997. doi:10.1002/pro.5560060406. (Cited on pages 25, 26, and 34.)

C. M. Pennartz, R. F. Ameerun, H. J. Groenewegen, and F. H. L. da Silva. Synaptic plasticity in an in vitro slice preparation of the rat nucleus accumbens. *Eur J Neurosci*, 5(2):107–117, 1993. (Cited on page 115.)

S. Pepke, T. Kinzer-Ursem, S. Mihalas, and M. B. Kennedy. A dynamic model of interactions of Ca2+, calmodulin, and catalytic subunits of Ca2+/calmodulin-dependent protein kinase II. *PLoS Comput Biol*, 6(2):e1000675, 2010. doi:10.1371/journal.pcbi.1000675. (Cited on page 20.)

B. A. Perrino, A. J. Wilson, P. Ellison, and L. H. Clapp. Substrate selectivity and sensitivity to inhibition by FK506 and cyclosporin A of calcineurin heterodimers composed of the alpha or beta catalytic

subunit. *Eur J Biochem*, 269(14):3540–3548, 2002. (Cited on pages 30 and 32.)

J. D. Petersen, X. Chen, L. Vinade, A. Dosemeci, J. E. Lisman, and T. S. Reese. Distribution of postsynaptic density (PSD)-95 and Ca2+/calmodulin-dependent protein kinase II at the PSD. *J Neurosci*, 23(35):11270–11278, 2003. (Cited on pages 33 and 104.)

R. S. Petralia, N. Sans, Y.-X. Wang, and R. J. Wenthold. Ontogeny of postsynaptic density proteins at glutamatergic synapses. *Mol Cell Neurosci*, 29(3):436–452, 2005. doi:10.1016/j.mcn.2005.03.013. (Cited on pages 112 and 119.)

J. J. Petrozzino, L. D. P. Miller, and J. A. Connor. Micromolar Ca2+ transients in dendritic spines of hippocampal pyramidal neurons in brain slice. *Neuron*, 14(6):1223–1231, 1995. (Cited on pages 54 and 55.)

J. C. Piña-Crespo and A. J. Gibb. Subtypes of NMDA receptors in new-born rat hippocampal granule cells. *J Physiol*, 541(Pt 1):41–64, 2002. (Cited on page 104.)

F. E. Pontieri, G. Tanda, and G. D. Chiara. Intravenous cocaine, morphine, and amphetamine preferentially increase extracellular dopamine in the "shell" as compared with the "core" of the rat nucleus accumbens. *Proc Natl Acad Sci U S A*, 92(26):12304–12308, 1995. (Cited on page 1.)

M. M. Poo. Neurotrophins as synaptic modulators. *Nat Rev Neurosci*, 2(1):24–32, 2001. doi:10.1038/35049004. (Cited on pages 8 and 114.)

R. Pulido, A. Zúñiga, and A. Ullrich. PTP-SL and STEP protein tyrosine phosphatases regulate the activation of the extracellular signal-regulated kinases ERK1 and ERK2 by association through a kinase interaction motif. *EMBO J*, 17(24):7337–7350, 1998. doi: 10.1093/emboj/17.24.7337. (Cited on page 58.)

A. R. Quintana, D. Wang, J. E. Forbes, and M. N. Waxham. Kinetics of calmodulin binding to calcineurin. *Biochem Biophys Res Commun*, 334(2):674–680, 2005. doi:10.1016/j.bbrc.2005.06.152. (Cited on pages 30 and 32.)

C. Racca, F. A. Stephenson, P. Streit, J. D. Roberts, and P. Somogyi. NMDA receptor content of synapses in stratum radiatum of the hippocampal CA1 area. *J Neurosci*, 20(7):2512–2522, 2000. (Cited on page 104.)

T. W. Robbins and B. J. Everitt. Limbic-striatal memory systems and drug addiction. *Neurobiol Learn Mem*, 78(3):625–636, 2002. (Cited on page 1.)

M. J. Robinson and M. H. Cobb. Mitogen-activated protein kinase pathways. *Curr Opin Cell Biol*, 9(2):180–186, 1997. (Cited on page 58.)

T. E. Robinson, G. Gorny, E. Mitton, and B. Kolb. Cocaine self-administration alters the morphology of dendrites and dendritic spines in the nucleus accumbens and neocortex. *Synapse*, 39(3):257–266, 2001. doi:3.0.CO;2-1. (Cited on page 117.)

T. E. Robinson, G. Gorny, V. R. Savage, and B. Kolb. Widespread but regionally specific effects of experimenter- versus self-administered morphine on dendritic spines in the nucleus accumbens, hippocampus, and neocortex of adult rats. *Synapse*, 46(4):271–279, 2002. doi: 10.1002/syn.10146. (Cited on page 118.)

T. E. Robinson and B. Kolb. Persistent structural modifications in nucleus accumbens and prefrontal cortex neurons produced by previous experience with amphetamine. *J Neurosci*, 17(21):8491–8497, 1997. (Cited on pages 117 and 118.)

T. E. Robinson and B. Kolb. Alterations in the morphology of dendrites and dendritic spines in the nucleus accumbens and prefrontal cortex following repeated treatment with amphetamine or cocaine. *Eur J Neurosci*, 11(5):1598–1604, 1999a. (Cited on pages 57, 117, and 118.)

T. E. Robinson and B. Kolb. Morphine alters the structure of neurons in the nucleus accumbens and neocortex of rats. *Synapse*, 33(2):160–162, 1999b. doi:3.0.CO;2-S. (Cited on page 118.)

T. E. Robinson and B. Kolb. Structural plasticity associated with exposure to drugs of abuse. *Neuropharmacology*, 47 Suppl 1:33–46,

2004. doi:10.1016/j.neuropharm.2004.06.025. (Cited on pages 8 and 117.)

O. S. Rosenberg, S. Deindl, R.-J. Sung, A. C. Nairn, and J. Kuriyan. Structure of the autoinhibited kinase domain of CaMKII and SAXS analysis of the holoenzyme. *Cell*, 123(5):849–860, 2005. doi:10.1016/j.cell.2005.10.029. (Cited on pages 19 and 44.)

M. M. Rubin and J. P. Changeux. On the nature of allosteric transitions: implications of non-exclusive ligand binding. *J Mol Biol*, 21(2):265–274, 1966. (Cited on page 25.)

G. Rumbaugh, J. P. Adams, J. H. Kim, and R. L. Huganir. SynGAP regulates synaptic strength and mitogen-activated protein kinases in cultured neurons. *Proc Natl Acad Sci U S A*, 103(12):4344–4351, 2006. doi:10.1073/pnas.0600084103. (Cited on page 60.)

D. A. Rusakov, M. G. Stewart, and S. M. Korogod. Branching of active dendritic spines as a mechanism for controlling synaptic efficacy. *Neuroscience*, 75(1):315–323, 1996. (Cited on page 117.)

B. L. Sabatini, T. G. Oertner, and K. Svoboda. The life cycle of Ca(2+) ions in dendritic spines. *Neuron*, 33(3):439–452, 2002. (Cited on pages 18, 21, 35, 46, 48, and 78.)

C. Sala, S. Rudolph-Correia, and M. Sheng. Developmentally regulated NMDA receptor-dependent dephosphorylation of cAMP response element-binding protein (CREB) in hippocampal neurons. *J Neurosci*, 20(10):3529–3536, 2000. (Cited on page 8.)

J. Salzmann, C. Marie-Claire, S. L. Guen, B. P. Roques, and F. Noble. Importance of ERK activation in behavioral and biochemical effects induced by MDMA in mice. *Br J Pharmacol*, 140(5):831–838, 2003. doi:10.1038/sj.bjp.0705506. (Cited on pages 58 and 111.)

F. Sananbenesi, A. Fischer, C. Schrick, J. Spiess, and J. Radulovic. Phosphorylation of hippocampal Erk-1/2, Elk-1, and p90-Rsk-1 during contextual fear conditioning: interactions between Erk-1/2 and Elk-1. *Mol Cell Neurosci*, 21(3):463–476, 2002. (Cited on page 57.)

S. Sasagawa, Y. ichi Ozaki, K. Fujita, and S. Kuroda. Prediction and validation of the distinct dynamics of transient and sustained ERK

activation. *Nat Cell Biol*, 7(4):365–373, 2005. doi:10.1038/ncb1233. (Cited on pages 71, 103, and 104.)

M. Sato, T. Ozawa, K. Inukai, T. Asano, and Y. Umezawa. Fluorescent indicators for imaging protein phosphorylation in single living cells. *Nat Biotechnol*, 20(3):287–294, 2002. doi:10.1038/nbt0302-287. (Cited on page 122.)

M. Saxena, S. Williams, K. Taskén, and T. Mustelin. Crosstalk between cAMP-dependent kinase and MAP kinase through a protein tyrosine phosphatase. *Nat Cell Biol*, 1(5):305–311, 1999. doi: 10.1038/13024. (Cited on page 58.)

R. H. Scannevin and R. L. Huganir. Postsynaptic organization and regulation of excitatory synapses. *Nat Rev Neurosci*, 1(2):133–141, 2000. doi:10.1038/35039075. (Cited on page 123.)

G. E. Schafe, K. Nader, H. T. Blair, and J. E. LeDoux. Memory consolidation of Pavlovian fear conditioning: a cellular and molecular perspective. *Trends Neurosci*, 24(9):540–546, 2001. (Cited on page 6.)

A. J. Scheetz, A. C. Nairn, and M. Constantine-Paton. NMDA receptor-mediated control of protein synthesis at developing synapses. *Nat Neurosci*, 3(3):211–216, 2000. doi:10.1038/72915. (Cited on page 6.)

N. L. Schramm, R. E. Egli, and D. G. Winder. LTP in the mouse nucleus accumbens is developmentally regulated. *Synapse*, 45(4):213–219, 2002. doi:10.1002/syn.10104. (Cited on page 115.)

W. Schultz. Getting formal with dopamine and reward. *Neuron*, 36(2):241–263, 2002. (Cited on page 116.)

D. W. Self, K.-H. Choi, D. Simmons, J. R. Walker, and C. S. Smagula. Extinction training regulates neuroadaptive responses to withdrawal from chronic cocaine self-administration. *Learn Mem*, 11(5):648–657, 2004. doi:10.1101/lm.81404. (Cited on page 115.)

K. Shen and T. Meyer. Dynamic control of CaMKII translocation and localization in hippocampal neurons by NMDA receptor stimulation. *Science*, 284(5411):162–166, 1999. (Cited on page 122.)

M. Sheng, J. Cummings, L. A. Roldan, Y. N. Jan, and L. Y. Jan. Changing subunit composition of heteromeric NMDA receptors during development of rat cortex. *Nature*, 368(6467):144–147, 1994. doi: 10.1038/368144a0. (Cited on page 59.)

M. Sheng and C. Sala. PDZ domains and the organization of supramolecular complexes. *Annu Rev Neurosci*, 24:1–29, 2001. doi: 10.1146/annurev.neuro.24.1.1. (Cited on page 123.)

S. Shi, Y. Hayashi, J. A. Esteban, and R. Malinow. Subunit-specific rules governing AMPA receptor trafficking to synapses in hippocampal pyramidal neurons. *Cell*, 105(3):331–343, 2001. (Cited on pages 57 and 122.)

J. M. Shifman, M. H. Choi, S. Mihalas, S. L. Mayo, and M. B. Kennedy. Ca2+/calmodulin-dependent protein kinase II (CaMKII) is activated by calmodulin with two bound calciums. *Proc Natl Acad Sci U S A*, 103(38):13968–13973, 2006. doi:10.1073/pnas.0606433103. (Cited on pages 19, 26, and 34.)

S. Y. Shvartsman, C. B. Muratov, and D. A. Lauffenburger. Modeling and computational analysis of EGF receptor-mediated cell communication in Drosophila oogenesis. *Development*, 129(11):2577–2589, 2002. (Cited on page 16.)

L. T. Singer, R. Arendt, S. Minnes, K. Farkas, A. Salvator, H. L. Kirchner, and R. Kliegman. Cognitive and motor outcomes of cocaine-exposed infants. *JAMA*, 287(15):1952–1960, 2002. (Cited on page 120.)

G. L. Snyder, A. A. Fienberg, R. L. Huganir, and P. Greengard. A dopamine/D1 receptor/protein kinase A/dopamine- and cAMP-regulated phosphoprotein (Mr 32 kDa)/protein phosphatase-1 pathway regulates dephosphorylation of the NMDA receptor. *J Neurosci*, 18(24):10297–10303, 1998. (Cited on page 13.)

G. D. Stanwood and P. Levitt. Drug exposure early in life: functional repercussions of changing neuropharmacology during sensitive periods of brain development. *Curr Opin Pharmacol*, 4(1):65–71, 2004. doi:10.1016/j.coph.2003.09.003. (Cited on page 120.)

M. I. Stefan, S. J. Edelstein, and N. Le Novère. An allosteric model of calmodulin explains differential activation of PP2B and CaMKII. *Proc Natl Acad Sci U S A*, 105(31):10768–10773, 2008. doi:10.1073/pnas.0804672105. (Cited on pages 19, 21, 22, 25, 27, 31, 32, and 34.)

O. Steward and W. B. Levy. Preferential localization of polyribosomes under the base of dendritic spines in granule cells of the dentate gyrus. *J Neurosci*, 2(3):284–291, 1982. (Cited on page 6.)

O. Steward and E. M. Schuman. Protein synthesis at synaptic sites on dendrites. *Annu Rev Neurosci*, 24:299–325, 2001. doi:10.1146/annurev.neuro.24.1.299. (Cited on page 6.)

M. G. Stewart and D. A. Rusakov. Morphological changes associated with stages of memory formation in the chick following passive avoidance training. *Behav Brain Res*, 66(1-2):21–28, 1995. (Cited on page 117.)

A. Stipanovich, E. Valjent, M. Matamales, A. Nishi, J.-H. Ahn, M. Maroteaux, J. Bertran-Gonzalez, K. Brami-Cherrier, H. Enslen, A.-G. Corbillé, O. Filhol, A. C. Nairn, P. Greengard, D. Hervé, and J.-A. Girault. A phosphatase cascade by which rewarding stimuli control nucleosomal response. *Nature*, 453(7197):879–884, 2008. doi:10.1038/nature06994. (Cited on pages 13 and 114.)

S. Strack, M. A. Barban, B. E. Wadzinski, and R. J. Colbran. Differential inactivation of postsynaptic density-associated and soluble Ca2+/calmodulin-dependent protein kinase II by protein phosphatases 1 and 2A. *J Neurochem*, 68(5):2119–2128, 1997a. (Cited on page 20.)

S. Strack, S. Choi, D. M. Lovinger, and R. J. Colbran. Translocation of autophosphorylated calcium/calmodulin-dependent protein kinase II to the postsynaptic density. *J Biol Chem*, 272(21):13467–13470, 1997b. (Cited on pages 60 and 122.)

S. Strack, R. B. McNeill, and R. J. Colbran. Mechanism and regulation of calcium/calmodulin-dependent protein kinase II targeting to the NR2B subunit of the N-methyl-D-aspartate receptor. *J Biol Chem*, 275(31):23798–23806, 2000. doi:10.1074/jbc.M001471200. (Cited on pages 60 and 122.)

P. Svenningsson, A. A. Fienberg, P. B. Allen, C. L. Moine, M. Lindskog, G. Fisone, P. Greengard, and B. B. Fredholm. Dopamine D(1) receptor-induced gene transcription is modulated by DARPP-32. *J Neurochem*, 75(1):248–257, 2000. (Cited on page 13.)

P. Svenningsson, A. Nishi, G. Fisone, J.-A. Girault, A. C. Nairn, and P. Greengard. DARPP-32: an integrator of neurotransmission. *Annu Rev Pharmacol Toxicol*, 44:269–296, 2004. doi:10.1146/annurev. pharmtox.44.101802.121415. (Cited on page 30.)

K. Takahashi, K. Kaizu, B. Hu, and M. Tomita. A multi-algorithm, multi-timescale method for cell simulation. *Bioinformatics*, 20(4):538–546, 2004. doi:10.1093/bioinformatics/btg442. (Cited on page 23.)

Y. Takumi, V. Ramírez-León, P. Laake, E. Rinvik, and O. P. Ottersen. Different modes of expression of AMPA and NMDA receptors in hippocampal synapses. *Nat Neurosci*, 2(7):618–624, 1999. doi:10. 1038/10172. (Cited on page 124.)

X. Tao, S. Finkbeiner, D. B. Arnold, A. J. Shaywitz, and M. E. Greenberg. Ca2+ influx regulates BDNF transcription by a CREB family transcription factor-dependent mechanism. *Neuron*, 20(4):709–726, 1998. (Cited on page 8.)

Y. Teh and G. Rangaiah. A Study of Equation-Solving and Gibbs Free Energy Minimization Methods for Phase Equilibrium Calculations. *Chemical Engineering Research and Design*, 80(7):745 – 759, 2002. ISSN 0263-8762. doi:DOI:10.1205/026387602320776821. (Cited on page 122.)

G. M. Thomas and R. L. Huganir. MAPK cascade signalling and synaptic plasticity. *Nat Rev Neurosci*, 5(3):173–183, 2004. doi: 10.1038/nrn1346. (Cited on pages 57 and 58.)

M. J. Thomas, C. Beurrier, A. Bonci, and R. C. Malenka. Long-term depression in the nucleus accumbens: a neural correlate of behavioral sensitization to cocaine. *Nat Neurosci*, 4(12):1217–1223, 2001. doi:10.1038/nn757. (Cited on page 115.)

T. Tian, A. Harding, K. Inder, S. Plowman, R. G. Parton, and J. F. Hancock. Plasma membrane nanoswitches generate high-fidelity

Ras signal transduction. *Nat Cell Biol*, 9(8):905–914, 2007. doi:10. 1038/ncb1615. (Cited on page 17.)

A. Y. Ting, K. H. Kain, R. L. Klemke, and R. Y. Tsien. Genetically encoded fluorescent reporters of protein tyrosine kinase activities in living cells. *Proc Natl Acad Sci U S A*, 98(26):15003–15008, 2001. doi:10.1073/pnas.211564598. (Cited on page 122.)

D. P. Tölle and N. Le Novère. Particle-based stochastic simulation in systems biology. *Curr Bioinformatics*, 1:315–320, 2006. (Cited on pages 15, 17, and 123.)

N. Toni, P. A. Buchs, I. Nikonenko, C. R. Bron, and D. Muller. LTP promotes formation of multiple spine synapses between a single axon terminal and a dendrite. *Nature*, 402(6760):421–425, 1999. doi: 10.1038/46574. (Cited on page 5.)

R. Y. Tsien, B. J. Bacskai, and S. R. Adams. FRET for studying intracellular signalling. *Trends Cell Biol*, 3(7):242–245, 1993. (Cited on page 122.)

A. Tzortzopoulos, S. L. Best, D. Kalamida, and K. Török. Ca2+/calmodulin-dependent activation and inactivation mechanisms of alphaCaMKII and phospho-Thr286-alphaCaMKII. *Biochemistry*, 43(20):6270–6280, 2004. doi:10.1021/bi035449u. (Cited on page 102.)

A. Tzortzopoulos and K. Török. Mechanism of the T286A-mutant alphaCaMKII interactions with Ca2+/calmodulin and ATP. *Biochemistry*, 43(21):6404–6414, 2004. doi:10.1021/bi036224m. (Cited on page 32.)

M. A. Ungless, J. L. Whistler, R. C. Malenka, and A. Bonci. Single cocaine exposure in vivo induces long-term potentiation in dopamine neurons. *Nature*, 411(6837):583–587, 2001. doi:10.1038/35079077. (Cited on page 118.)

H. Urakubo, M. Honda, R. C. Froemke, and S. Kuroda. Requirement of an allosteric kinetics of nmda receptors for spike timing-dependent plasticity. *J Neurosci*, 28(13):3310–3323, 2008. doi: 10.1523/JNEUROSCI.0303-08.2008. (Cited on page 20.)

H. Usui, R. Inoue, O. Tanabe, Y. Nishito, M. Shimizu, H. Hayashi, H. Kagamiyama, and M. Takeda. Activation of protein phosphatase 2A by cAMP-dependent protein kinase-catalyzed phosphorylation of the 74-kDa B″ (delta) regulatory subunit in vitro and identification of the phosphorylation sites. *FEBS Lett*, 430(3):312–316, 1998. (Cited on page 67.)

E. Valjent, J. C. Corvol, C. Pages, M. J. Besson, R. Maldonado, and J. Caboche. Involvement of the extracellular signal-regulated kinase cascade for cocaine-rewarding properties. *J Neurosci*, 20(23):8701–8709, 2000. (Cited on pages 58, 111, and 117.)

E. Valjent, V. Pascoli, P. Svenningsson, S. Paul, H. Enslen, J.-C. Corvol, A. Stipanovich, J. Caboche, P. J. Lombroso, A. C. Nairn, P. Greengard, D. Hervé, and J.-A. Girault. Regulation of a protein phosphatase cascade allows convergent dopamine and glutamate signals to activate ERK in the striatum. *Proc Natl Acad Sci U S A*, 102(2):491–496, 2005. doi:10.1073/pnas.0408305102. (Cited on pages 58, 59, 78, 80, 82, 86, 89, 98, and 111.)

L. E. Vazquez, H.-J. Chen, I. Sokolova, I. Knuesel, and M. B. Kennedy. SynGAP regulates spine formation. *J Neurosci*, 24(40):8862–8872, 2004. doi:10.1523/JNEUROSCI.3213-04.2004. (Cited on page 60.)

J. D. Violin, J. Zhang, R. Y. Tsien, and A. C. Newton. A genetically encoded fluorescent reporter reveals oscillatory phosphorylation by protein kinase c. *J Cell Biol*, 161(5):899–909, 2003. doi:10.1083/jcb.200302125. (Cited on page 122.)

N. Volfovsky, H. Parnas, M. Segal, and E. Korkotian. Geometry of dendritic spines affects calcium dynamics in hippocampal neurons: theory and experiments. *J Neurophysiol*, 82(1):450–462, 1999. (Cited on page 124.)

S. I. Walaas, D. W. Aswad, and P. Greengard. A dopamine- and cyclic AMP-regulated phosphoprotein enriched in dopamine-innervated brain regions. *Nature*, 301(5895):69–71, 1983. (Cited on page 11.)

L. Wang and C. N. Kim. On the feasibility and reliability of nonlinear kinetic parameter estimation for a multi-component photocatalytic

process. *Korean Journal of Chemical Engineering*, 18(5):652–661, 2001. (Cited on page 122.)

M. O. West, L. L. Peoples, A. J. Michael, J. K. Chapin, and D. J. Woodward. Low-dose amphetamine elevates movement-related firing of rat striatal neurons. *Brain Res*, 745(1-2):331–335, 1997. (Cited on page 118.)

J. R. Wickens, A. J. Begg, and G. W. Arbuthnott. Dopamine reverses the depression of rat corticostriatal synapses which normally follows high-frequency stimulation of cortex in vitro. *Neuroscience*, 70(1):1–5, 1996. (Cited on page 116.)

J. R. Wickens, J. N. J. Reynolds, and B. I. Hyland. Neural mechanisms of reward-related motor learning. *Curr Opin Neurobiol*, 13(6):685–690, 2003. (Cited on page 14.)

C. J. Wilson and Y. Kawaguchi. The origins of two-state spontaneous membrane potential fluctuations of neostriatal spiny neurons. *J Neurosci*, 16(7):2397–2410, 1996. (Cited on page 116.)

R. A. Wise. Drug-activation of brain reward pathways. *Drug Alcohol Depend*, 51(1-2):13–22, 1998. (Cited on page 1.)

D. Wolf and R. Moros. Estimating rate constants of heterogeneous catalytic reactions without supposition of rate determining surface steps – an application of a genetic algorithm. *Chemical Engineering Science*, 52(7):1189 – 1199, 1997. ISSN 0009-2509. doi:DOI:10.1016/S0009-2509(96)00479-4. (Cited on page 122.)

M. E. Wolf. The role of excitatory amino acids in behavioral sensitization to psychomotor stimulants. *Prog Neurobiol*, 54(6):679–720, 1998. (Cited on page 117.)

M. E. Wolf, X. Sun, S. Mangiavacchi, and S. Z. Chao. Psychomotor stimulants and neuronal plasticity. *Neuropharmacology*, 47 Suppl 1:61–79, 2004. doi:10.1016/j.neuropharm.2004.07.006. (Cited on pages 56 and 116.)

G. Y. Wu, K. Deisseroth, and R. W. Tsien. Activity-dependent CREB phosphorylation: convergence of a fast, sensitive calmodulin kinase pathway and a slow, less sensitive mitogen-activated protein kinase

pathway. *Proc Natl Acad Sci U S A*, 98(5):2808–2813, 2001a. doi: 10.1073/pnas.051634198. (Cited on page 8.)

G. Y. Wu, K. Deisseroth, and R. W. Tsien. Spaced stimuli stabilize MAPK pathway activation and its effects on dendritic morphology. *Nat Neurosci*, 4(2):151–158, 2001b. doi:10.1038/83976. (Cited on pages 57, 111, and 117.)

Z. Xia and D. R. Storm. The role of calmodulin as a signal integrator for synaptic plasticity. *Nat Rev Neurosci*, 6(4):267–276, 2005. doi: 10.1038/nrn1647. (Cited on page 50.)

J. Xing, D. D. Ginty, and M. E. Greenberg. Coupling of the RAS-MAPK pathway to gene activation by RSK2, a growth factor-regulated CREB kinase. *Science*, 273(5277):959–963, 1996. (Cited on page 57.)

Z. Yan, L. Hsieh-Wilson, J. Feng, K. Tomizawa, P. B. Allen, A. A. Fienberg, A. C. Nairn, and P. Greengard. Protein phosphatase 1 modulation of neostriatal AMPA channels: regulation by DARPP-32 and spinophilin. *Nat Neurosci*, 2(1):13–17, 1999. doi:10.1038/4516. (Cited on page 13.)

S. N. Yang, Y. G. Tang, and R. S. Zucke. Selective induction of LTP and LTD by postsynaptic [Ca2+]i elevation. *J Neurophysiol*, 81(2):781–787, 1999. (Cited on pages 18, 20, and 54.)

R. Yuste and T. Bonhoeffer. Morphological changes in dendritic spines associated with long-term synaptic plasticity. *Annu Rev Neurosci*, 24:1071–1089, 2001. doi:10.1146/annurev.neuro.24.1.1071. (Cited on pages 5 and 123.)

A. M. Zhabotinsky. Bistability in the Ca(2+)/calmodulin-dependent protein kinase-phosphatase system. *Biophys J*, 79(5):2211–2221, 2000. doi:10.1016/S0006-3495(00)76469-1. (Cited on pages 33, 44, and 102.)

J. Zhang, Y. Ma, S. S. Taylor, and R. Y. Tsien. Genetically encoded reporters of protein kinase A activity reveal impact of substrate tethering. *Proc Natl Acad Sci U S A*, 98(26):14997–15002, 2001. doi: 10.1073/pnas.211566798. (Cited on page 122.)

Y. Zhao and Z. Y. Zhang. The mechanism of dephosphorylation of extracellular signal-regulated kinase 2 by mitogen-activated protein kinase phosphatase 3. *J Biol Chem*, 276(34):32382–32391, 2001. doi: 10.1074/jbc.M103369200. (Cited on pages 71 and 72.)

B. Zhou, Z.-X. Wang, Y. Zhao, D. L. Brautigan, and Z.-Y. Zhang. The specificity of extracellular signal-regulated kinase 2 dephosphorylation by protein phosphatases. *J Biol Chem*, 277(35):31818–31825, 2002. doi:10.1074/jbc.M203969200. (Cited on pages 58, 72, and 73.)

J. J. Zhu, Y. Qin, M. Zhao, L. V. Aelst, and R. Malinow. Ras and Rap control AMPA receptor trafficking during synaptic plasticity. *Cell*, 110(4):443–455, 2002. (Cited on pages 57 and 112.)

## LIST OF ACRONYMS

AC . . . . . . . . . . . . adenylyl cyclase

AMP . . . . . . . . . . adenosine monophosphate

AMPA . . . . . . . . . $\alpha$-amino-3-hydroxy-5-methyl-4-isoxazolepropionic acid

BDNF . . . . . . . . . brain-derived neurotrophic factor

CaMKII . . . . . . . calcium/calmodulin-dependent protein kinase II

cAMP . . . . . . . . . cyclic adenosine monophosphate

CDK5 . . . . . . . . . cyclin-dependent protein kinase 5

cGMP . . . . . . . . . cyclic guanosine monophosphate

CK1 . . . . . . . . . . casein kinase 1

CK2 . . . . . . . . . . casein kinase 2

CREB . . . . . . . . . cyclic AMP-response-element-binding protein

DARPP-32 . . . . . dopamine- and cAMP-regulated phosphoprotein of 32 kDa

ERK . . . . . . . . . . extracellular signal regulated kinase

ERK1/2 . . . . . . . extracellular signal regulated kinases-1/2

ERK2 . . . . . . . . . extracellular signal regulated kinase-2

FRET . . . . . . . . . fluorescence resonance energy transfer

$G\alpha_{olf}$ . . . . . . . . . olfactory isoform of GTP-binding protein $\alpha$ subunit

GPCRs . . . . . . . . G-protein coupled receptors

I1 . . . . . . . . . . . . . inhibitor I

LTD . . . . . . . . . . long-term depression

LTP . . . . . . . . . . .    long-term potentiation

MAL . . . . . . . . . .    Mass Action Law

MAP . . . . . . . . . .    mitogen-activated protein

MAPK . . . . . . . .    mitogen-activated protein kinase

MEK . . . . . . . . . .    MAPK/ERK kinase

MKP . . . . . . . . . .    mitogen-activated protein kinase phosphatase

MSK . . . . . . . . . .    mitogen- and stress-activated kinases

MSN . . . . . . . . . .    medium-sized spiny neuron

MTs . . . . . . . . . . .    microtubules

NAc . . . . . . . . . . .    nucleus accumbens

NMDA . . . . . . . .    $N$-methyl-D-aspartate

NMDAR . . . . . .    $N$-methyl-D-aspartate receptor

NO . . . . . . . . . . . .    nitric oxide

ODE . . . . . . . . . .    ordinary differential equation

PDE . . . . . . . . . . .    cyclic nucleotide phosphodiesterase

PDE . . . . . . . . . . .    partial differential equations

PKA . . . . . . . . . . .    cyclic AMP-dependent protein kinase

PKC . . . . . . . . . . .    protein kinase C

PKG . . . . . . . . . .    cyclic GMP-dependent protein kinase

PP1 . . . . . . . . . . .    protein phosphatase 1

PP2A . . . . . . . . . .    protein phosphatase 2A

PP2B . . . . . . . . . .    protein phosphatase 2B

PP2C . . . . . . . . . .    protein phosphatase 2C

PSD . . . . . . . . . . .    postsynaptic density

RAS-GAP . . . . . .    Ras GTPase activating protein

Ras-GEF ...... Ras guanine nucleotide exchange factor protein

Ras-GRF ...... Ras guanine nucleotide releasing factor protein

RSK .......... ribosomal protein S6 kinases

sGC .......... soluble guanylyl cyclase

SPRCs ........ synapse-associated polyribosome complexes

STEP ......... striatal-enriched tyrosine phosphatase

SynGAP ....... synaptic Ras GTPase activating protein

TC ........... tautomycetin

VTA .......... ventral tegmental area

# A

- M. J. Schilstra, **L. Li**, J. Matthews, A. Finney, M. Hucka, and N. Le Novère. CellML2SBML: conversion of CellML into SBML. Bioinformatics, 22(8):1018-1020, 2006.

- N. Le Novère, B. Bornstein, A. Broicher, M. Courtot, M. Donizelli, H. Dharuri, **L. Li**, H. Sauro, M. Schilstra, B. Shapiro, J. L. Snoep, and M. Hucka. Biomodels database: a free, centralized database of curated, published, quantitative kinetic models of biochemical and cellular systems. Nucleic Acids Res, 34(Database issue):D689-D691, 2006.

- N. Le Novère, **L. Li**, and J.-A. Girault. DARPP-32: molecular integration of phosphorylation potential. Cell Mol Life Sci, 65(14):2125-2127, 2008.

- N. Le Novère, M. Hucka, H. Mi, S. Moodie, F. Schreiber, A. Sorokin, E. Demir, K. Wegner, M. I. Aladjem, S. M. Wimalaratne, F. T. Bergman, R. Gauges, P. Ghazal, H. Kawaji, **L. Li**, Y. Matsuoka, A. Villéger, S. E. Boyd, L. Calzone, M. Courtot, U. Dogrusoz, T. C. Freeman, A. Funahashi, S. Ghosh, A. Jouraku, S. Kim, F. Kolpakov, A. Luna, S. Sahle, E. Schmidt, S. Watterson, G. Wu, I. Goryanin, D. B. Kell, C. Sander, H. Sauro, J. L. Snoep, K. Kohn, and H. Kitano. The systems biology graphical notation. Nat Biotechnol, 27(8):735-741, 2009.

- C. Li, M. Donizelli, N. Rodriguez, H. Dharuri, L. Endler, V. Chelliah, **L. Li**, E. He, A. Henry, M. I. Stefan, J. L. Snoep, M. Hucka, N. Le Novère and C. Laibe. BioModels Database: An enhanced, curated and annotated resource for published quantitative kinetic models. *submitted*

- **L. Li**, M. I. Stefan, N. Le Novère. Postsynaptic calcium affects the ratio of PP2B and CaMKII activation. *submitted*

- **L. Li**, M. S. Matamales, N. Le Novère, J.-A. Girault. NMDA receptor controls PP1 dual regulations on ERK2 activity. *in preparation*